



# **University of Nottingham**

Department of Architecture and Built Environment

Faculty of Engineering

PhD Thesis Title

Theoretical and Experimental investigation of a Solar Free-Piston Stirling Engine (FPSE) using a flexible bellow for water pumping/power generation

PhD Student: Mohamed Shalak

Student ID: 4296705

Primary Supervisor: Dr. Rabah Boukhanouf

Secondary Supervisor: Dr. John Calautit

The thesis was submitted to the University of Nottingham for the degree of  
Doctor of Philosophy

Year: 2022

## Abstract:

Fossil fuels are the primary energy source globally and currently represent more than 80% of the overall energy consumption. Fossil fuels such as natural gas, oil and coal remain the principal fuels for supply and off-grid power generation in remote areas. Concerns over the negative environmental impact of greenhouse gases emission have shifted toward deploying and developing renewable and low carbon energy technologies. In the last decades, many sustainable and clean energy alternatives have been exploited to make energy and power generation clean and affordable to mitigate the negative impact of fossil fuels on the environment. The Stirling engine is considered one of the most promising solutions of sustainable power technologies to generate electricity from external heat sources.

This research develops the computer model of a free-piston Stirling engine (FPSE) prototype operated by a solar simulator for small-scale power generation. The mathematical model was based on solving the working fluid's mass, energy and momentum conservation equations in different engine components. The engine's performance was evaluated based on the other three models: Schmidt, Adiabatic and Simple analysis. It is found that Simple analysis gave the most accurate result because the model considers the heat losses of the Stirling cycle. This research also investigated a novel design of a solar Free-piston Stirling engine for power generation and water pumping, which can be used in remote world regions. The design incorporates flexible bellows or diaphragm working as a power piston and two pre-compressed springs to support the displacer. This mechanical arrangement of the moving components in the engine reduces mechanical friction and air leakage. The experimentally testable FPSE was carried out, including a linear electric generator to develop and validate the theoretical simulation model. It was

demonstrated the engine could operate successfully at an input heat temperature of 300C°, at 1 bar pressure and a frequency of 10 Hz. Moreover, a novel design is added to the engine to convert the linear motion to rotary motion. Overall, the engine's measured power and efficiency are low, and more tests of increasing the pressure of the engine for more than 1 bar are required to obtain better performance.

## Contents

Abstract: .....	2
List of Figures .....	8
List of Tables .....	10
Nomenclature .....	11
Acknowledgement .....	13
Chapter 1: .....	14
Introduction .....	14
1.1 Background .....	14
1.2 Research Question and Research Gap .....	15
1.3 The Main Research Aim .....	16
1.4 Methodology of research .....	17
1.5 Thesis outline .....	18
Chapter 2: .....	20
Review of solar power generators .....	20
2.1 Solar Power .....	20
2.2 Direct solar conversion to electrical power .....	21
2.2.1 Photovoltaic system (PV) .....	21
2.3 Indirect solar conversion to electrical power .....	23
2.3.1 Parabolic trough concentrator .....	23
2.3.2 Linear Fresnel reflector .....	25
2.3.3 Solar tower .....	26
2.3.4 Parabolic dish concentrators .....	27
2.4 Summary .....	28
Chapter 3: .....	30
Review of Stirling Engine Technology .....	30
3.1 Brief overview .....	30
3.2 Operation principle of Stirling engine .....	32
3.3 Main parts of Stirling engine .....	33
3.3.1 Power piston .....	34
3.3.2 Displacer: .....	34
3.3.3 Heater .....	35
3.3.4 Cooler .....	35
3.3.5 Regenerator .....	35
3.4 Stirling Cycle .....	36

3.4.1	Isothermal compression process at constant temperature (1-2).....	36
3.4.2	Regenerative process at (constant volume) heating (2-3).....	37
3.4.3	Isothermal expansion process at constant temperature (3-4).....	37
3.4.4	Regenerative process at (constant volume) cooling (4-1) .....	37
3.5	Real Stirling Cycle .....	37
3.6	Stirling engine Classification.....	39
3.6.1	Alpha Type .....	39
3.6.2	Beta Type .....	40
3.6.3	Gama Type.....	40
3.7	Free Piston Stirling Engine (FPSE) .....	41
3.8	Classification and types of (FPSE) .....	43
3.8.1	Single acting (FPSE) .....	43
3.9	Diaphragm free-piston Stirling machine.....	45
3.10	Solar Stirling engine .....	46
3.11	Design, development and performance evaluation of Solar Stirling engine....	47
3.12	Parabolic Dish Technology .....	49
3.13	Dish mounted storage and Hybridisation.....	52
3.14	The Receiver.....	53
3.15	Applications of Solar Stirling engine .....	54
3.15.1	Solar Stirling electric power generation system .....	54
3.15.2	Solar Stirling power plants .....	56
3.15.3	Solar Stirling of irrigation system .....	56
3.16	Mathematical models of Stirling engine cycle.....	60
3.17	Zero dimensional model .....	60
3.18	First Order Model (Schmidt Analysis) .....	62
3.18.1	Heat transfer in Schmidt analysis .....	65
3.19	Second Order Model (Adiabatic Analysis) .....	68
3.20	Simple Analysis .....	73
3.21	Third-Order Model (Nodal analysis) .....	74
3.22	Dynamic Analysis of FPSE .....	75
3.23	Summary .....	79
Chapter 4:	.....	80
Computer Modelling and Simulation Analysis .....		80
4.1	The proposed mechanical arrangement for the FPSE .....	80
4.2	The design objectives.....	81

4.3	Thermodynamic Models .....	81
4.3.1	First-order model (Schmidt analysis) .....	82
4.3.2	Second-order model (Adiabatic analysis) .....	85
4.3.3	Simple analysis.....	90
4.4	Numerical simulation and results.....	92
4.5	Computer Model Results .....	93
4.6	Consideration-variable frequency versus power output and efficiency .....	100
4.7	Consideration-variable stroke versus power output and efficiency.....	103
4.8	Consideration-variable pressure versus power output and efficiency.....	105
Chapter 5: .....		107
The proof of concept engine design, fabrication and assembly.....		107
5.1	Introduction .....	107
5.2	Engine design and configuration .....	108
5.3	Displacer assembly manufacturing.....	109
5.3.1	Mechanical spring selection.....	110
5.4	Power piston.....	113
5.4.1	Design of Bellows and sizing .....	114
5.4.2	Fabrication process .....	115
5.4.3	Movement and Deflection .....	115
5.4.4	The characteristics design of Bellows.....	116
5.4.5	Diaphragm power piston manufacturing .....	116
5.5	Engine casing cylinder.....	117
5.6	Cooling coil.....	118
5.7	Regenerator .....	119
5.8	Solar simulator .....	120
5.9	Cover Simulator.....	121
5.10	Water jacket .....	122
5.11	Engine supporting frame .....	123
5.12	Linear to rotary motion conversion mechanism .....	124
5.12.1	Introduction.....	124
5.12.2	Advantages.....	124
5.13	Structural configuration of the prototype platform.....	124
5.14	The purpose of the design.....	125
5.15	The Lever design.....	127
5.16	The Conrods design .....	127

5.17	Bearings .....	128
5.18	Summary .....	129
	Chapter 6: .....	130
	Experimental set up of assembled engine.....	130
6.1	Instrument description .....	131
6.1.1	Thermocouple:.....	131
6.1.2	Data taker and data logger software:.....	131
6.1.3	Infrared thermometer .....	131
6.1.4	Oscilloscope .....	132
6.1.5	Pressure transducer .....	133
6.2	Engine start up procedures .....	134
6.3	Inspection and modification .....	135
6.4	Power piston operating frequency tuning .....	136
6.4	Steady state operation results .....	137
6.5	Water pump output.....	139
6.6	Power generation output .....	140
6.7	Engine lifting capacity.....	142
6.8	Summary of the experiment result compared to modelling result.....	143
	Chapter 7: .....	144
	Conclusion and future work.....	144
7.1	Contribution to the development of FPSE design and Novelty of the research	145
7.2	Recommendation for future work .....	145
	REFERENCES .....	147
	Appendices 1 The equations of Schmidt analysis .....	160
	Appendices 2 The equations of Adiabatic analysis .....	163
	Appendices 3 Matlab Computer Modelling (functions): .....	165
	Appendices 4 Matlab computer model result: .....	193

## List of Figures:

Figure 1.1: Power generation from various sources in the world [2].....	18
Figure 1.2: Flowchart of research approach.....	20
Figure 2.1: Classification of Solar power plant.....	21
Figure 2.2: Typical PV system.....	22
Figure 2.3: Principle working of PV system.....	24
Figure 2.4: Layout of parabolic trough concentrator technology.....	26
Figure 2.5: Schematic layout of Linear Fresnel Reflector system.....	27
Figure 2.6: Solar tower technology system.....	30
Figure 2.7: Parabolic dish concentrators with Stirling engine.....	33
Figure 3.1: Reverend Robert Stirling and his engine [59].....	33
Figure 3.2: Schematic principle of heat engine.....	36
Figure 3.3: The main components of Stirling engine.....	38
Figure 3.4: Description of each process of Ideal Stirling cycle.....	38
Figure 3.5: Real Stirling cycle in P-V diagram.....	40
Figure 3.6: P-V diagrams for practical Stirling engine.....	40
Figure 3.7: The diagram of Alpha Stirling engine [64].....	41
Figure 3.8: The diagram of Beta Stirling engine [72].....	42
Figure 3.9: The diagram of Gamma Stirling engine [72].....	43
Figure 3.10: Advanced Stirling Radioisotope Generator [75].....	45
Figure 3.11: The main components of FPSE [78].....	46
Figure 3.12: The movement of displacer and power piston with mechanical spring.....	47
Figure 3.13: Diaphragm free-piston Stirling engine [127].....	50
Figure 3.14: Schematic representation of dish Stirling engine.....	50
Figure 3.15. 2-stage parabolic dish-Stirling engine.....	51
Figure 3.16: The operation of parabolic reflector with sun radiation.....	52
Figure 3.17: (a) the Vanguard dish, (b) MDAC dish .....	53
Figure 3.18: Steps for designing parabolic solar dish.....	55
Figure 3.19: Thermal storage system based dish-Stirling power generation.....	57
Figure 3.20: Diagram of the thermal balance in the system.....	58
Figure 3.21: SUNPULSE Stirling System [45].....	60
Figure 3.22: Block diagram of the solar Stirling system with centrifugal pump.....	62
Figure 3.23: Schematic diagram of utilising heat rejected from Stirling engine.....	64
Figure 3.24: Beale number as a function of heater temperature [70].....	66
Figure 3.25: Ideal Isothermal Model [98].....	68
Figure 3.26: A generalized cell of working spaces in the engine.....	70
Figure 3.27: Sinusoidal volume variation of the compression and expansion space .....	71
Figure 3.28: The ideal adiabatic model in Stirling engine.....	72
Figure 3.29: Gamma Stirling engine components.....	78
Figure 3.30: Prototype engine and schematic diagram of Beta type.....	79
Figure 3.31: Diagram of Free-piston Vuilleumier Heat Pump (FVHP).....	82
Figure 3.32: Schematic components of proposed FPSE.....	83
Figure 4.1: Diagram of prototype FPSE components.....	87
Figure 4.2: Stirling thermodynamic cycle.....	94
Figure 4.3: Flow energy within each subsystem of the engine.....	97
Figure 4.4: Temperature and mass flow distribution.....	98

Figure 4.5: The progress function of the model simulation [72].....	99
Figure 4.6: PV Diagram in the simulation.....	100
Figure 4.7: Temperature change in the engine parts in complete cycle.....	101
Figure 4.8: Diagram of energy and work in the engine cells over the cycle.....	102
Figure 4.9: Pressure losses in heat exchanger over the cycle.....	103
Figure 4.10: Mass flow rate in the working space over the cycle.....	104
Figure 4.11: Engine Power output versus operating frequency for different values of external heat source temperature in Schmidt analysis.....	105
Figure 4.12: Engine Efficiency versus operating frequency for different values of external heat source temperature in Schmidt analysis.....	106
Figure 4.13: Engine Efficiency versus operating frequency for different values of external heat source temperature in Simple analysis.....	107
Figure 4.14: Engine Power output versus variable stroke in Schmidt and Simple analysis.....	110
Figure 4.15: Engine efficiency versus variable stroke in Schmidt and Simple analysis.....	112
Figure 4.16: Engine Power output versus variable pressure in Schmidt and Simple analysis.....	113
Figure 4.17: Engine efficiency versus variable pressure in Schmidt and Simple analysis.....	114
Figure 5.1: The main parts of the engine design.....	119
Figure 5.2: Inside the helical spring of the displacer .....	120
Figure 5.3: The components of the displacer.....	121
Figure 5.4: The combined displacer with the cylinder.....	122
Figure 5.5: Power piston of bellow design.....	123
Figure 5.6: Diaphragm of engine power piston.....	124
Figure 5.7: The engine casing cylinder.....	126
Figure 5.8: Cooling coil design.....	127
Figure 5.9: The regenerator inside the displacer cylinder.....	128
Figure 5.10: Solar simulator .....	128
Figure 5.11: The focal point, diameter of concentrator and the focal length of concentrator.....	131
Figure 5.12: Cover simulator of the engine.....	132
Figure 5.13: Water jacket cooling design.....	133
Figure 5.14: The support frame of the engine.....	134
Figure 5.15: The diagram configuration of the prototype.....	135
Figure 5.16: Two (one way bearing) design.....	136
Figure 5.17: The lever design.....	137
Figure 5.18: The conrods design.....	137
Figure 5.19: Sprag clutch one way bearing.....	138
Figure 6.1: Instruments laboratory of the rig .....	139
Figure 6.2: Data taker DT500.....	140
Figure 6.3: Fluke 64 MAX infrared thermometer.....	141
Figure 6.4: GW-INSTEK oscilloscope.....	142
Figure 6.5: The UNIK5000-PTX5072 pressure transducer.....	143
Figure 6.6: Resistance design high temperature gasket.....	144
Figure 6.7: One of the four sets of flat plates with springs .....	145
Figure 6.8: A magnet lump weight and coil transducer.....	146
Figure 6.9: The operation frequency diagram .....	147
Figure 6.10: The operation voltage output diagram.....	148
Figure 6.11: Water pump installed on the rotary output shaft.....	149
Figure 6.12: Small power generation installed on the rotary output shaft.....	150
Figure 6.13: Power output from electric generator.....	151
Figure 6.14: The rotary shaft of engine lifting amount of weight.....	152

## List of Tables:

Table 3.1: Best reported dish-Stirling systems.....	52
Table 4.1: Dimensions of the parts engine.....	94
Table 4.2: Operation parameters of the engine.....	95
Table 4.3: The numerical results from the computer analysis.....	96
Table 5.1: The design characteristics of the bellows.....	116
Table 5.2: Sprag clutch one way bearing specifications.....	129
Table 6.1 comparison of experimental result and modelling result at 300 C° heat in.....	144

## Nomenclature

<b>Symbol</b>	<b>Description</b>
A	cross sectional area, m <sup>2</sup>
B <sub>n</sub>	Beale number
C	damping coefficient, N/m
C <sub>p</sub>	gas specific heat capacity at constant pressure, J/kg.K
C <sub>v</sub>	gas specific heat capacity at constant volume, J/kg.K
f	frequency, Hz
g <sub>A</sub>	mass flow rate
K	spring rate, N/m
M	mass (kg)
$\dot{m}$	mass flow rate (kg/s)
n <sub>w</sub>	number of convolutions
NTU	number of transfer unites
NST	Stanton number
P	Pressure, N/m <sup>2</sup>
P <sub>m</sub>	mean pressure, N/m <sup>2</sup>
Q	heat transferred, W
R	gas constant, J/mol.K
$\dot{x}$	velocity, m/s
$\ddot{x}$	acceleration, m/s <sup>2</sup>
T	temperature, °C
t	thickness, mm
V	volume, m <sup>3</sup>
W	output power, W

### Greek letter

ε	heat exchanger effectiveness
δ	bellow and diaphragm deflection, mm
λ	natural frequency, Hz
η	thermal efficiency
θ	cyclic angle, degree

$\mu$	Poisson's ratio of the diaphragm
$\rho$	density, kg/m <sup>3</sup>
$\varphi$	phase angle, degree

## Subscripts

C	cooled temperature
diss	dissipated
H	hot temperature
c	Compression space
k	Cooler
r	Regenerator
h	Heater
e	Expansion space
cl	Clearance volume
sw	Swept volume
i, j	Space directions
i,o	in and out

## Acknowledgement

I wish to express my sincere appreciation to my supervisor Dr.Rabah Boukhanouf for his invaluable support and encouragement throughout my study.

Also, I will like to give special thanks to my parents and my wife for their constant care, financial and moral support throughout my study.

Finally, I would like to thank my Libyan embassy for their financial support.

# Chapter 1:

## Introduction

### 1.1 Background

The consumption of energy derived from fossil fuels plays a vital role in every field of human activity. It is a significant factor that contributed to the development of successive civilisations. However, it was not until the start of the industrial revolution that the utilisation of fossil fuel resources in manufacturing processes contributed to what we know today as global warming. Energy consumption today is in ascending trend it is expected that this will double in the next 50 years [1]. Therefore, many developed countries have decided to reduce carbon emissions and develop sustainable technologies to mitigate climate change. As shown in Figure (1.1), fossil fuels power constitutes the largest share of power generation globally.

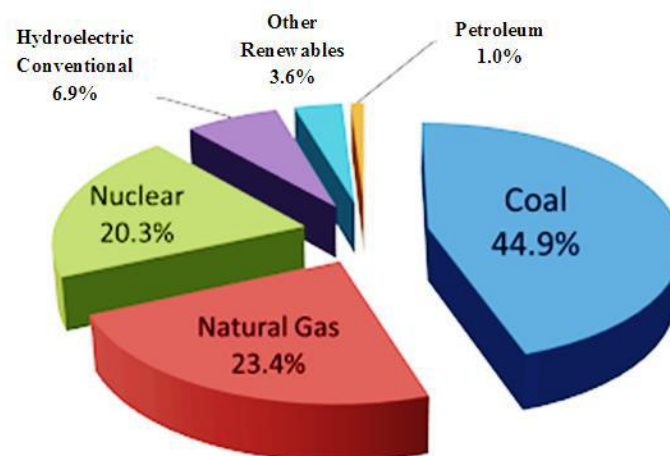


Figure 2.1: Power generation from various sources in the world [2]

It has been recognised that the use of fossil fuels for power generation has to be reduced to a sustainable level. Recently, there has been a massive investment in renewable energy development, with clean energy market revenues growing from about \$110 billion in 2006 to \$450 billion in 2016 [3]. This is driven by many countries' energy decarbonisation policies set ambitious targets to reduce carbon emissions. For instance, The UK has set a target to reduce CO<sub>2</sub> emissions by 80% by 2050 compared to the 1990 emission level [1].

Therefore, it is essential to further the development of clean, sustainable and affordable sources of energy such as geothermal, solar and biomass.

In this context, this research was undertaken to develop a solar-driven heat engine according to the Stirling cycle for application in remote parts of the world where solar energy resources are available for harvesting. The novelty of the design is utilising a flexible bellow as a power piston.

## 1.2 Research Question and research gap:

- **Question 1:**
  - What are the available small scale solar energy conversion technologies for power generation application in remote area?
  
- **Question 2:**
  - Which technology is affordable, reliable and required less maintenance for small scale power generation application in remote areas?
  
- **Question 3:**
  - How to design and develop a novel type of renewable driven small scale power generator for Libyan conditions?

- **Question 4:**
- What are the mathematical models for design and performance optimisation of Stirling engine?
  
- **Question 5:**
- How to optimise the components of the power generation system?
  
- **Question 6:**
- Building a proof-of-concept to validate the computer model?

### 1.3 The Main Research Aim:

The aim of the thesis is to propose one of the solutions that would make groundwater pumping sustainable or produce power generation and reduce carbon emissions. Mainly, this thesis discusses the ability to use solar energy to operate water pumps or generate electricity by using a free-piston Stirling engine. It provides the design elements for the solar free-piston Stirling engine. It discusses its applications for two operations that can be applied in rural areas: (a) as a water pump for usage in a drip irrigation system. (b) As a power, the generator to drive any electric application. The tasks of the objectives are:

- Conduct a comprehensive assessment of the literature review on power generation, focusing on renewable technologies, and identify the research gap in Stirling engine technology. The literature review covers renewable power generating cycles, such as photovoltaic system (PV), concentrating solar power (CSP) and the Stirling cycle.
- Find out the most efficient renewable technologies of small-scale power generation in remote areas and study them in greater depth.

- Assessment and review of the previous Stirling engine design and determine each design's limitation.
- Investigate a mathematical model that integrates the heat transfer, thermodynamics and mechanical efficiency for the simulation of Stirling engine systems. Furthermore, the model must consider the thermodynamic cycle using first, second and simple mathematical models and develop Matlab computer code.
- Specify and build the conceptual novel design of the solar-powered Stirling engine following input parameters of the engine design in mathematical modelling.
- Test and present a summary of the experimental set-up of the engine.

#### 1.4 Methodology of research:

The research study looked into making a free-piston Stirling engine with bellows and a rubber diaphragm as a power piston. Both quantitative and qualitative research methods were used in this study. Material selection, physical prototype fabrication, concept outline and a lab test rig are all parts of the quantitative research method. Meanwhile, the qualitative research method consists of Understanding theoretical principles of mathematical modelling and developing thermodynamic and dynamic modelling of Stirling cycle by utilising high-level computer language to provide the proposed design of free piston Stirling engine in this thesis.

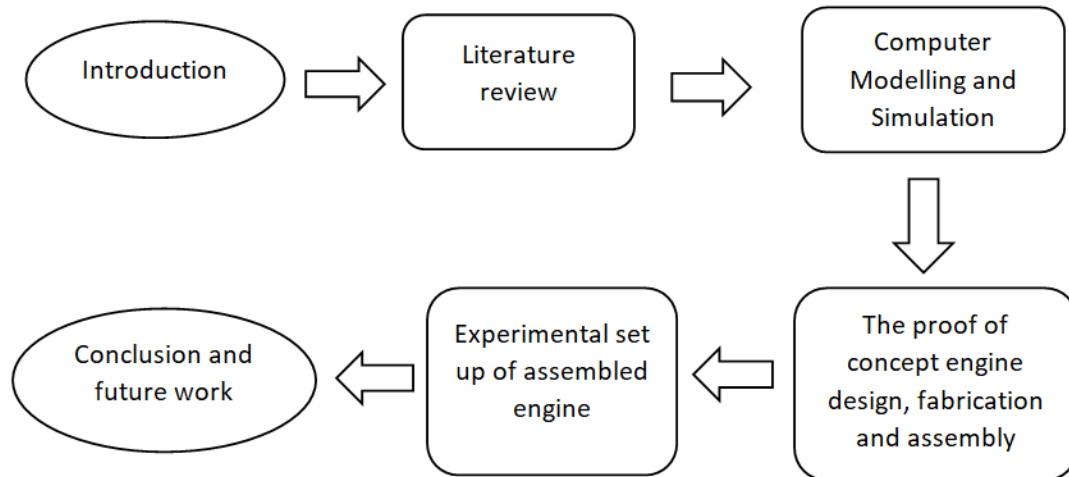


Figure 1.2: Flowchart of research approach

## 1.5 Thesis outline:

The thesis is divided into eight chapters. The description of each is as follows:

**Chapter 1:** Introduction: the underlying issues that serve as a motivation for this thesis are presented. The research objectives, the methodology of the research and the contribution to knowledge are also explained.

**Chapter 2:** Review of solar power generation technology: This chapter reviews direct and indirect solar conversion to electrical power technologies, focusing more on solar Stirling engine technology.

**Chapter 3:** Review of Stirling engine mechanical arrangements: the ideal thermodynamic Stirling engine cycle, the main parts of the Stirling engine and the Stirling engine classification are reviewed with mainly focused on recent improvements in the free-piston Stirling engine to broaden the knowledge of the Stirling engine cycle in power generation.

**Chapter 4:** Mathematical models of Stirling engine cycle: several thermodynamic Stirling engine cycle analysis methods are reviewed. The thermodynamic process of

the energy flow and the principle of the dynamic interaction of moving parts are also explained.

**Chapter 5:** Computer modelling and simulation analysis: this chapter describes the simulation model in detail. The equations of the simulation model are defined before the engine's design because the simulation model will approximate the prototype dimensions and specify the operating parameters.

**Chapter 6:** The proof-of-concept engine design, fabrication and assembly: The conceptual design of the solar free-piston Stirling engine is described in this chapter. The prototype manufacturing process is described, and the rationale for choosing the displacer and power piston design is presented. It also describes the novel method of using the prototype in pumping water for irrigation and power generator.

**Chapter 7:** Experimental set-up of assembled engine: the components used to build a test rig and measuring instruments used for experiments are explained. The experimental results for the rig are discussed and summarized.

**Chapter 8:** Conclusion and future work: a brief conclusion is explained for the thesis, and a few recommendations are presented in this section for future work.

# Chapter 2:

## Review of solar power generators

### 2.1 Solar Power:

The consumption of fossil fuels in thermal energy and electricity generation impacts the environment. The development of alternative energy sources has become the primary concern in the policy and decision-making of governments. This has led to the rise in research, investments and development of solar power devices that can generate electricity from the sun [4]. The major technologies of solar power have different electricity generation processes

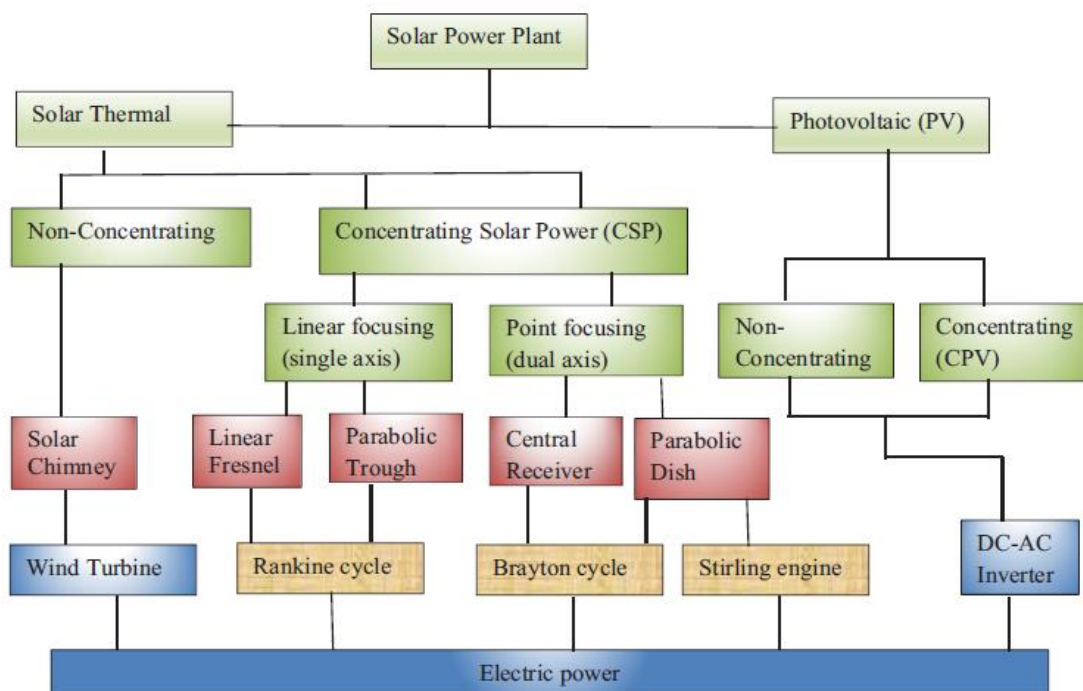


Figure 2.1: Classification of Solar power plant

As shown in Figure 2.1, solar energy can be exploited by converting solar radiation directly into electrical power or indirectly by heating a thermos fluid to drive a heat

engine. To increase the specific power generation of equipment, the diluted nature of solar energy often requires concentration using parabolic dishes and troughs of Fresnel lenses. The following solar technologies are being deployed in many parts of the world.

## 2.2 Direct solar conversion to electrical power:

### 2.2.1 Photovoltaic system (PV):

Recently, the most common PV systems design is the rack rooftop solar system, whereas the structure of building-integrated photovoltaics (BIPV) has been widely promoted by governments [5]. PV systems have several advantages: there is no depletion of resources while generating electricity, the operation has no noise environmental harm, and it requires minimum maintenance [6].

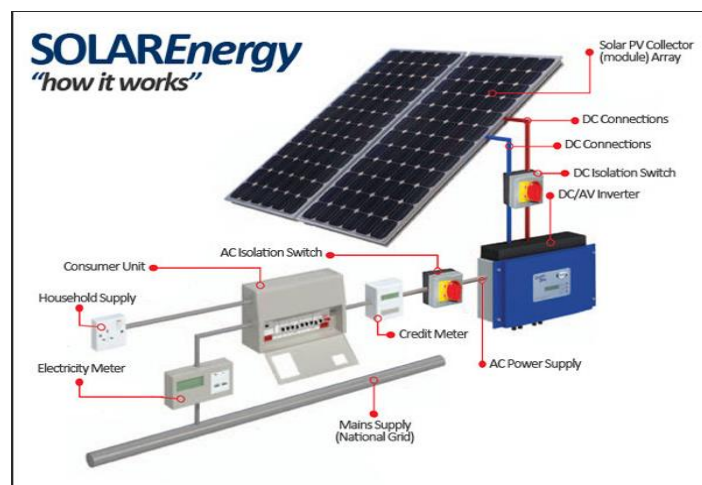


Figure 2.2: Typical PV system

As can be seen, the above Figure (2.2) shows that the PV system works by collecting solar energy from sunlight and converting it to (DC) electricity. An inverter then converts this DC electricity into (AC power).

Photovoltaic power generation is primarily based on the photoelectric effect, which is achieved by solar cells that capture and convert solar energy into electricity. Solar radiation that reaches the semiconductor's outer layer is partly reflected, while the remainder is absorbed and transmitted by the semiconductor. Some of the received solar energy is transformed into heat. In contrast, others generate electron-hole pairs separated by the semiconductor PN junction before being collected, as shown in Figure 2.3[7].

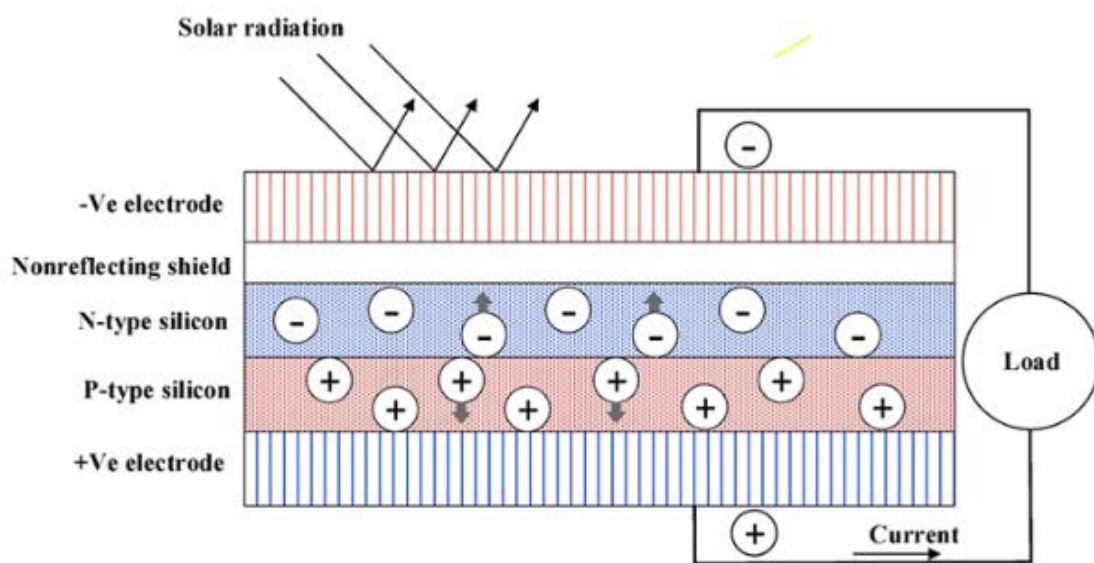


Figure 2.3: Principle working of PV system

According to the IEA's roadmap, solar capacity added worldwide will reach 4600GW, accounting for around 16 percent of total power generation [8]. As a result, PV will provide a clean and sustainable tool for power generation worldwide. PV cells can collect up to 80% of the solar light that falls on their surface, but their power conversion efficiency is currently only 12 to 18%, with a record efficiency of 24.7 percent. The remaining solar energy is converted to heat, boosting the temperature of the PV-cell to 40 degrees Celsius above ambient. Operating temperature, Irradiance, dust, humidity, and other variables all affect the electricity conversion

efficiency of PV modules[9]. One of the most significant issues in PV electricity production is the high working temperature of the panels.

Furthermore, single and multi-crystalline silicon cells account for about 85 percent to 90 percent of the PV market. Thin-film PV panels, which come in various shapes and sizes, account for ten to fifteen percent of the PV market. Thin-film cells are less expensive and less efficient than crystalline silicon cells. However, significant progress has been achieved in this area worldwide, with research revealing that PV panels composed of various materials have been developed in recent years[10].

## 2.3 Indirect solar conversion to electrical power:

Four CSP technologies have a different working processes, and economic maturity is already incorporated in the power and heat industry at the global level. These include: parabolic dish concentrators, parabolic trough concentrators, linear Fresnel reflectors and solar towers [11]. Detailed descriptions of the technologies' thermodynamic performance and operating principles are presented in the following subsections.

### 2.3.1 Parabolic trough concentrator:

Nowadays, the operation of parabolic trough concentrator (PTC) technology is mostly versatile of the other technologies [12]. As it can be seen in Figure (2.4) the curved parabolic shaped mirrors are utilised to concentrate incident solar radiation on a coated steel pipe. Also, the structure of concentrator provides firm support to the receiver tube and mirror, while the drive of collector assembly is designed with a tracker, which make it flexible and enable to track the path of the sun [13,14].

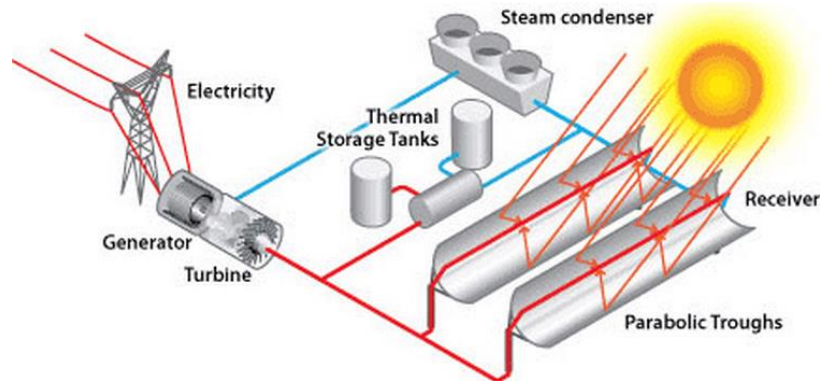


Figure 2.4: Layout of parabolic trough concentrator technology

To avoid misalignments that result in performance losses, the parabolic shape of the mirrors and the location of the receiver at the parabola's focal line should always be maintained. As a result, adequate structural framework design is critical. Bending and torsion of the framework, which are mostly caused by self-weight and wind forces, are the most significant mechanical qualities to consider during production. If the frame is not appropriately designed, these two characteristics will have an impact on performance [15].

The technology uses a heat transfer fluid (HTF) for instance synthetic oil which can be heated up to 400 °C then passes through the receiver tube. The function of thermal oil is to generate steam by transferring heat from receiver tube to heat exchanger. The steam is further superheated in order to run the turbines for electricity generation. However, thermal oils are not the perfect working fluid for parabolic trough collectors, because they have some technical limitation by the maximum operating temperature. Selecting the appropriate heat transfer fluid and storage medium is a key technological issue for the future success of CSP technology. Batuecas et al investigate the utilise of molten salts in thermal energy storage is the most competitive option between thermal efficiency and economy makes CSP. Also, using molten salts in thermal energy storage systems presents higher operating temperatures than synthetic oil[16].

### **2.3.2 Linear Fresnel reflector:**

The first commercial Linear Fresnel reflector plant was built in Spain which is connected to the local electricity grid in 2009 and has a capacity of 1.5 MW [17]. The process of Linear Fresnel reflector (LFR) is similar to the parabolic trough concentrator but utilises downward facing receiver which receive sunlight radiation from focal point of the reflectors. Typical Fresnel systems use 10–20 discrete, lengthy reflecting segments instead of a single trough collector, as shown in Figure. These large, flat mirrors may be turned along their long axes, which are oriented north–south, like a parabolic trough, to track the Sun through the sky. The cost of the collecting field is significantly reduced when flat mirrors are used instead of parabolic mirrors. Furthermore, unlike a parabolic trough, the collection of mirrors directing sunlight onto a single receiver can be significantly larger [18]. This type of system also allows the flat solar mirrors to remain near the ground, avoiding wind loads.

Current designs for the linear solar fresnel system heat water to produce steam at 545oF in the absorber tubes. Solar collection efficiency is lower too, with a maximum of 70%. In order to increase efficiency, Fresnel reflector plants often use direct steam heat collection systems instead of the oil heat transfer fluid to drive a turbine in a standard Rankine cycle to produce electricity, avoiding the need for a heat exchanger [19]. The steam leaves the turbine and becomes cooled to liquid state in the condenser as shown in Figure 2.5.

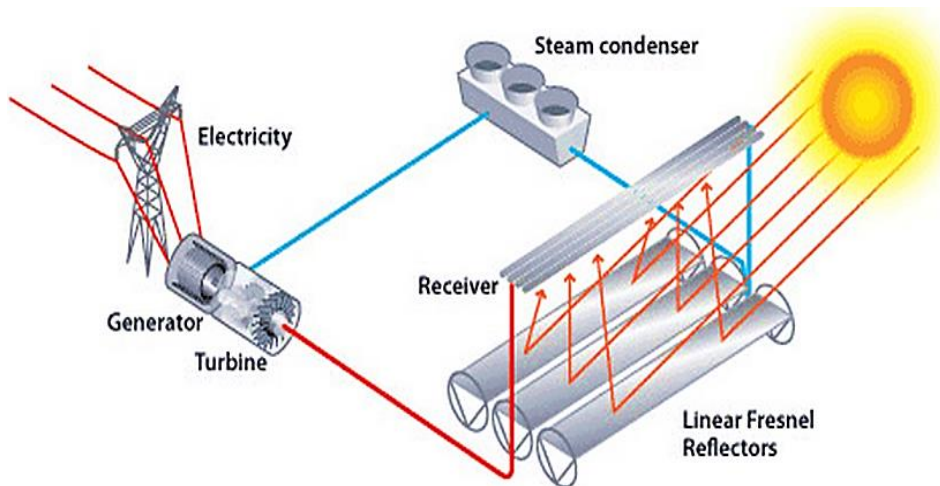


Figure 2.5: Schematic layout of Linear Fresnel Reflector system

### 2.3.3 Solar tower:

A solar tower (ST) is a type of solar furnace where usually hundreds of giant mirrors reflectors with two-axis sun tracking, called heliostats are used to concentrate the sun rays on a central receiver at the top of tower. Solar tower has a higher thermal conversion efficiency, greater power conversion efficiency and higher operating temperature than the line focus concentrate technologies due to the mechanism of two-axis tracking [20,21]. The temperature at the receiver can be up to  $1200^{\circ}\text{C}$ . The heat-transfer medium in this central receiver absorbs the highly concentrated radiation reflected by the heliostats and converts it to thermal energy to be used for the subsequent generation of superheated steam for turbine operation [22]. However, a major challenge in solar tower plant is the intermittency of the Sun's availability due to weather, and other issues include the mismatch in energy production and utilization, which has adverse effects on the overall efficiency of the system. This mismatch can be effectively damped by introducing an energy thermal storage unit that will store the surplus energy by renewable means or the off-peak electricity by all types of resources. The stored energy can be used in case of non-

availability of renewable sources [23]. As it can be seen in Figure (2.6) presents a schematic view of the solar power plant.

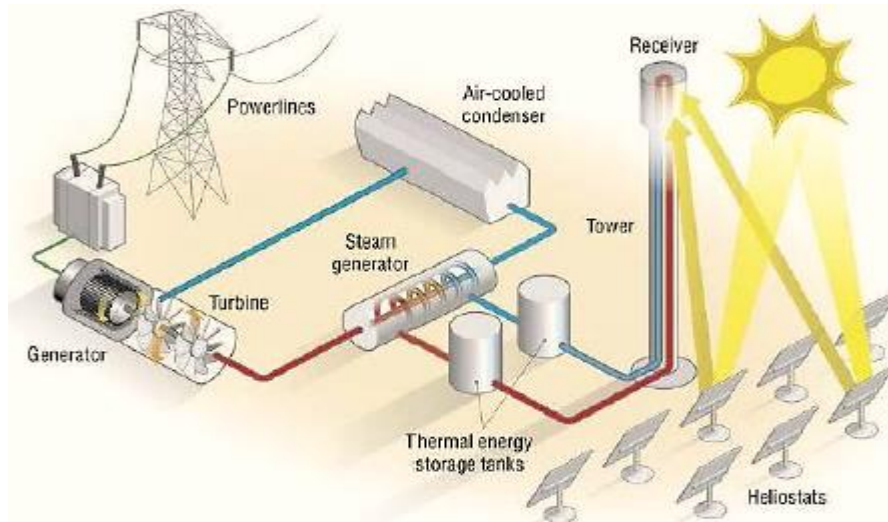


Figure 2.6: Solar tower technology system

#### 2.3.4 Parabolic dish concentrators:

It is used to focus solar radiation onto a focal point of the receiver which generate the heat at the receiver. The thermal heat is used to power an independent generator such as Stirling machines. The temperature can be reached up to 750 °C depending on the type of thermal property of heat transfer [24,25].

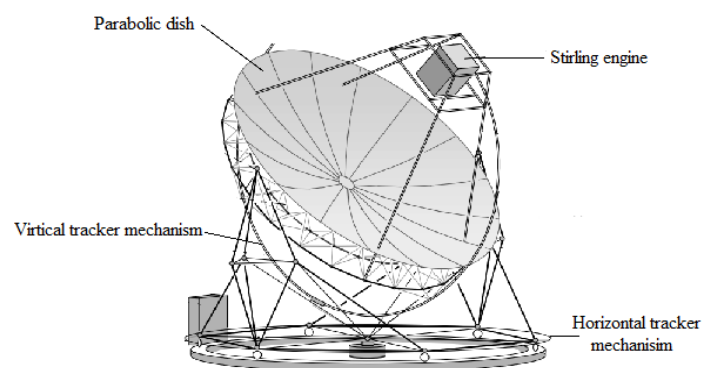


Figure 2.7: Parabolic dish concentrators with Stirling engine

Parabolic dish concentrators systems are characterized by high efficiency, autonomous operation, modularity, and an inherent hybrid capability (the ability to operate on either solar energy or a fossil fuel, or both). A number of thermodynamic cycles and working fluids have been considered for dish/engine systems. These include Brayton cycles, both open and closed cycles; Rankine cycles, using water or an organic working fluid; and Stirling cycles. Among these, Stirling engines have been mainly used and developed in the US and Europe [26,27]. The Parabolic dish concentrators systems seem potential to become one of the least expensive sources of renewable energy due to their high solar-to-electric conversion efficiency (29.4% reported in 1984, and a new record of 31.25% in 2007[28]). However, Parabolic dish concentrators systems are quite heavy with very high costs. Also, because of the high pressure (>20 MPa) and high temperature (>700 °C), the engine are expensive to make[29].

## **2.4 Summary:**

In this chapter, different technologies of small scale solar power plants are reviewed to understand their operating principles, with more focus on solar thermal plants. Also, the chapter gives a review of recent studies of development, design and performance of solar Stirling engine technology in order to assist and improve the performance and design of solar power Stirling engine (SPSE) in this project. The application of power generation and irrigation system in solar Stirling engine are investigated. It is found also, thermal efficiency of solar Stirling engine specifically working at high pressure and high temperature is affected some factors such as air leakage, heat losses and damping losses. However, in this research a flexible bellow is proposed to be incorporated into a simple design of solar free piston Stirling engine operating at low pressure, low temperature and low frequency working by

solar simulator. Furthermore, most research focused on the design of dish-Stirling system in the field of solar energy. A proper design of solar collector can increase the efficiency of the Stirling engine. Therefore, in this research a solar simulator will be designed and utilised as a heat source to operate the engine instead of burning fuel.

# Chapter 3:

## Review of Stirling Engine Technology

### 3.1 Brief overview:

The Stirling engine was invented by Reverend Robert Stirling in 1816 who is a Minister in the Church of Scotland as it can be seen in Figure (3.1) Robert Stirling and his brother James introduced two inventions, the hot air engine and the thermal regenerator (economiser) [58]. Being the first for patent, thereafter the cycle identified as Stirling cycle. During his life, Stirling continued to develop the design of closed cycle regenerative with external combustion. In the late 1930's, Philips started working on Stirling machines in order to develop the efficiency, speed and power density of Stirling machines. Philips considered the importance of working and processing on large Stirling engines. He switched to lighter working fluid such as helium and hydrogen to permit high power density and high speed.

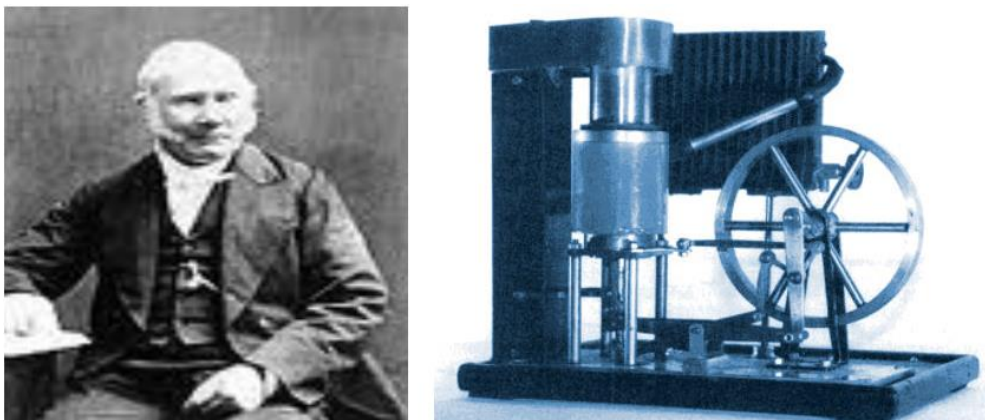


Figure 3.1: Reverend Robert Stirling and his engine [59]

On the other hand, there were outstanding contributions made by other acting independently of Philips. Most notable is the work of William Beale. The work of Philips became interested by Beale in the early 1960's [60]. He studied the mechanical movement of Stirling engine and concluded that the kinematic linkage coupling the crankshaft and reciprocating displacer and pistons could be neglected. Therefore, the Free Piston Stirling Engine was invented. Beale established the company Sunpower Inc, Ohio and became successful in developing the free piston system. In 1970's, The Japanese Government Ministry of International Trade funded a project on four engines from 3kw to 30kw. The fuel used as natural gas fired and the system were intended to be used as drivers for heat pumps and cogeneration. The technology of solar-powered Stirling engine began in 1978 USA, where engineers at Ford Motor Company developed designs of solar-powered Stirling engine. In 1996, the system of Stirling energy in USA has worked on this technology and bring Sun Catcher to the market which is 25kW solar dish Stirling system that is designed to automatically track the sun due to collect and focus solar energy on to a power conversion unit, which generates electricity [61].

Stirling machines defined as a form of heat engine utilising expansion and compression at different temperatures of a gaseous working fluid for their operation. The Stirling engine contain a novel component called thermal regenerator which is a form of heat exchanger acting as a thermodynamic sponge reciprocally accepting and rejecting heat to and from the working fluid. This improves in recycling a large fraction of the energy flow from one cycle to the next. Stirling engines present high thermal efficiency between hot and cold temperature limits due to the regenerator [62]. Stirling machines might be used as a heat pump or refrigerator, rising heat from a low temperature source and rejecting it at a high temperature with work input. They

may also be used as a prime mover taking heat from a high temperature source, then converting some of the heat to work and rejecting heat at a lower temperature [63].

In Stirling engine, the working fluid of air or other gas in Stirling cycle undergoes an expansion and compression at different level temperature which converting the thermal energy into mechanical energy [58]. There are many applications of Stirling engine that has found during the past and now, for instance, combined heat power, marine vessels, cryogenic cooling, and power units in space missions. Moreover, the advantages of Stirling engine that flexible to operate on a wide range of heat sources and requiring little maintenance. In addition, the operation of Stirling engine generate low vibration and silence of operation. The overall efficiency can be very high, due to function of the temperature of hot and cold sources. However, the main limitations of Stirling engine that have slow thermal response to the load variation and low power comparing to weight ratio [64].

### **3.2 Operation principle of Stirling engine:**

The basic concept of the Stirling engine is a simple one and the operation is similar to the other of heat engines. The operation begins of thermal energy portion supply from a high temperature of heat source which converted to mechanical energy and the remaining waste heat is rejected into low temperature sink. Figure (3.2) presents the diagram of heat engine operating between two levels of temperature and producing useful work.

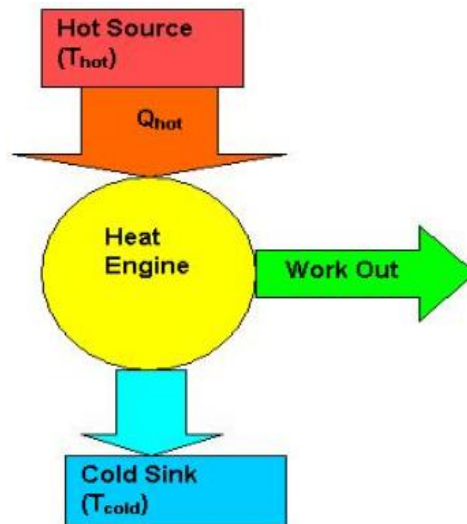


Figure 3.2: Schematic principle of heat engine

### 3.3 Main parts of Stirling engine:

The components of Stirling engine is simple, it is composed of two heat exchanger, two moving pistons and a thermal regenerator. Figure (3.3) shows the main parts of Stirling engine where it is presented that the cylinder house a power piston at the cold end, and a displacer at the hot end.

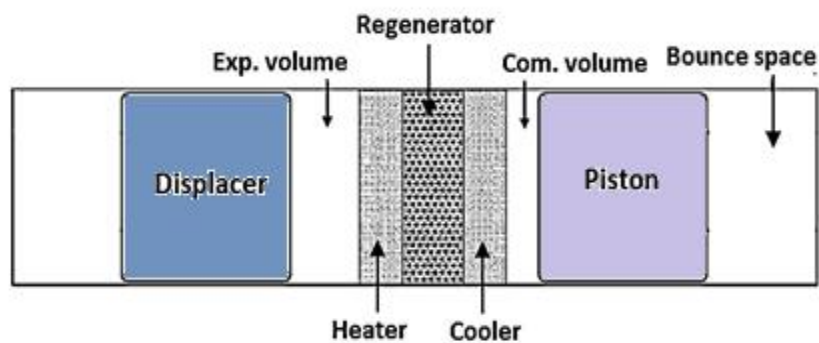


Figure 3.3: The main components of Stirling engine

The function and the process of each components are described below:

### **3.3.1 Power piston:**

The function of power piston in Stirling engine is similar to the piston of internal combustion engine. Its job to convert the engine pressure variation into a reciprocating movement which transmit power. To maintain the required pressure variation, the piston tightly sealed against the cylinder wall by the piston ring. Also, the piston rings can be made of rubber, metal or other appropriate materials. Moreover, lubricant is used between the piston rings and the cylinder wall, in order to prevent excessive friction. Utilising more lubricant will effect on regenerator to become blocked and lose effectiveness, due to the lubricant will not evaporate subsequently condense inside the regenerator [65].

### **3.3.2 Displacer:**

The displacer describes as a lightweight piston that reciprocate between the expansion and compression spaces shuttling the working fluid forth and back over the heat exchanger (heater, cooler, and regenerator). The displacer consumes a small mechanical power of the engine, because of moving the working fluid. In the regenerator, there is viscous losses of the working fluid which make a pressure difference ( $\Delta P$ ) between the displacer ends. The displacer is subjected at highest temperature from external heat source which separate the expansion space at high temperature and the compression space at low temperature [66]. Moreover, the displacer is designed and constructed in a ratio of its diameter to length (1:2.5) in order to reduce heat conduction. Utilising a seal between the cylinder wall and displacer in order to prevent passing working fluid to the heat exchanger. However, there is no need for the seal in small Stirling engines, due to the regenerator is installed in the displacer [61].

### **3.3.3 Heater:**

The heater is an essential part of Stirling engine which all heat released from external source is transferred to the enclosed working fluid in Stirling engine. Moreover, the effective design of heater depending on the kind of heat source and its temperature. The external surface of heater is exposed to the low pressure environment and high temperature while the internal surface is exposed to the high pressure of the working fluid. Therefore, the heater of Stirling engine is manufactured from expensive stainless steels. Recently, usually utilising a complex bundle of tubes that located within the combustion chamber [67].

### **3.3.4 Cooler:**

The cooler is a part of heat exchanger that operates at cold temperature, therefore the cooler can be made from cheaper materials such as aluminium or copper alloys. Once the working fluid produce work to the power piston, the heat is rejected from engine. Most Stirling engines designs have adopted the method of water cooling, where the simple air cooled fins around the compression space immersed in the bundle tubes of water cooling jacket [68].

### **3.3.5 Regenerator:**

The regenerator was invented by Robert Stirling in 1816 which was the most important aspect of his invention. Usually, the regenerator made of a matrix of metal strips or wires. The regenerator is installed in the engine to store the heat as working fluid is moving from the expansion to the compression space, which lead to obtain high performance of Stirling engine operation. Moreover, the matrix of regenerator should have high heat capacity at reasonable dimension, due to the thermal heat capacity of the regenerator material effect on its efficiency [68].

### 3.4 Stirling Cycle:

The Stirling cycle is considered as a reversible cycle in which all the processes of heat transfer are assumed to be reversible. All heat loss through viscous, friction in the regeneration process and dead volume are neglected, where the motion of displacer and power piston is discontinuous to produce the output of working fluid. As it can be seen in Figure (3.4) below, that presents PV diagram of ideal Stirling cycle and the movement of the piston and displacer. The following thermodynamic processes are explained [66].

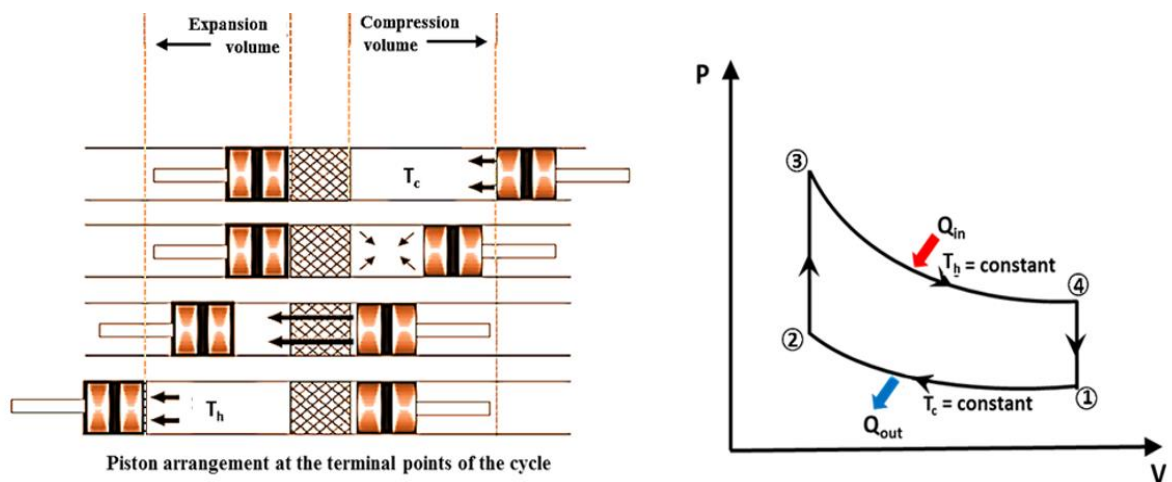


Figure 3.4: Description of each process of Ideal Stirling cycle

#### 3.4.1 Isothermal compression process at constant temperature (1-2):

Initially, all working fluid is assumed to be in the compression space at its minimum temperature ( $T_c$ ) and pressure ( $P_1$ ), however the volume ( $V_1$ ) is at the maximum. At the temperature of heat sink ( $T_c$ ), the working fluid is compressed where the heat is rejected to the surrounding. During this process, the working fluid is compressed by power piston from pressure ( $P_1$  to  $P_2$ ), while the position of displacer is at the top of cylinder.

#### **3.4.2 Regenerative process at (constant volume) heating (2-3):**

At this stage, the working fluid is moved swiftly from the compression space to the expansion space, where the temperature and pressure of working fluid increased to  $T_h$  and  $P_2$  respectively. However, the heat transferred from the regenerator to the working fluid at constant volume. Also, the displacer moves from the hot end to the cold end which displaces all the working fluid through the heat exchangers into the expansion space.

#### **3.4.3 Isothermal expansion process at constant temperature (3-4):**

The working fluid at state-3 expands isothermally in the cylinder at the maximum temperature and pressure, while also at minimum volume. During the expansion process more heat is added to the working fluid to keep the system at constant temperature. The expansion of the working fluid allowed to do useful work on the power piston.

#### **3.4.4 Regenerative process at (constant volume) cooling (4-1):**

The working fluid is compressed by moving from the expansion space to the compression space through the regenerator, which absorbs the heat and its temperature  $T_c$  decreases to the lowest point. The working fluid transfers heat to the regenerator at constant volume.

### **3.5 Real Stirling Cycle:**

As discussed above that there are many assumptions in ideal thermodynamic Stirling cycle, however most of these assumptions are not possible in real Stirling cycle, due to the motion of displacer and power piston is continuous [69]. The

continuous motion of displacer and power piston makes the boundaries of each thermodynamic Stirling processes not clearly classified and represented by a smooth elliptical shape diagram as presented in Figure (3.5).

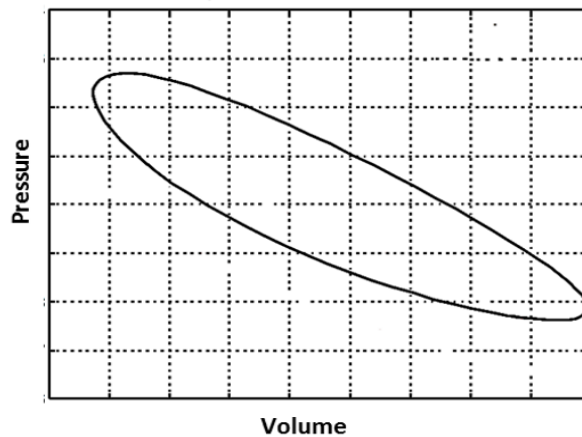


Figure 3.5: Real Stirling cycle in P-V diagram

The processes of expansion and compression do not take place wholly in one diagram, therefore the real Stirling P-V diagram can be drawn in three diagrams, one for the expansion space, one for the compression space and one for the total enclosed volume, which includes the dead space, see Figure (3.6).

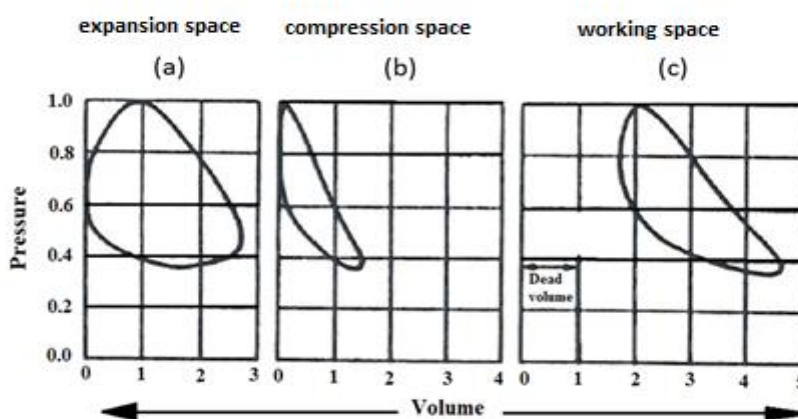


Figure 3.6: P-V diagrams for practical Stirling engine

As it can be seen in the above figure that (a) presents the expansion space diagram, (b) shows the compression space diagram and (c) presents total working-space. The definition of dead space is the part of the working space that not swept by one of the pistons, and include void volumes of the regenerator and other heat exchangers. Moreover, as shown in Figure 3.5, the P-V diagram for the expansion space represents the gross work of the cycle is done at high temperature, whereas the compression space diagram represents the work of the output is done at low temperature. Therefore, the variation in these areas diagram is the net cycle output that providing useful power to the engine [70].

### **3.6 Stirling engine Classification:**

There are several configurations of Stirling engine that have different purposes and operation which also classified into four essential configuration: Alpha type, Beta, Gamma and Free piston. All these configurations have approximately same working space which based on gas expansion and thermodynamic laws at higher temperature.

#### **3.6.1 Alpha Type:**

The alpha type uses two power pistons and no displacer that mounted in series cylinder with a heater, cooler and regenerator. The cylinder contains two spaces, the compression space (cold cylinder) and expansion space (hot cylinder), as it is shown in Figure (3.7). The alpha engine has several problems related to the sealing, due to movement of the piston at expansion space under high temperature.

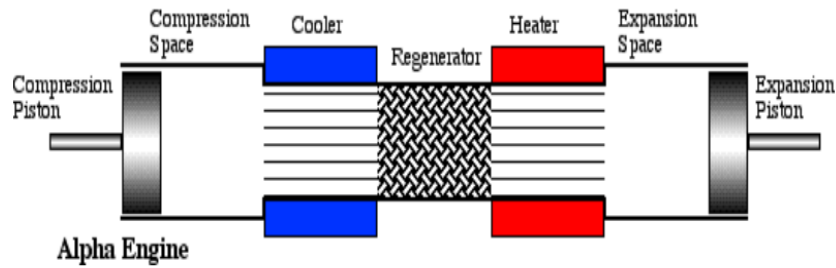


Figure 3.7: The diagram of Alpha Stirling engine [64]

### 3.6.2 Beta Type:

Beta engine is formed with the piston and the displacer are placed in the same cylinder as shown in Figure (3.8). The displacer is moveable part which shuttle the working gas from hot heat exchanger (expansion space) to the cold heat exchanger (compression space) and does not extract any power. The advantages of Beta design that higher power, compression and efficiency can be obtained due to lower dead volume [71].

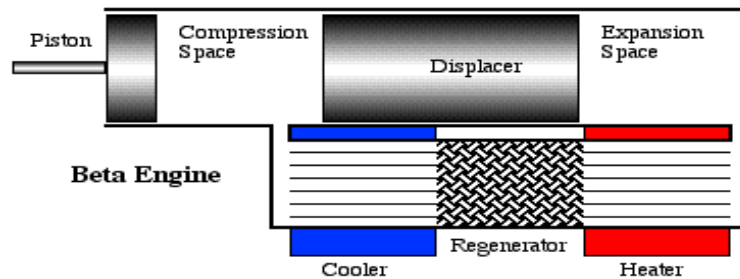


Figure 3.8: The diagram of Beta Stirling engine [72]

### 3.6.3 Gama Type:

A gamma Stirling is similar to Beta type, in which the displacer and the power piston attached in a separate cylinder as shown in Figure (3.9). This configuration has lower compression ratio, however is mechanically simpler and commonly used in multi-cylinder Stirling engines. Also, Gamma type is mechanically more efficient than

other types. However, it contains higher dead volumes particularly in connecting pipe which connect the lower part of the expansion to the compression [71].

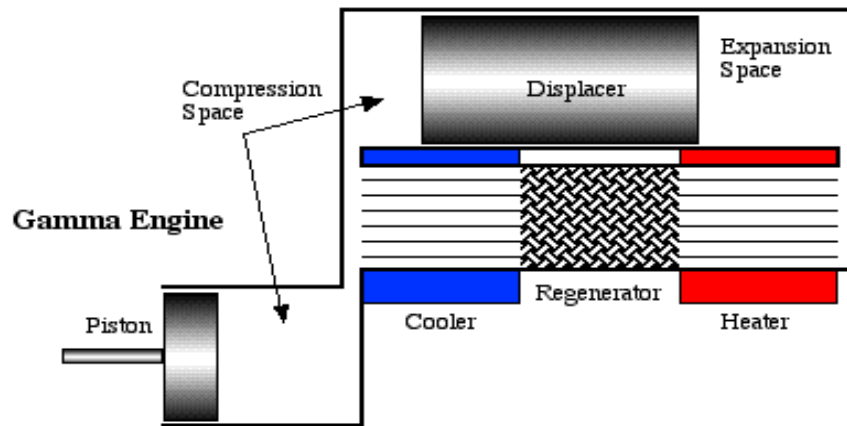


Figure 3.9: The diagram of Gamma Stirling engine [72]

### 3.7 Free Piston Stirling Engine (FPSE):

The free-piston Stirling engine was invented by William Beale in 1964 which is defined as a dynamic resonant system operating at almost constant frequency. The FPSE technology based on the Beta type of Stirling engine that was developed to mitigate the problems of technical barrier leakage. In addition, FPSE configuration is expected to be as a simple and unique mechanical arrangement in which the mechanical contact, wear and friction are eliminated. FPSE utilise working gas such as gas spring in order to provide a sufficient movement to the various components of the engine (displacer and power piston) [73].

The main advantages of FPSE are known as a simpler mechanical design and there is no lateral loads that minimise wear and a following extended lifetime in comparison with classical Stirling engines. Free piston Stirling engine contributed in development of space mission applications such as radioisotope generator [74], as shown in Figure (3.10).

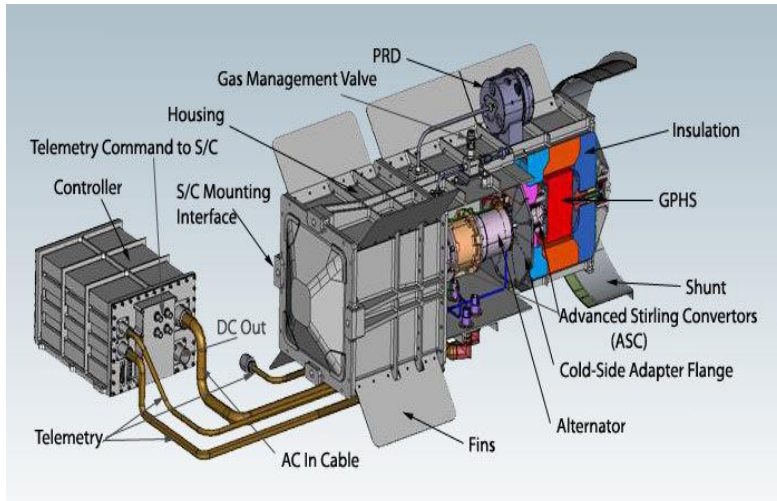


Figure 3.10: Advanced Stirling Radioisotope Generator [75]

In spite its advantages, the optimisation and development of FPSE is a difficult task because of several practical difficulties. The phase angle and stroke are both set up and affected by thermodynamic and dynamic parameters. Moving parts of FPSE are driven by both gas springs pressures and working fluid. Moreover, the volume of pressure and pressure losses through heat exchanger are modified by the displacement of displacer and piston [76].

It can be considered that free piston Stirling engine contains essential three components, a lightweight displacer, a heavy piston and a cylinder sealed at the top end as shown in Figure (3.11). The shaft of displacer passes through the piston. The displacer rod and displacer are hollow from inside and they can be open at the lower end, so in this case their interior is part of the bounce space [77]. The working space represented by the compression space below the displacer and the expansion space above the displacer. The regenerator is an important component in FPSE which install between displacer and cylinder wall and this serves as the regenerative heat exchanger to improve the performance of the engine

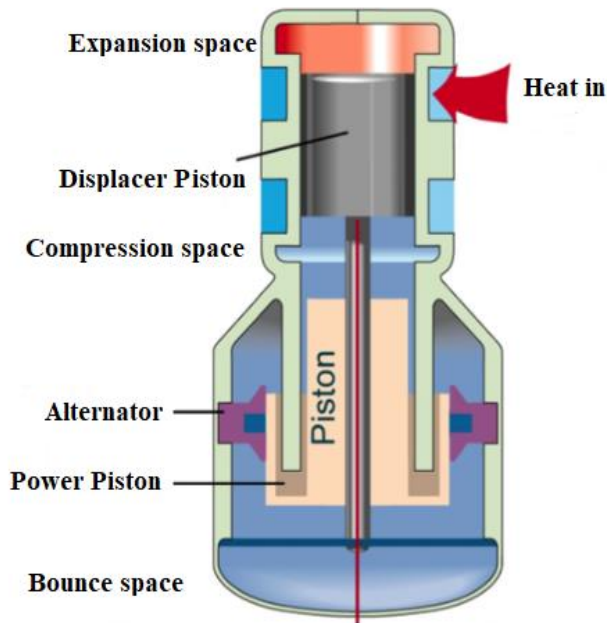


Figure 3.11: The main components of FPSE [78]

### 3.8 Classification and types of (FPSE):

The free piston Stirling engine has many types and arrangements and the principle components of each type is similar to the another which have at least one oscillating component driven by fluid pressure forces.

#### 3.8.1 Single acting (FPSE):

The displacer and the piston are located in one cylinder which involves three difference masses of the components, however, commonly one of these masses is large which considered as infinite mass in comparison with other two [73]. Usually, the mass of the cylinder is the large one, hence, the cylinder mass assumed to be a rigid part and only mass of the piston and the displacer are considered in the dynamic analysis (two mass system analysis). The design of three-mass is commonly utilised in water pump system where the cylinder oscillates to move the plunger, then reciprocating water pump.

There are different types of mechanical springs that are used in free-piston Stirling engines, hence the design of FPSE depends on the way the displacer is driven. The design can be divided into three main groups [73], as shown in Figure (3.12). The first design (a) is the displacer sprung to the piston, where the piston and the displacer can be connected by a mechanical spring. The second design (b) is the displacer sprung to the ground where the dynamic forces of the displacer are separated from other forces acting on the power piston. The third one (c) in this case, the power piston and the displacer are sprung to the common ground.

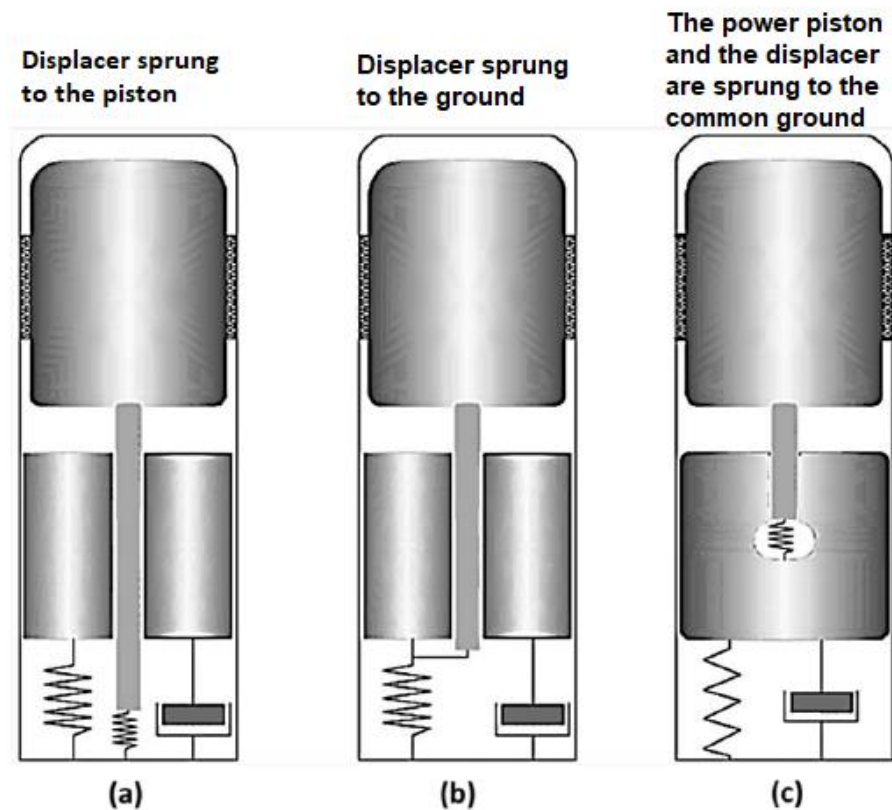


Figure 3.12: The movement of displacer and power piston with mechanical spring

### 3.9 Diaphragm free-piston Stirling machine:

There are several difficulties and disadvantages of Free-piston Stirling engine such as friction and wear in the moving components and gas leakage between the compression and expansion spaces. The first heat engine in diaphragm design that operating on the Stirling thermodynamic cycle was invented by Cooke-Yarborough in 1967. He installed a metal diaphragm oscillating instead of the piston at high frequencies from 50 to 140 Hz in order to reduce and evaluate the difficulties of friction and wear [73]. The idea of utilising metal diaphragm in FPSE cryocooler is to avoid sealants and make the displacer to oscillate without moving seals or rubbing, hence improving the mechanism life span and increase thermal efficiency. As it can

be seen in Figure (3.13) shows a flexible diaphragm that proposed to replace the power piston.

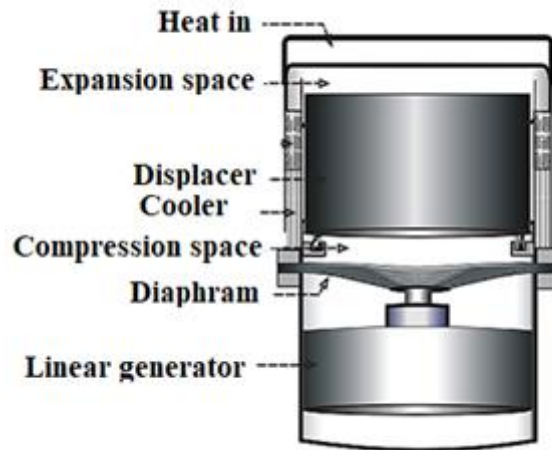


Figure 3.13: Diaphragm free-piston Stirling engine [127]

### 3.10 Solar Stirling engine:

In 1908, Hooper and Reader started to develop a solar Stirling engine. Recently in 1987, Meijer invented the design of Stirling cycle heat engine operating with a dish concentrator in order to generate electricity [30]. Among many types of solar-based technology, the systems of solar Stirling engine have been accounted to have the highest efficiency of solar electrical conversion. The system of solar dish Stirling system consists of a Stirling engine, a power generator and a parabolic collector arrangement, as it can be seen in Figure (3.14). There are two main components of the collector system: a thermal receiver and a solar concentrator. The purpose of the collector system is to runs the Stirling engine by delivering thermal energy.

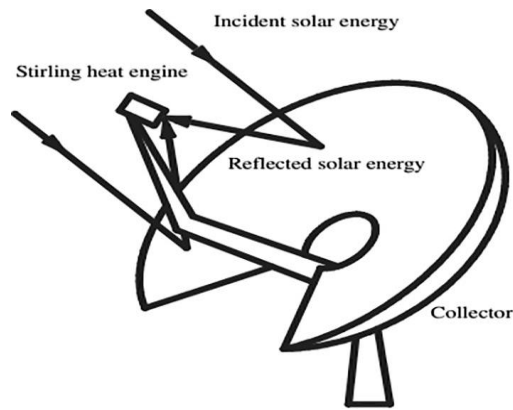


Figure 3.14: Schematic representation of dish Stirling engine

The design of parabolic dish is utilised to focus solar radiation on the receiver's aperture. The receiver consists of an absorber and aperture which occur mechanical energy in the Stirling engine and eventually electricity is generated [31]. In USA 2010, solar dish-Stirling technology power plant was commenced to operate the first large capacity (1.5 MW), [32]. Recently, most of the research is primarily focused on the performance enhancement, modelling and simulation of solar Stirling engines. Nowadays, the design of dish-Stirling system is the research hotspot in the field of solar energy [31].

### **3.11 Design, development and performance evaluation of Solar Stirling engine:**

In this section, the review of recent and last advances in the performance and development of the solar Stirling engine is presented. Moreover, several research papers related to the design, modelling, simulation and optimization studies are discussed.

Beltran et al. [33] developed a mathematical model and a case study that represents the optical operation of a solar parabolic dish concentrator with cavity receiver for a Stirling engine. The main focus was on the optimization and design of the thermal

performance of parabolic dish collectors. It is also considered the analysis of the radiation losses in the receiver. In addition, graphical process for design obtained to utilise the results generated by the simulator. Ferreira et al. [34] also proposed a mathematical model to study and design of a solar dish collector. The main aim of the study was to reduce the cost of dish collector and figure out the availability of amount heat to the Stirling engine. The researchers obtained the optimal results for a solar collector dish with a dish diameter of 6.58 m and a rim angle of about 41 C° and an aperture receiver of 0.12 m for an optimal cost of 4717 €. Moreover, the researchers considered the possibility of obtain an ideal thermodynamic efficiency of 64%.

On the other hand, Srinivas et al. [35] investigated the heat transfer and thermodynamic analysis of solar Stirling engine for five variable working fluids under specific conditions to select the suitable working fluid for the Stirling engine. It was considered that helium has been selected as the optimal working gas to develop the performance characteristics. In addition, the impact of maximum engine pressure, receiver gas temperature and concentration ratio on output power and efficiency also investigated. The specific output power and overall efficiency were estimated as 2.7 kw/litter of helium and 10% respectively at 540 W/m<sup>2</sup> of solar direct normal irradiation.

Shendage et al. [36] performed a second order analysis for a Beta configuration Stirling engine. The researchers focused to provide the optimal operating temperature range to obtain the maximum efficiency. The analysis presents that the system have an overall efficiency of 25% in the optimum temperature range of 750 – 1000 K. Sookramoon et al. [37] developed a parabolic dish-Stirling engine with two axis sun tracking system as shown in Figure (3.15). It is found that the maximum

concentrator efficiency was around 26%, it is also recommended that the efficiency can be increased by the following: increase the aperture area to add more heat input, increase the hot end of the engine and increase the cooling by adding more fins, redesign the shape of sub dish and study the heat loss from the receiver such as radiation and convection loss.



Figure 3.15. 2-stage parabolic dish-Stirling engine

### 3.12 Parabolic Dish Technology:

The design of parabolic dish has several essential components, described here as the reflector, tracking system, support structure, foundation, receiver support and receiver. The structure of reflector must maintain structural integrity and optical accuracy under gravitational loads and wind while in various orientations. During the operation, the reflector also has to be rotated about two-axes to focus point directly towards the sun always [38].

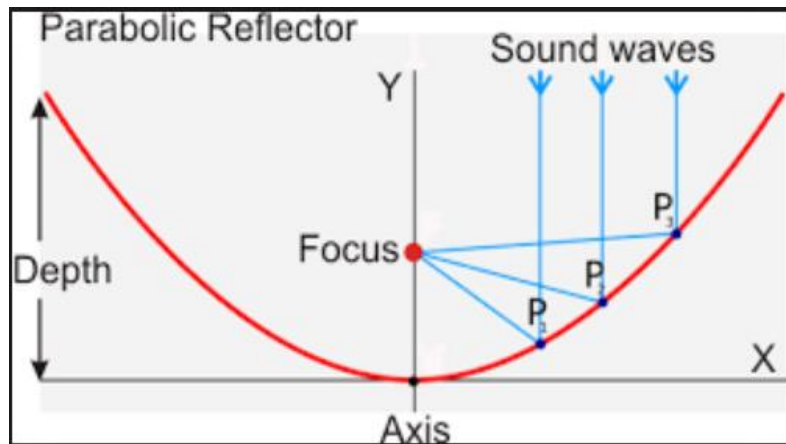


Figure 3.16: The operation of parabolic reflector with sun radiation

Vanguard dish system contains up to 336 mirror facets mounted on a truss structure and rack as it can be seen in Figure (3.17,a). The design of mirror facets are constructed of thin glass mirrors and the tracking system has a standard azimuth rotation system. The MDAC dish designed of 82 mirror facets to provide 459 an aperture area of about 88 m<sup>2</sup> as shown in Figure (3.17,b), [39]. On the other hand, the design Stirling energy systems (SES) provides a new and better performance of 31.25% of net efficiency, the reflector structure has a significantly modified by using stamped steel mirror construction with a thin glass reflective surface as shown in Figure (3.17,c). Moreover, Ripasso dish design tested in 2012 and gives an electric net efficiency of 32% on a 28 °C day with Stirling engine. The mirror facets are made up of a glass mirror bonded to a reinforced plastic composite as shown in Figure (3.17,d), [38,40].



(a)



(b)



(c)



(d)

Figure 3.17: (a) The Vanguard dish, (b) MDAC dish, (c) SES SunCatcher dish, (d) Rispasso dish

Therefore, table (3.1) below describes the optimised solar to electric efficiency for dish-Stirling systems.

Table 3.1: Best reported dish-Stirling systems

Dish system	Original Stirling engine	Gross efficiency (at generator)	Net efficiency	Year
Vanguard	USAB 4-95	31.6%	29.4%	1984
MDAC	USAB 4-95	31.4%	30.0%	1985
SES MPP	USAB 4-95	-	31.25%	2008
Ripasso	USAB 4-95	-	32%	2011

Moreover, the steps for designing parabolic solar dish can be seen in Figure (3.18), [41]:

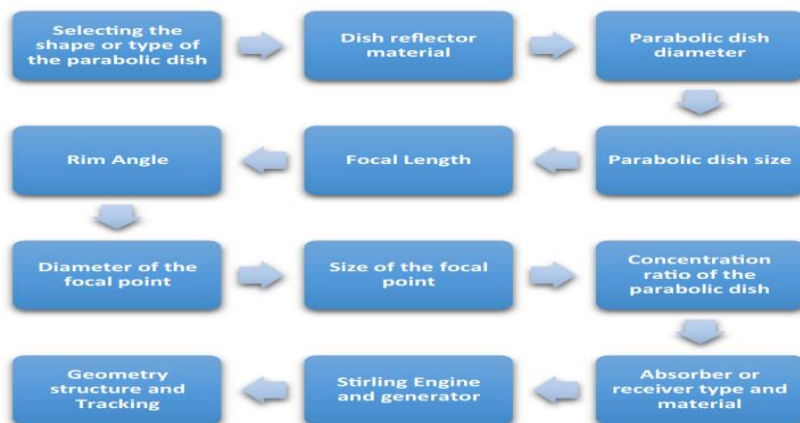


Figure 3.18: Steps for designing parabolic solar dish

### 3.13 Dish mounted storage and Hybridisation:

Recently, the combination of thermal energy storage or hybridization with the solar dish-Stirling engine has become popularity in the research arena. As it can be seen in Figure (3.19), thermal storage units and engine are installed at the back of the

parabolic dish in order to optimise the structure design. The thermal storage system reduce the dependency of solar energy source and more continuous working of the system. Moreover, the researchers found that thermal storage system for parabolic dish-Stirling engine can achieve a significant reduction in levelized cost of energy (LCOE), [42].

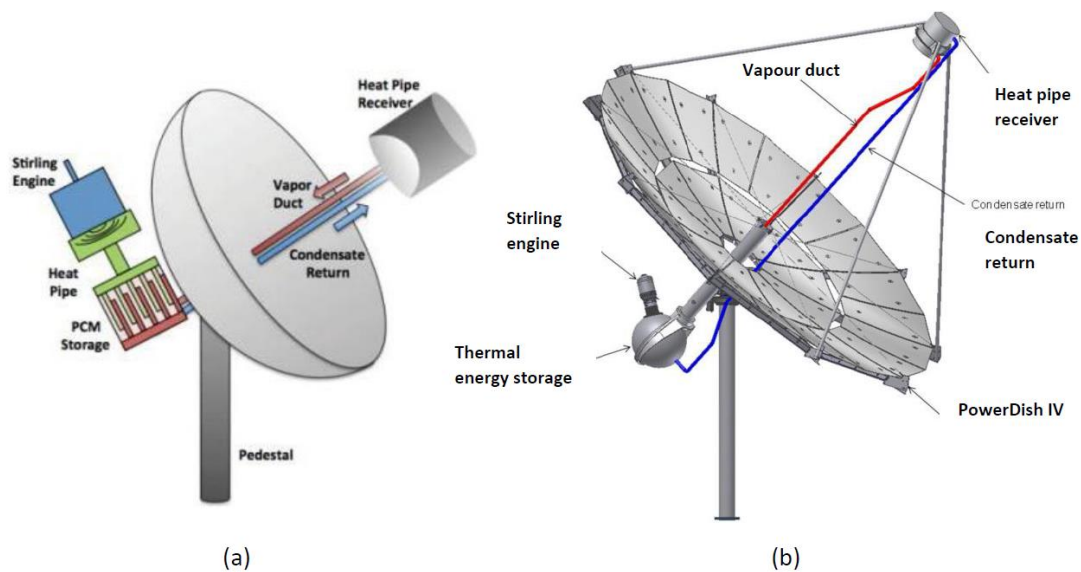


Figure 3.19: Thermal storage system based dish-Stirling power generation

### 3.14 The Receiver:

The receiver is an essential part in the system of dish-Stirling. It contains the aperture that receive the solar radiations delivered by the dish and the absorber that converts the thermal energy to the working fluid in the Stirling engine. Recently, the receiver has been developed in many researchers in order to make the optimum design. In this section, a review of recent progress, development and design of receiver system is presented.

Nowadays, the design of receiver that contains heat pipe receivers are quite commonly and utilised a mixture of potassium and sodium for heat transfer process within the receiver [42]. The design of cavity receivers are utilised mostly in dish-Stirling systems, where the aperture receives the solar radiations. After that the absorber converts the solar energy into heat energy and transfer to the working fluid in Stirling engine. The range of the temperature in this process are higher (973 – 1073 K), [43]. Garrido et al. investigated a study of radiation analysis in the receiver by considering the effect of re-reflection and re-radiation in order to obtain the efficiency and the lifespan. Three different cavity shapes were studied and performed, reverse-conical, diamond-shaped and cylindrical. It was found that the reverse-conical cavity design can obtain the optimum radiation efficiency with lowest radiation losses [43].

On the other hand, the performance of receiver that using hot chamber installed with the absorber is more efficient than the absorber with no hot chamber [44]. Moreover, it is found that a high receiver absorptivity and short aperture radius make the receiver cavity become much more efficient [45].

### **3.15 Applications of Solar Stirling engine:**

There are several applications of solar Stirling engine system. Recent works and development that related to the application of power generation and water pumping are reviewed in this section.

#### **3.15.1 Solar Stirling electric power generation system:**

Castellanos et al. presented a methodology to calculate the appropriate characterize and angles of the solar tracking control system. Mathematical analysis was performed in order to obtain the maximum temperature and the thermal efficiency of

the solar Stirling system. The maximum working temperature in the receiver was found 1596 K, and the thermodynamic efficiency of the receiver also was obtained between 84% and 88%, [46]. On the other hand, Yang et al. introduced a new design of cylindrical linear magnetic gear composite generator that can increase the drive speed of the generator mover and boost the overall efficiency of the solar dish-Stirling system [47].

Mendoza et al. [48] validated experimental results of the dish Stirling system generates power of 1.00 KW with mathematical model as shown in Figure (3.20) that present the thermal balance of the system. The experimental results showed that the overall efficiency is about 21% in comparison with the mathematical model of 24%. The maximum values of deviation reached to 12%, which are caused by errors in the adjustments of the non-measurable parameters and the inaccuracies in the measures.

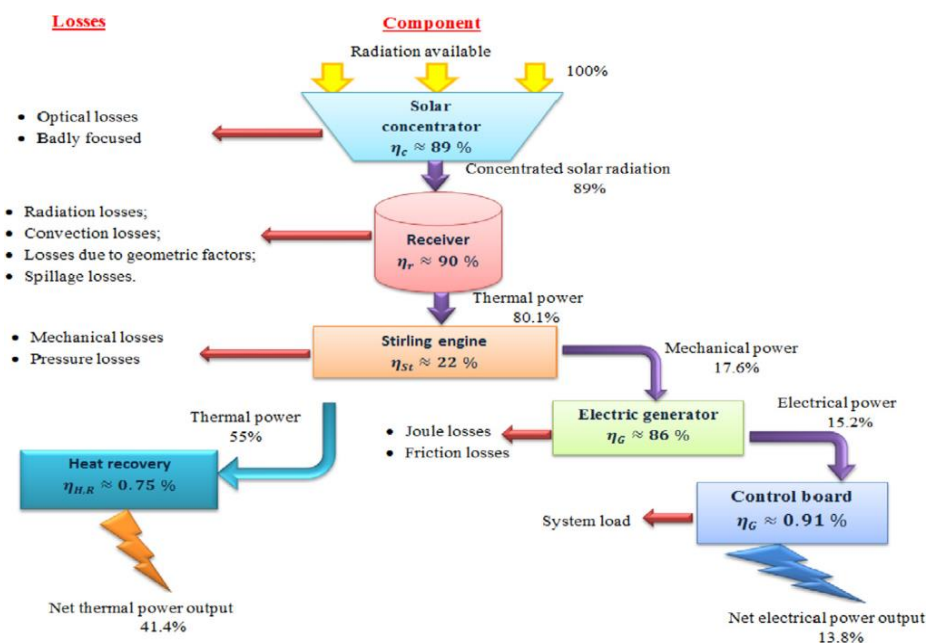


Figure 3.20: Diagram of the thermal balance in the system

### **3.15.2 Solar Stirling power plants:**

The company called Infinia Corporation has built the first concentrating solar power (CSP) systems in 1.5 MW capacity provided to US army in Utah state, USA. The CSP plant consists of 429 Infinia Dish power system based on dish-Stirling CSP technology [49]. Abbas et al. investigated the economic and technical analysis of 100MW dish-Stirling using hydrogen as working fluid and based on solar thermal power plant for electricity generation. Moreover, the plant was evaluated and tested for several different locations in Sahara of Algeria country. It was observed that the operation of the plant in desert region decreases the economic performance, whereas the annual electric energy output increased [50]. Another study is carried out by Bakos and Antoniadis investigated the possibility to install 10MW dish-Stirling power plant in Greece. The performance of the plant was obtained by carrying out simulation study and a concentrating solar system was proposed that contains the first mirror in order to concentrate the sun rays on the secondary mirror which deliver the solar radiation into the receiver system. The study concluded with output power generation 11.19 GWh annual energy that could be generated from the dish-Stirling system. Furthermore, the economics of the project was performed [51].

### **3.15.3 Solar Stirling of irrigation system:**

The research on solar thermal technology for water pumping are minimal, there is quite few data available on the feasibility of irrigation technology. Rankine cycle systems are the most common technology that used for thermal power generation utilised for irrigation, however the system can only be used for large scale [52]. Therefore, recently developed studies focused more on solar Stirling engine technology utilising for pumping water. These systems are compact and easy to manufacture, however, the output power is low. The investigation of Stirling cycle

system mostly focused to reduce the cost, therefore the research deeply investigated on low and medium power solar collection temperatures with a difference of 60-95 °C. The output power of Stirling engine can be increased with higher temperatures. Wazed et al. reviews the drip irrigation method which the liquid piston pumps water directly to storage tank which is then irrigate field using the drip irrigation method [53]. The company from Germany SUNORBIT that innovate the system of concentrate solar capable to produce up to 1500 W, 10m head, and 80,000 L/day known as the SUNPULSE. See Figure (3.21). This system utilises a dish concentrator with a storage of heat powering a gamma type Stirling engine. The system is estimated to cost 2500 \$, and tested across Europe, Asia, Africa and Australia.



Figure 3.21: SUNPULSE Stirling System [45]

In another research study, Saini, et al [54] proposed a new design of solar Stirling engine of water pump. The idea of project was the way of driving the centrifugal pump and parabolic mirror is used to concentrate the solar radiation onto the Stirling engine, as shown in Figure (3.22). The author concluded that this design is the most

economical and efficient way of driving the centrifugal pump. Bumataria and Patel [55] reviewed applications of the solar Stirling engine for water pumping in remote areas. It is found that the theoretically designed of the engine will provide efficiency of about 52% to 72%. Moreover, the speed of the engine should be designed as the speed of centrifugal pump available in the market.

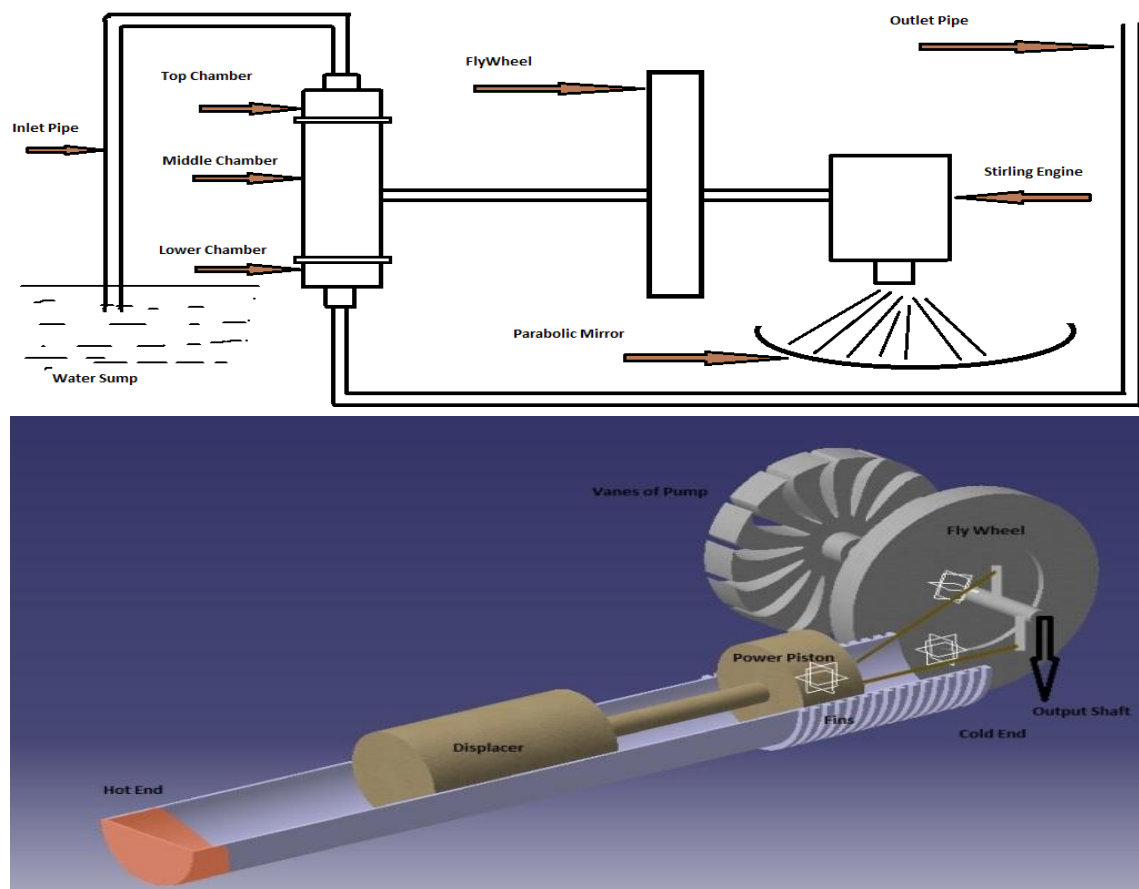


Figure 3.22: Block diagram of the solar Stirling system with centrifugal pump

In another research, Gadelkareem et al. [56] proposed a design of cold and hot drinking water dispenser operating on the heat rejected from the Stirling cycle. The mathematical model was formulated based on Schmidt analysis to evaluate the performance of the machine. The commercial advantage of this proposed is that it can produce hot water up to 95°C without using heating elements, which consume more electricity. It is also suggested that the Stirling heat pump/refrigerator can be

fabricated according to the optimised result obtained from mathematical model. Al-Dafaie et al. [57] proposed an idea of utilising rejected heat from solar Stirling engines for water distillation as shown in Figure (3.23) where the heat rejected from the cold chamber in the engine is utilised to evaporate water, and then condensing it on a cold surface. A simple analysis is carried out to present the economic advantages of utilising rejected heat from the engine for water distillation. The author recommended to consider more for design of the condenser system.

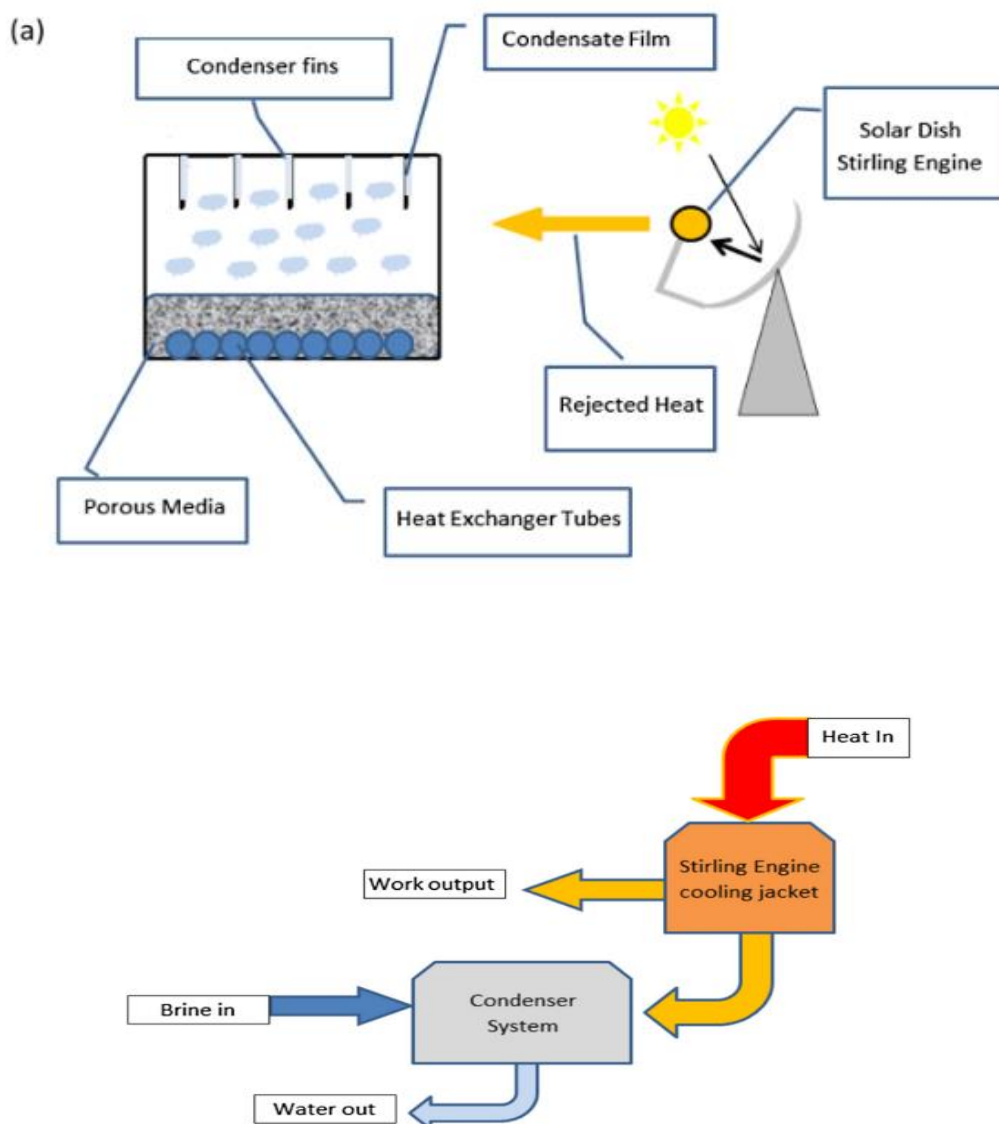


Figure 3.23: Schematic diagram of utilising heat rejected from Stirling engine

### 3.16 Mathematical models of Stirling engine cycle:

The behaviour and the operation of Stirling engine demand to understand the thermodynamic process of the energy flow and the principle of dynamic interaction of moving parts. The energy supplied from extract heat source, in order to make the variation of the working pressure and volume. The analysis of mathematical models and computer simulation use variable parameters such as thermal efficiency, heat energy inputs and power output to approximate the preliminary design factors and predict the operating parameters [79]. In this section, the accuracy and complexity mathematical modelling of the zero order, first order, second order and third order of Stirling engines are presented. Furthermore, this chapter provides a critical review of the recent studies on these modelling with focus on the most common analysis that provide the optimum design and performance of Stirling engine.

### 3.17 Zero dimensional model:

The zero dimensional model is the simplest model and empirical method to modelling the Stirling engine rather than the mathematical model. William Beale proposed the zero analysis of the Stirling engine as a result of processing many experimental of statistical data. The principle of zero modelling requires and focuses on more experimental observation other than the specific mathematical method [80].

The below empirical equation can calculate the power output of the Stirling engine:

$$W = B_n P_m f V_{sw} \quad (3.1)$$

Where  $W$  is the output power of Stirling engine in watts,  $B_n$  is referred as parameter of Beal number,  $f$  is the operation frequency in Hz,  $P_m$  is the mean cycle pressure in bar,  $V_{sw}$  is the swept volume of the power piston in  $\text{cm}^3$ . The Beal number equation is described as a function of the heat sink and heat source as:

$$B_n = 0.035 \frac{T_h - T_c}{T_h + T_c} \quad (3.2)$$

Where  $T_c$  is the cold temperature at the compression space and  $T_h$  is the hot temperature at the compression space in Kelvin unit. In addition, the relationship between the Beale number and temperature ratio is presented in Figure (3.24), which can be used to determine the output power of Stirling engine and the design [81].

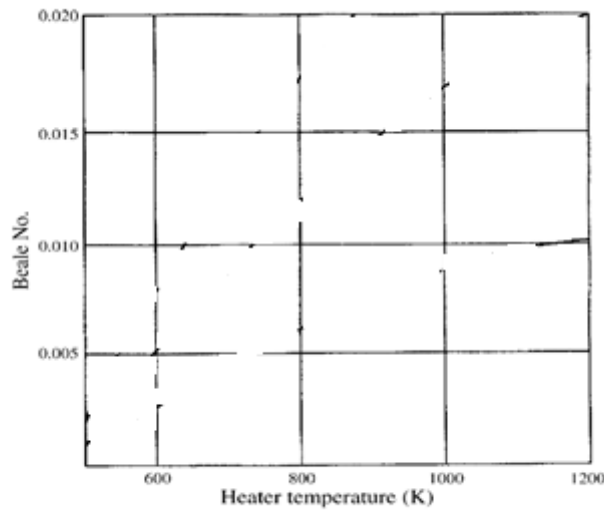


Figure 3.24: Beale number as a function of heater temperature [70]

Moreover, Walker, Senft, and West improved the Beale number correlation which used to determine the Stirling engine shaft power output, the equation expressed as follows:

$$P = p_m V_p f F \left[ \frac{1 - \tau}{1 + \tau} \right] \quad (3.3)$$

Where,  $P$  is the power output of the Stirling engine in Watt,  $\tau$  is the working fluid temperature ratio,  $V_p$  is the displacement of power piston in  $m^3$ ,  $f$  is the cycle frequency in Hz and  $P_m$  is mean cycle pressure in  $N/m^2$ . In the ideal cycle, the factor  $F$  does not consider into account the friction,  $m \eta$  loss etc. the value of  $F$  that may be

used in practical is 0.25 to 0.35 [81]. In another estimation of Zeroth analysis, the power output of the Stirling engine can be calculated by added the heat input values of heat source as follows [81]:

$$P = \eta_H \eta_{mech} \eta_{thermo} E_c Q_{in}$$

Where,  $Q_{in}$  is the heat input,  $\eta_H$ ,  $\eta_{mech}$  and  $\eta_{thermo}$  are the heat source, mechanical and the thermodynamic efficiency of the Stirling engine, respectively,  $E_c$  is the Stirling engine coefficient in the range between 0.55 to 0.88.

### **3.18 First Order Model (Schmidt Analysis):**

One of the first thermodynamic models for Stirling engines that based on algebraic equations and use the energy and mass conservation to predict the performance of the engine and to estimate the relationship between the power output and the overall size of the engine [82]. In 1871, Gustav Schmidt developed the first mathematical model of ideal Stirling cycle. The Schmidt analysis is considered as the simplest model of the Stirling cycle and close to the operation of real Stirling cycle, due to it gives sinusoidal volume variation of the working spaces. The Schmidt analysis is widely used for optimising the design of the Stirling engine, in particular the design of small scale engines. The assumptions of this analysis that the temperature of the expansion space is constant and the same with heater temperature, and also the temperature of the compression space is constant and equal with cooler temperature [83]. Moreover, the Schmidt analysis depends on certain conditions and assumptions that have to be implemented and applied, the engine speed is constant, the effectiveness of the regenerator is ideal, and the working fluid, pressure losses and leakage are neglected.

On the other hand, there are several factors and variables that have to be taken into account of Schmidt analysis [77]:

- The expansion and compression swept volumes.
- The movement of reciprocating elements in the engine, which is sinusoidal motion in real cycle.
- Dead space in the working space.
- The volume variations and the phase angle in the compression and the expansion spaces.

As it can be seen in Figure (3.25) presents ideal isothermal model of Alpha-type Stirling engine. The working space of the engine divided into expansion space (e), heater (h), regenerator (r), cooler (k) and compression space (c). Each part considered as a cell of constant properties and all spaces are connected in series.

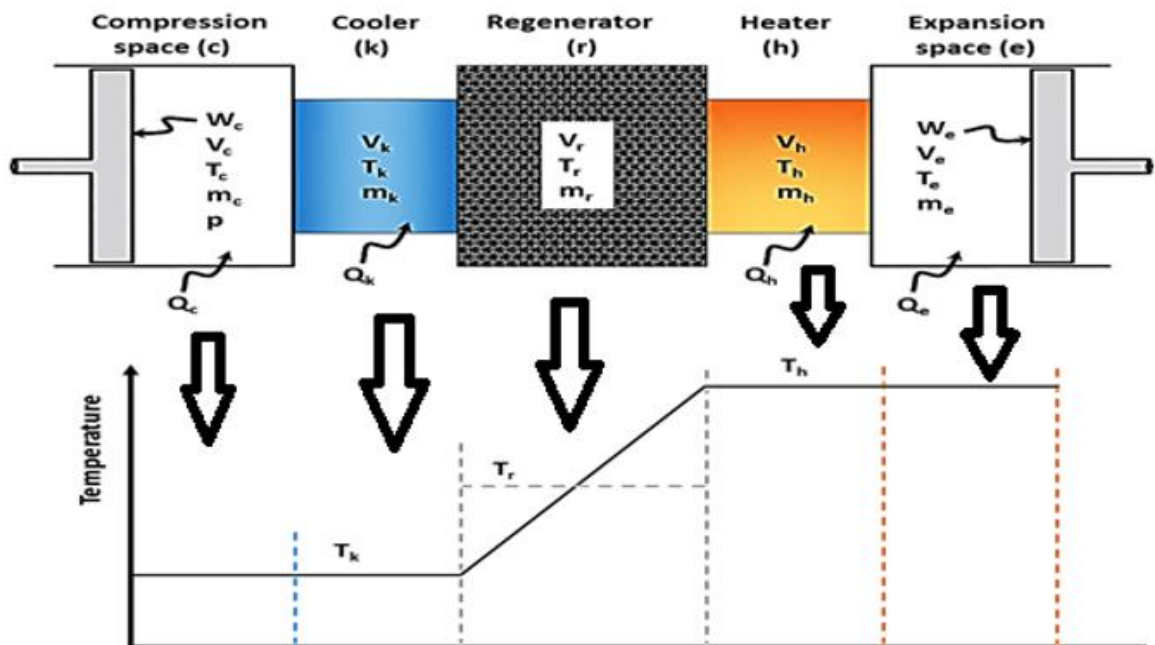


Figure 3.25: Ideal Isothermal Model [98]

The Schmidt analysis started with an assumption that the total mass of the working fluid in the engine is constant.

$$M = m_c + m_k + m_r + m_h + m_e \quad (3.4)$$

Where, ( $m_c$ ,  $m_k$ ,  $m_r$ ,  $m_h$  and  $m_e$ ) refer to the mass working fluid property in the compression space, cooler, regenerator, heater and the expansion space.

Also, it is assumed that the ideal gas law is applied in each working control spaces, as follows:

$$PV = mRT \quad (3.5)$$

Where the properties of the working fluid are described by the volume  $V$  ( $m^3$ ), pressure  $P$  ( $N/m^2$ ), mass  $m$  ( $kg$ ), temperature  $T$  ( $k$ ) and the gas constant  $R$  ( $J/kg.k$ ).

By substituting equation (3.5) into equation (3.4), the equation can be written as:

$$M = \frac{P \left( \frac{V_c}{T_k} + \frac{V_k}{T_k} + \frac{V_r}{T_r} + \frac{V_h}{T_h} + \frac{V_e}{T_h} \right)}{R} \quad (3.6)$$

As the temperature of the regenerator depends on the cooler and heater temperatures and acts as thermal store of the working fluid which shuttled between the compression and expansion space. Therefore, the regenerator temperature in ideal analysis considered as linearly distributed and  $T_r$  is given by:

$$T_r = \frac{(T_h - T_k)}{\ln \left( \frac{T_h}{T_k} \right)} \quad (3.7)$$

By substituting equation 3.7 into equation 3.6 and calculating as working pressure in the engine, it can be rewritten as:

$$P = \frac{MR}{\left( \frac{V_c}{T_k} + \frac{V_k}{T_k} + \frac{V_r \ln\left(\frac{T_h}{T_k}\right)}{(T_h - T_k)} + \frac{V_h}{T_h} + \frac{V_e}{T_h} \right)} \quad (3.8)$$

Over a complete cycle, the work output of the engine ( $W$ ) is the algebraic sum of the work done by expansion and compression spaces. This is expressed as follow:

$$W = W_e + W_c$$

$$W = \oint PdV_c + \oint PdV_e$$

$$W = \oint P \left( \frac{dV_c}{d\theta} + \frac{dV_e}{d\theta} \right) d\theta \quad (3.9)$$

Where  $\theta$  is crank angle.

### 3.18.1 Heat transfer in Schmidt analysis:

The investigation of heat transfer in Schmidt analysis considered as the energy conservation equation for working gas. As it can be seen in Figure (3.26) presents a generalized cell of control volume which may be either reduced a heat exchanger cell or working space cell. The enthalpy is transferred and added into the cell by means of mass flow ( $m_i$ ) and temperature ( $T_i$ ) and out of the cell by temperature ( $T_o$ ) and mass flow ( $m_o$ ).

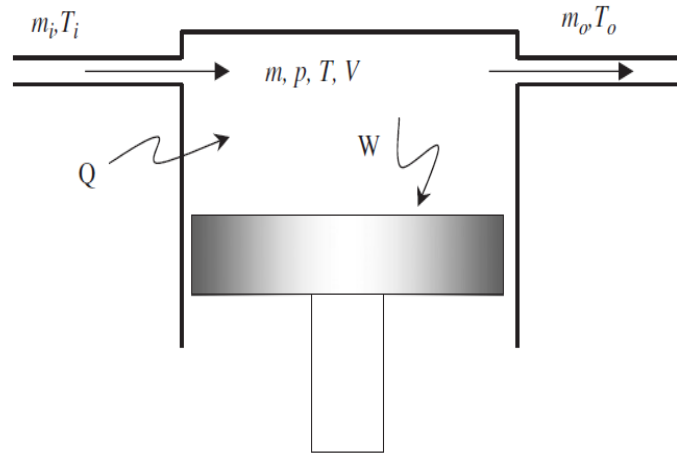


Figure 3.26: A generalized cell of working spaces in the engine

Therefore, the energy conservation in control volume of generalized cell stated as:

*(Rate of heat transfer into cell) + (Net enthalpy convected to cell) + (Rate of work done on surrounding) = (Rate of internal energy increase in the cell)*

Mathematically the statement expresses as:

$$\Delta Q + (C_p T_i m_i - C_p T_o m_o) = \Delta W + C_v \Delta(mT) \quad (3.10)$$

Where  $C_v$  and  $C_p$  are the specific heat capacities of the gas at constant volume and pressure respectively. Equation (3.10) is well-known as a classical form of the energy equation for non-steady flow. However, in Schmidt analysis for the expansion and compression spaces as well as for the cooler and the heater, it is considered that  $T_i = T_o = T$ . Therefore,

$$\Delta Q = C_p T(m_o - m_i) + C_v T \Delta m + \Delta W \quad (3.11)$$

From mass conservation law, the mass flow difference  $(m_o - m_i)$  is simply the mass accumulation rate within the cell, and for ideal gas ( $R = C_p - C_v$ ). The equation can be simplified for net heat transferred to the working gas over the cycle as:

$$Q = RT\phi Dm + \phi \Delta W \quad (3.12)$$

On the other hand, Schmidt investigated his analysis in the case of sinusoidal volume variation of compression and expansion spaces with respect to the cycle angle  $\theta$ , as shown in Figure (3.27). In this case, the volume variation of the compression and expansion space considered as sinusoidal and also  $\alpha$  is the phase shift angle of the expansion space volume variation with respect to the volume variation of the compression space.

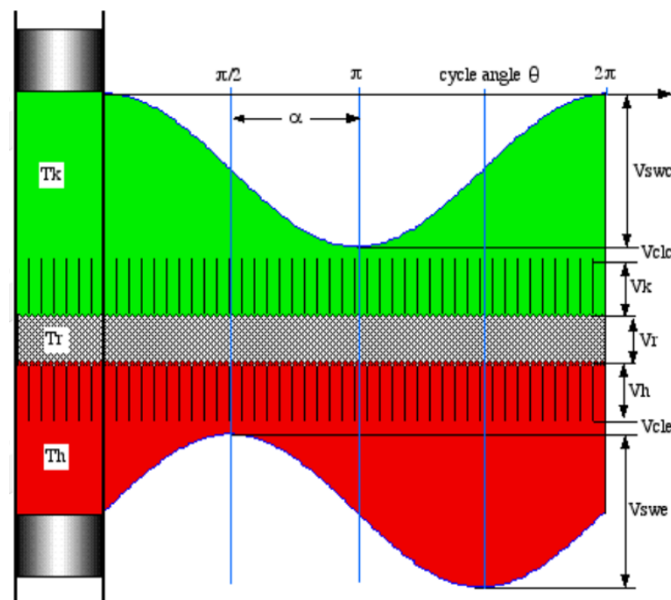


Figure 3.27: Sinusoidal volume variation of the compression and expansion space [99]

Readers refer to Appendix 1: for the derivation of Schmidt analysis equations.

Recently, many research works are focused to develop first order model and more thermodynamic analysis of several parameters are added to the model in order to obtain accuracy result of the performance and design. Bataineh [84] have developed mathematical modelling of first order by considering the regeneration, pumping and thermal losses in the analysis. In this case, the geometric and operating parameters are optimized and hence obtain a significant improvement of engine performance.

However, the heat capacity and the volume of the regenerator have a major effect on the engine performance, thus the effectiveness of the regenerator should be considered in any analysis. In [85] the authors focused and described in details the influence of the phase angle and the frequency on the operational performance by using several working fluid (air, helium and hydrogen). This analysis gives an observed result that the hydrogen has the maximum power output of about 8.8 kW for 80° phase angle, and 118 Hz frequency.

Furthermore, Chong et al [86] applied Schmidt analysis to perform a newly proposed hybrid dense-array concentrator photovoltaic and low temperature differential (LTD) Stirling engine. It is concluded that the highest efficiency of the hybrid system is about 38%.

### **3.19 Second Order Model (Adiabatic Analysis):**

The adiabatic analysis of the Stirling engine is a further developed and more realistic than the first order model. It is more accuracy approach to the modelling of Stirling engine that calculates the friction and thermal losses during engine operation. In 1960, Finkelstein developed the first analysis of second order model (adiabatic analysis), [70]. However, Urieli and Berchwitz investigated and developed the adiabatic analysis and took into account the impact of non-ideal heat exchangers and applied the equations of heat transfer to obtain the heater and cooler gas temperature [87].

As it can be seen in Figure (3.28) shows the temperature gradient in adiabatic analysis for each control volumes of the Stirling engine. The temperature of the cooler and heater are assumed to be constant, and also the compression and expansion control volumes are assumed to be adiabatic and under constant

temperature. The constant working fluid temperature in the heater and the cooler are,  $T_h$  and  $T_k$ , respectively. Moreover, there is a wire matrix regenerator that set in a linear distribution [88]. The performed work in adiabatic analysis depends on the changes in the volume of the expansion and compression spaces and the heat is transferred from outside to the working fluid in the heater and the cooler which are  $Q_h$  and  $Q_k$  respectively [89].

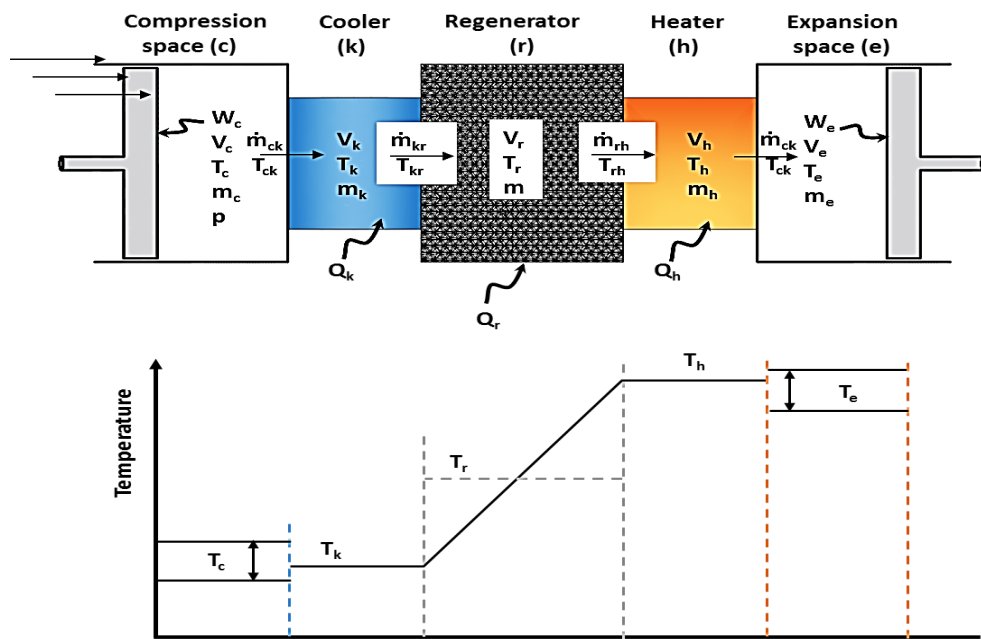


Figure 3.28: The ideal adiabatic model in Stirling engine

In adiabatic analysis, the equation of ideal gas can be applied in each control volume, in order to obtain the required differential equations and review the heat transfer in the cooler and the heater. Therefore, the energy equation for variable control volumes can be defined as:

$$\Delta Q + (C_p T_{ig} A_i - C_p T_{og} A_o) = \Delta W + C_v \Delta(mT) \quad (3.13)$$

Where  $C_p$  and  $C_v$  are the specific heat capacity of gas at constant pressure and constant volume. Also, the equation for pressure and volume can be written as:

$$pV = mRT \quad (3.14)$$

The differential form of equation (3.34) is written as follows:

$$\frac{\Delta p}{P} + \frac{\Delta v}{V} = \frac{\Delta m}{m} + \frac{\Delta T}{T} \quad (3.15)$$

It is assumed that the mass conservation of working gas in the components of the engine is the first step in adiabatic analysis [41]:

$$m_c + m_k + m_r + m_h + m_e = M \quad (3.16)$$

Readers refer to Appendix (2): for the derivation of Adiabatic analysis equations.

Alfarawi et al [71] developed a non-ideal adiabatic analysis for Gamma-type Stirling engine (ST05 CNC) and validated against experimental measurements. The modelling was reconfigured with six engine cells to contain connecting pipe that represent as a dead volume into the analysis, as shown in Figure (3.29). As it is considered to be adiabatic analysis which no heat is transferred to the surrounding and the energy is transported from cell to cell by means of enthalpy change based on mass flow and upstream temperature.

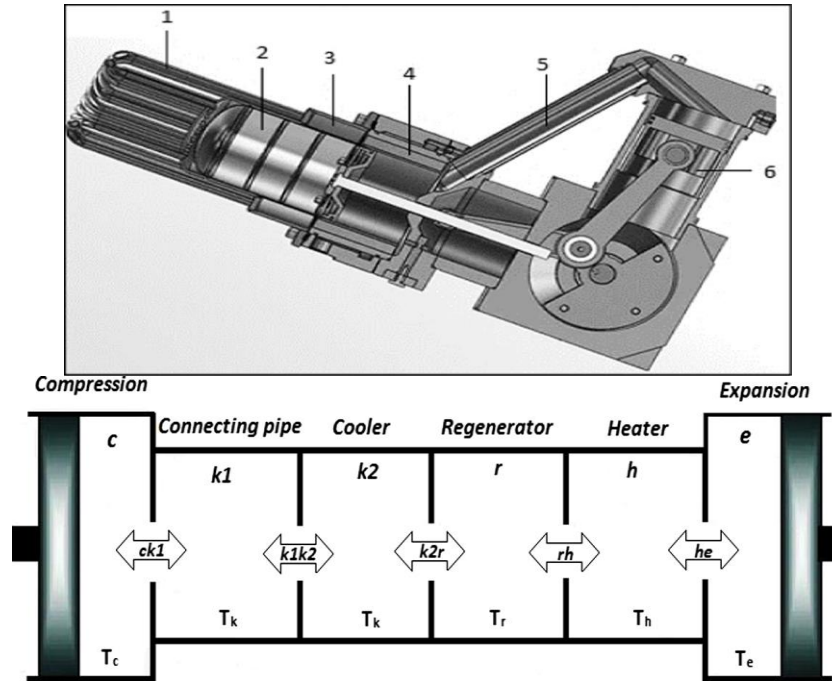


Figure 3.29: Gamma Stirling engine components: 1 - Heater, 2 - Displacer piston, 3 - Regenerator, 4 - Cooler, 5 - Connecting pipe, 6 - Power piston.

Therefore, it is observed that the heat transfer to the cooler and connecting pipe obtained as:

$$\Delta Q_k = C_v(V_{k1} + V_{k2}) \frac{dp}{R} - C_p(T_{ck1}m_{ck1} - T_k m_{k2r}) \quad (3.17)$$

As it can be seen from above equation that the author considered the volume of connecting tubes ( $V_{k1}$ ) in the analysis. The volume variation is obtained based on crank radius, compression and expansion swept volumes. Also, the author assumed the pressure to be uniform through the engine spaces. The conduction losses and shuttle are accounted for, as well as mechanical losses. It found that as the connecting pipe diameter reduced by 50%, the power shaft and thermal efficiency of the engine are significantly enhanced. Cheng et al [90] also investigated a non-ideal adiabatic model which includes the heat loss due to imperfect regeneration and friction power loss due to pressure drop. He also added Senft's theory [91] to the

analysis in order to estimate the effectiveness of the mechanism and the shaft power output. It is also assumed that the pressure is uniform throughout engine space, the temperature distribution in the regenerator is different from heater to the cooler, and the compression and expansion chamber are insulated.

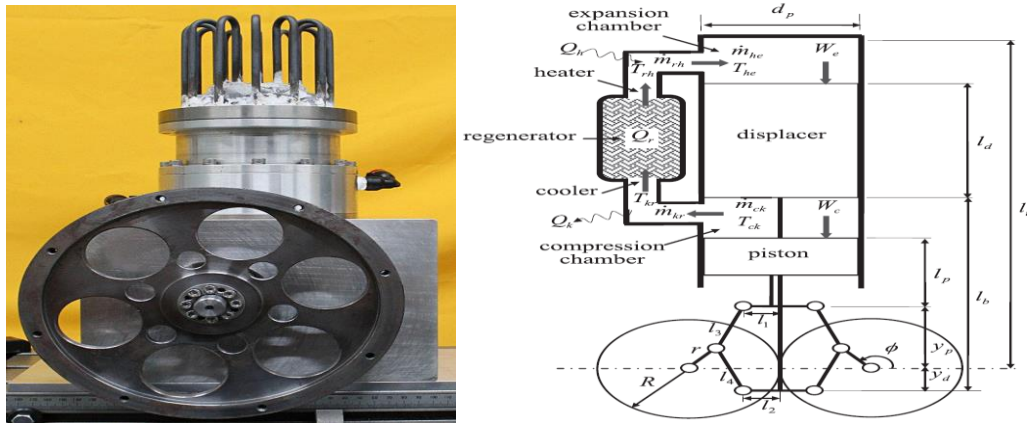


Figure 3.30: Prototype engine and schematic diagram of Beta type with rhombic drive mechanism[91]

The displacement equations of the displacer and the piston are defined as:

$$\gamma_p = r \sin\phi + \sqrt{l_3^2 - (R - l_1 + r \cos\phi)^2} \quad (3.18)$$

$$\gamma_d = r \sin\phi - \sqrt{l_4^2 - (R - l_2 + r \cos\phi)^2} \quad (3.19)$$

Thus, the volume variation of compression and expansion spaces are determined by,

$$V_e = A_d(l_t - l_d - l_b - \gamma_d) \quad (3.20)$$

$$V_c = A_p(\gamma_d + l_b - l_p - \gamma_p) \quad (3.21)$$

The study concluded that the shaft power output can be obtained numerically, with help of Senft's theory. It was observed that using helium as working fluid give much higher shaft power output than using air. On the other hand, Ni et al. [92] developed a

thermodynamic model of second order called Improved Simple Analytical Model (ISAM) which carefully considered the power and heat losses in the analysis. The analysis result well agreed with experimental result, however, several factors could be considered in ISAM modelling in order to improve an accuracy of second order model. For instance, the mass and heat transfer equations of oscillating flow could be studied specifically in high rotary speed. Furthermore, the excess gas leakage loss in the displacer also have to be considered in ISAM analysis.

### 3.20 Simple Analysis:

Urieli and Berchowitx developed simple analysis by calculating and considering the effectiveness of the heat exchanger (heater, cooler and regenerator). They proposed a definition of regenerator effectiveness as [87]:

$$\varepsilon = \frac{\textit{The amount of heat transferred unidirectionally to the working gas in the regenerator section over the cycle}}{\textit{The equivalent amount of heat transferred in the regenerator section of the Ideal Adiabatic model}}$$

On other hand, Babaelahi et al. modified the original simple analysis and developed a new thermal model called Simple-II which include the effect of heat rejection and absorption between the compression and expansion spaces. Therefore, new form of conservation equations can be stated as [93]:

$$\Delta Q - \Delta Q_{shuttle} + (\dot{m}_i C_p T_i - \dot{m}_o C_p T_o) = \Delta W + c_v \Delta(mT) \quad (3.22)$$

Where,  $\Delta Q$  is heat rejection or absorption from (or into) the working fluid,  $\Delta W$  is the net output work and  $\Delta Q_{shuttle}$  is the heat loss due to shuttle conduction by the displacer. The result of the new model was evaluated and validated with previous

experimental results. Also, it is concluded that the regenerator was responsible for the greater part of heat losses due to thermal ineffectiveness and pressure drop, respectively.

### 3.21 Third-Order Model (Nodal analysis):

It was first proposed by Finkelstein [94] which also known as nodal analysis models where the model subdivided the working space into control volume (nodes). The one-dimensional conservation equation of momentum, mass and energy are adopted in each control volume. Although, an adiabatic analysis has reliable accuracy result, but there is no cyclic information. Third order analysis provides relatively comprehensive operational information about the heat and flow characteristics inside a Stirling engine [92]. In this analysis, each control volume is defined by a set of differential equations of energy conservation, momentum and mass. Therefore, applying energy conservation to each control volume (node) as follows [80,95]:

$$\frac{\Delta Q_{in}}{\Delta t} - Q_{loss} + C_p(T_i m_i - T_{i-1} m_{i-1}) = C_v \frac{d}{dt}(m_n T_n) + \Delta W_n \quad (3.23)$$

Where,  $Q_{in}$  is the heat energy supplied in each node,  $Q_{loss}$  is the heat losses from each node,  $T_i$  is the temperature transferred between nodes,  $T_n$  is the temperature of each node,  $m_i$  is the mass transferred between nodes,  $m_n$  is the mass of each node,  $C_p$  is the specific heat capacity of the working fluid at constant pressure,  $C_v$  is the specific heat capacity of the working fluid at constant volume and  $W_n$  is the work in each node.

Recently, many research studies have focused to improve the nodal analysis. For instance, in the research of [92], the author combined the third-order with a second-order model to provide an accurate result and detailed information of the total thermal efficiency power output with variant pressure and speed. On other hand, several algorithm have been used with third-order model such as multi-objectives optimization to optimize the performance of Stirling engine [96,97,98]. Karabulut et al [92] applied a third order model on alpha type Stirling engine and utilized Schmidt formula in order to calculate the pressure of nodal volume. The author divided the working space of the engine into 27 nodal volumes which indicates the hot and cold cylinders from the left to the right. He also used a coordinate system of dynamic analysis which applied to the engine in order to calculate the locations of the hot and the cold pistons. Thus, the volumes of the hot and the cold cylinders are determined. Several speeds were applied and tested. It was found that the speed of Stirling engine related to the friction causes a weakness performance.

In another research, Toghyani et al [96] has developed the third order thermodynamic analysis to optimize the efficiency, output power and the pressure drop of GPU3 Stirling engine. Multi-objective optimization with four variable decision make were applied in order to enhance the performance of the engine. It was observed that the analysis indicated a good improvement of efficiency and output power.

### **3.22 Dynamic Analysis of FPSE:**

The design of Free-piston Stirling engines (FPSEs) were developed in order to avoid problematic mechanical link by connecting the displacer and the piston to a flexure spring. Therefore, FPSEs become simpler in structural configuration of the

components than kinematic engines [99]. However, there are many complicated problems in piston dynamics due to undetermined motions which caused by the flexion spring. Eventually, the dynamic analysis is very important to design FPSEs based on the theory of mechanical vibration with Stirling thermodynamics. It is seen that the first analysis conducted on the dynamic behaviour of the free piston Stirling engines was performed by Beale [100]. The free piston Stirling engines treated as a dynamic system having two degree of freedom by assuming the casing to be constant [101,102]. The solution of the dynamic model was achieved analytically in these studies by converting to the linear form. Engines whose power is removed via the casing can be developed using a three-degree-of-freedom dynamic model.

Recently, many research works have developed different mathematical models to improve the design and performance of FPSE, each model includes features and drawbacks. In [101] research work presented a novel mathematical model based on genetic algorithm for FPSE considering the design variables such as spring stiffness and mass for both displacer and power piston. It was concluded that the outcome of the simulation predicted the engine operating frequency with a low error 3%.

Boucher et al.[103] carried out the analysis of a free piston Stirling engine possessing a piston and two displacers as moving component and predicted design parameters for 1 kW power output. Also dynamic analysis, which is a very essential model for an optimal design of FPSE, Karabulut [104] presented a nonlinear dynamic analysis of FPSE which considered the length of the piston displacer strokes. The dynamic model derived on the closed and open cycle of FPSE and the analysis indicated that the free piston can operate stability on closed cycle within a small range of (700K) hot end temperature.

On the other hand, Hofacker et al. [102] investigated and developed a novel design of free piston Stirling engine system called liquid free piston Stirling engine (LFPSE), the displacer piston and power piston are liquid pistons formed by trapping water between elastomeric membranes. The damping and spring elements of the system are compactly contained within the elasticity of the membrane material. Comprehensive mathematical modelling of dynamic analysis which include development of the dynamic of working fluid pressure, cold, hot and tuning liquid columns and power piston. It was shown that the results of mathematical model are in a good accordance with the experimental results. Chen et al. [105] developed a novel design of free-piston Vuilleumier heat pumps (FVHP) which utilized for residential heating and cooling as shown in Figure (3.31). The study presented a dynamic model based on dwell-motion which includes mechanical spring, friction, pressure, gravity and viscous damping. The results showed that an improved design of the system and reduce the overall system cost.

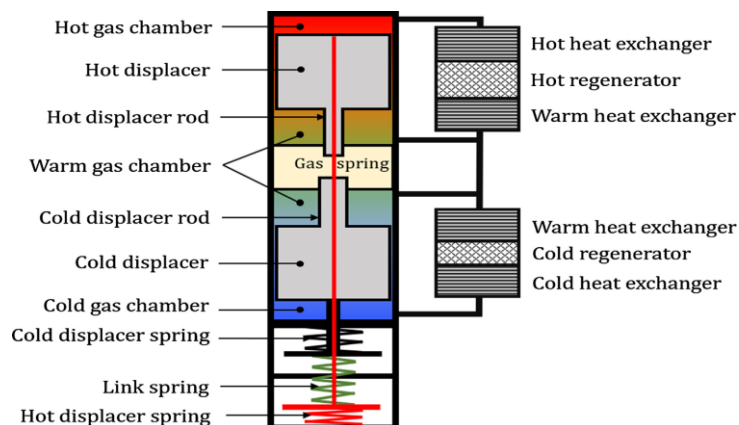


Figure 3.31: Diagram of Free-piston Vuilleumier Heat Pump (FVHP)

In another research [106] Saleh et al. describe a novel design approach of FPSE based on multiple-scale perturbation method. This method can be used to effectively simplify nonlinearities that are unavoidable in a nonlinear dynamic system. A comprehensive mathematical models are applied and the classical Schmidt assumptions are used in the model except finite heat transfer between heat exchanger and working fluid. Non-linear spring are added to the design as shown in Figure (4.9). It was found that the efficiency, power piston stroke and frequency are respectively as 7.1 %, 3.46 W and 71.1 rad/s, which also showed that a good agreed with experimental results. The difficult task was predict the gas temperature in the heat exchangers of the FBSEs.

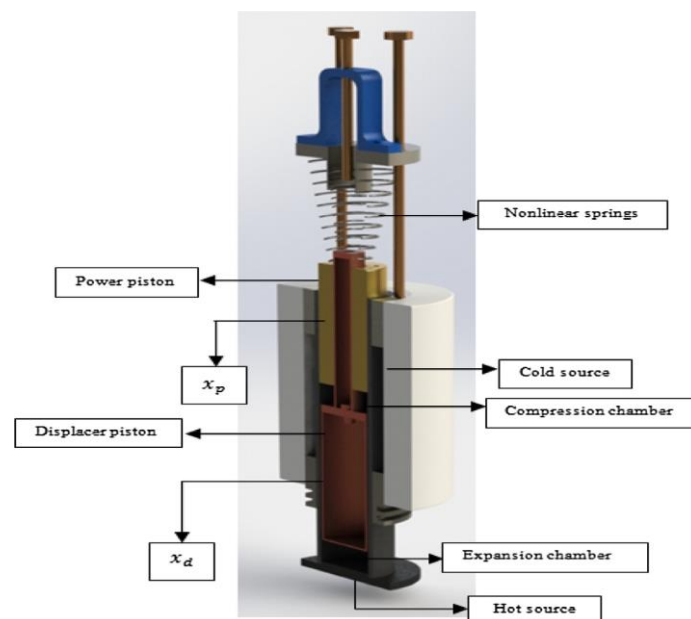


Figure 3.32: Schematic components of proposed FPSE

In order to design and construct free piston Stirling engine from a system dynamics point, it is necessary to consider and review several variation of dynamic model that can be applied on Stirling engine cycle.

### 3.23 Summary:

In many applications where conventional engines cannot be employed, Stirling engines have a tremendous deal of promise for commercial use (eg. For utilisation of renewable energies, waste heat etc.). Over the years, many successful and unsuccessful developments have been made for a variety of Stirling engine applications. It is also found, comparing to traditional kinematical Stirling engines, free piston Stirling engine-based units currently have the most successful uses on the market, despite the fact that the theoretical underpinnings of such FPSEs are less explored.

To improve performance of FPSEs further development of mathematical modelling of their working process for their designing optimisation is required and this is the purpose of this study. As mentioned above, several levels of mathematical models are developed in this work and calibrated against published experimental and theoretical data to evaluate their accuracy. Moreover, the components of the Stirling engine were reviewed and introduced, as well as the different types of Stirling engine designed were presented. Furthermore, the chapter presented the process of thermodynamic cycle of the Stirling engine in detail. Focused more on the different mechanical arrangements of Free-piston Stirling engine (FPSE) as this research is going to develop the design of FPSE for irrigation or power generation applications by using solar dish system. Finally, it is concluded that the different orders of the thermodynamic analysis were mathematically formulated and studied in order to optimise the design of the Stirling engine. In this research, first, second and simple model analysis is going to be applied in next chapter in order to optimise the design and operation parameters of the FPSE.

# Chapter 4:

## Computer Modelling and Simulation Analysis

### 4.1 The proposed mechanical arrangement for the FPSE:

The novel design of the free piston Stirling engine described and introduced in this study is based on the innovative design concept that uses a particular type of flexible bellows or diaphragms with a long lifetime and high reliability as a power piston. Several designs of diaphragm or bellows that can be practically installed have been proposed. However, the manufacturing and assembly issues have been considered to reduce the total cost and simplify the assembly. The flexure bellows provide advantages of compression space in the linear direction. The displacer is the bottom part of the engine, which contain two helical springs installed inside the displacer. Both springs are installed under a pre-compressed position to maintain the proper position of the displacer and align the displacer's oscillation during expansion and compression space. The displacer is placed between the cold end on the top and the hot space from the bottom of the engine; thus, a large temperature gradient will have occurred, which also obtains the specific operating frequency and stroke.

Furthermore, the displacer is designed to be a lightweight stainless steel metal cylinder clamped on the top by a bellow flange connected to the engine frame. The bellow, which represents the power piston, is proposed to be mounted on the top of the engine. The bellows generate the expansion and compression strokes. The mechanical arrangement of the component for the engine is shown in Figure 4.1.

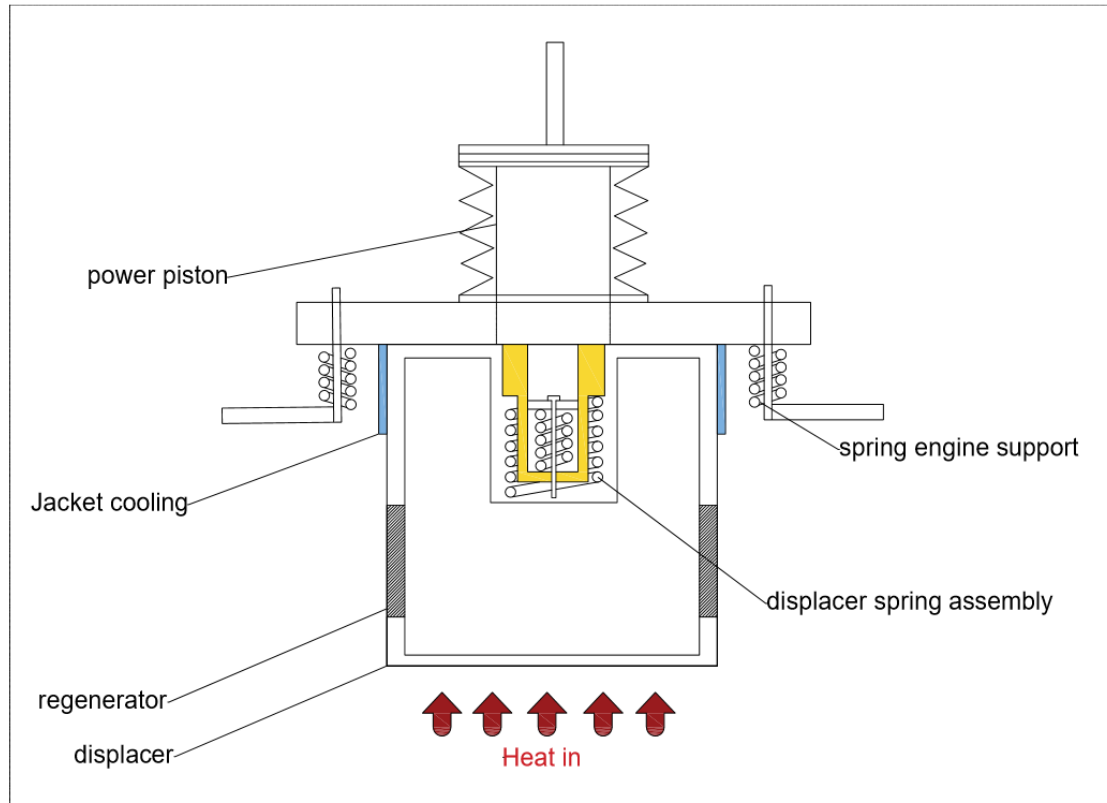


Figure 4.1: Diagram of prototype FPSE components

## 4.2 The design objectives:

The FPSE engine shown in Figure 4.1 was analysed and simulated in mathematical modelling to evaluate and validate its performance by considering pressure drop, heat pumping losses caused by fluid friction, and imperfections of the heat exchanger. The dimensions of the engine components and operating parameters are used in the mathematical model.

## 4.3 Thermodynamic Models:

The mathematical thermodynamic models used in this design of the Free Piston Stirling engine are classified into three types:

### 4.3.1 First-order model (Schmidt analysis):

Schmidt analysis is basic model, based on ideal conditions. They use adjustment factors to estimate the power output and thermal performance; this causes the results to be insufficiently reliable to determine the engine's actual performance and dimensions. This model also provides a quick way to study engine dimensions concerning power output, identifying the critical variables and their influence on the engine.

First of all, according to the Schmidt model, the amount of heat entering to the engine system comes from the heat simulator and heat absorbed by the regenerator:

$$Q_i = Q_h + Q_r \quad (4.1)$$

Since the ideal cycle is composed of two isotherms and two constant-volume processes, as shown from figure (4.2) that both heat enters the system of the engine and that which comes out given according to:

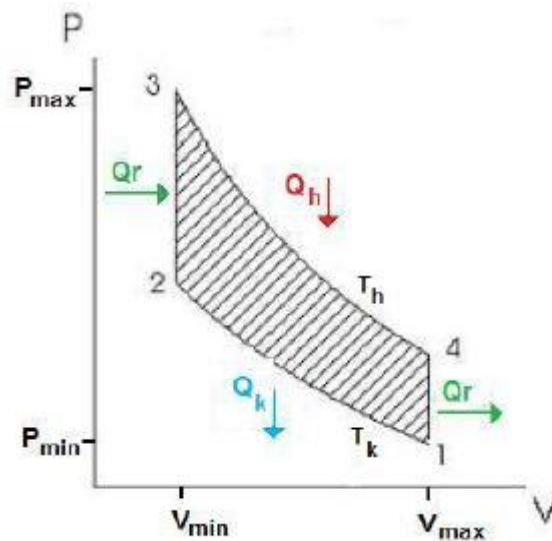


Figure 4.2: Stirling thermodynamic cycle

$$Q = C_v(T_h - T_k) + \int_{V_{min}}^{V_{max}} PV \quad (4.2)$$

Then, replacing  $P=RT/V$  into the integral and considering that the temperature (T) is constant on the hot side, you have [107]:

$$Q_i = Cv(T_h - T_k) + RT_h \ln\left(\frac{V_{min}}{V_{max}}\right) \quad (4.3)$$

Similarly, for the heat that leaves the system of the engine, we have [108]:

$$Q_o = Q_r + Q_k \quad (4.4)$$

$$Q_o = Cv(T_k - T_h) + RT_h \ln\left(\frac{V_{max}}{V_{min}}\right) \quad (4.5)$$

Where,

Qr: heat absorbed by the regenerator.

Qk: heat delivered by the cold source (cooler),

Q h: heat produced by the hot source (heater),

Cv: the specific capacity for constant volume (J / kgK),

Th: the temperature of the hot source in the Stirling cycle,

Tk: the temperature of the cold source,

R: the universal gas constant (J / kgK),

V min, V max: the specific volumes of the thermodynamic cycle (m<sup>3</sup> / kg)

We also assume that the entire gas (air) is distributed over three volumes:

The expansion volume (V<sub>E</sub>) at T<sub>E</sub> (k), the compression volume V<sub>C</sub> at T<sub>C</sub> (k), and the dead volume V<sub>D</sub> at T<sub>D</sub> (k). Therefore, the total amount of substance volume is [109]:

$$V = v_1 + v_2 + v_3 = \frac{P}{R} \left( \frac{V_E}{T_E} + \frac{V_C}{T_C} + \frac{V_D}{T_D} \right) \quad (4.6)$$

Where the expression for pressure expressed as:

$$P = \frac{VR}{\frac{V_E}{T_E} + \frac{V_C}{T_C} + \frac{V_D}{T_D}} \quad (4.7)$$

According to Schmidt assumption about the harmonic motion of the pistons, it is considered that [110]:

$$V_c = V_{clc} + \frac{V_{swc}(1+\cos\theta)}{2} \quad (4.8)$$

$$V_e = V_{cle} + \frac{V_{swe}(1+\cos(\theta+\alpha))}{2} \quad (4.9)$$

Where  $V_{sw}$  and  $V_{cl}$  are the swept and clearance volume respectively in ( $m^3$ ), and  $\Theta$  is the cycle angle and  $\alpha$  is the phase lag of the compression piston from the piston extension.

Also, the expression for average pressure per cycle takes the following form:

$$P_{mean} = \frac{MR}{2\pi S} \int_0^{2\pi} \frac{1}{(1 + b \cos \varphi)} d\theta \quad (4.10)$$

Therefore, the work done in the expansion space (J) is [111]:

$$W_E = \oint P_E \Delta V_E = -\frac{V_{swe} MR}{2s} \int_0^{2\pi} \frac{\sin(\theta + \alpha)}{1 + b \cos(\beta + \theta)} \Delta\theta \quad (4.11)$$

The work is under the compression (J):

$$W_C = \oint P_C \Delta V_C = \frac{V_{swc} MR}{2s} \int_0^{2\pi} \frac{\sin \theta}{1 + b \cos(\beta + \theta)} \Delta\theta \quad (4.12)$$

The total work per cycle is equal to:

$$W = W_E + W_C \quad (4.13)$$

Where,

$$\oint = \int_{\theta=0}^{2\pi} \quad \text{Which means cycle-by-cycle integration,}$$

Therefore, the overall efficiency of the engine can be found as [112]:

$$\eta = \frac{W}{Q_i} \quad (4.14)$$

performing numerical integration in the above equations, it is possible to analyse the operation parameter and identify the dependence dimension parameter of the engine in Schmidt approximation.

#### **4.3.2 Second-order model (Adiabatic analysis):**

Adiabatic analysis considers different equations for the resolution of the model. The significant advantage of this model with regarding the first order is that they have a more detailed analysis of both the losses thermals and those associated with pressure drops within the engine [113]. The way to find the equations that govern the model is to use the equations state and energy of the system. These equations will be complemented by the equations of continuity throughout the system.

Adiabatic model is going to determine the thermodynamic conditions of the engine in each of its parts, it will divide the rig into subsystems which interact with each other. These subsystems will be the compression space, expansion space, heater, cooler and regenerator. Thus, the subscripts will be the following:

e: Expansion space

c: Compression space

k: Cooler

h: Heater

r: Regenerative

i: Entrance to the engine

o: Output of the engine

The compression space refers to all the space in which there is gas at cold temperature. In the same way, the expansion refers to all the space in which there is gas at hot temperature, which is responsible for producing expansion work [111].

Thus, the energy flux in the different sections of the engine is shown in figure (4.3).

$$\begin{array}{|c|} \hline \text{Flow rate of} \\ \text{heat transfer} \\ \text{into the cell} \\ \hline \end{array}
 +
 \begin{array}{|c|} \hline \text{Net enthalpy} \\ \text{convicted into} \\ \text{the cell} \\ \hline \end{array}
 +
 \begin{array}{|c|} \hline \text{Rate of work} \\ \text{produced on the} \\ \text{surroundings} \\ \hline \end{array}
 =
 \begin{array}{|c|} \hline \text{Rate of increase} \\ \text{of internal} \\ \text{energy in the cell} \\ \hline \end{array}$$

Figure 4.3: Flow energy within each subsystem of the engine

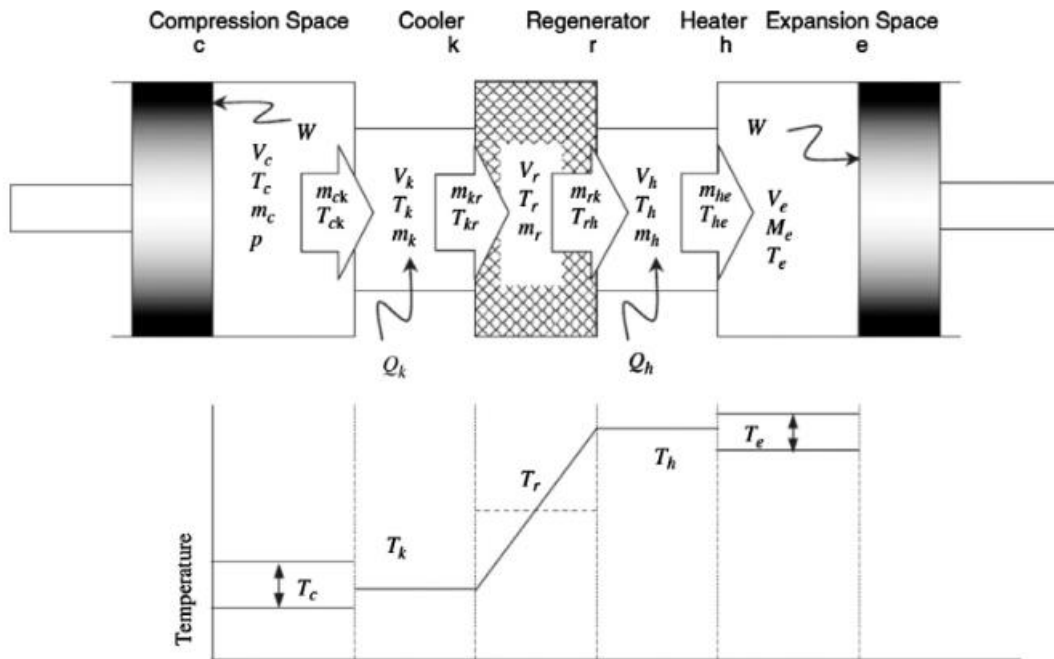


Figure 4.4: Temperature and mass flow distribution in each parts of Stirling engine based on ideal adiabatic model [111].

The temperature in the compression and expansion spaces ( $T_c$  and  $T_e$ ), as shown in the temperature distribution graphic in Figure 4.4, is not constant during the cycle, but varies according to the adiabatic compression and expansion that occurs in the working areas. As a result, the enthalpies flowing across the interfaces  $ck$  and  $he$  carry the temperatures of the next upstream cells, so temperatures  $T_{ck}$  and  $T_{he}$  are dependent on the flow direction.

In order to solve the ideal adiabatic model, total mass of the system should be assumed constant and then, using the energy equation and ideal gas equation of state, the equations required to measure the engine heat transfer, exerted work and

engine efficiency can be obtained. Figure (5.4) represent the five components of the Stirling cycle. Considering the coordinate system that is defined for the model, several variables and differential equations need to be solved to reach a solution for the engine cycle.

Mathematically, this becomes:

$$\Delta Q + (C_p T_i \dot{m}_i - C_p T_o \dot{m}_o) = \Delta W + C_v \Delta(\dot{m}T) \quad (4.15)$$

Where,  $C_p$  and  $C_v$  are the specific heat capacities of the gas, for pressure and volume constant respectively. The working gas is assumed to be ideal. Thus, the equation of state for each section is presented in its standard and differentiated form as follows [114]:

$$\frac{\Delta P}{P} + \frac{\Delta V}{V} = \frac{\Delta m}{m} + \frac{\Delta T}{T} \quad (4.16)$$

The starting point of the analysis is that the total mass of gas in the engine is constant, Thus:

$$m_c + m_k + m_r + m_h + m_e = M \quad (4.17)$$

Substitute having the ideal gas law in the previous equation, we have:

$$M = \frac{P \left( \frac{V_c}{T_k} + \frac{V_k}{T_k} + \frac{V_r}{T_r} + \frac{V_h}{T_h} + \frac{V_e}{T_e} \right)}{R} \quad (4.18)$$

As the temperature of the regenerator depends on the cooler and heater temperatures and acts as thermal store of the working fluid which shuttled between the compression and expansion space. Therefore, the regenerator temperature in ideal analysis considered as linearly distributed and  $T_r$  is given by:

$$T_r = \frac{(T_h - T_k)}{\ln\left(\frac{T_h}{T_k}\right)} \quad (4.19)$$

Solving the pressure in the previous equation (18) we have:

$$P = \frac{MR}{\left(\frac{V_c}{T_k} + \frac{V_k}{T_k} + \frac{V_r}{T_r} + \frac{V_h}{T_h} + \frac{V_e}{T_e}\right)} \quad (4.20)$$

Deriving the conservation of mass equation can be written as Eq.(21), since the temperature and the volume are constant [113]:

$$\Delta m_c + \Delta m_k + \Delta m_r + \Delta m_h + \Delta m_e = 0 \quad (4.21)$$

For heat exchanger, assuming volumes and temperatures are constants, the derived form of the equation of state reduces to[113]:

$$\frac{\Delta p}{P} = \frac{\Delta m}{m} \quad (4.22)$$

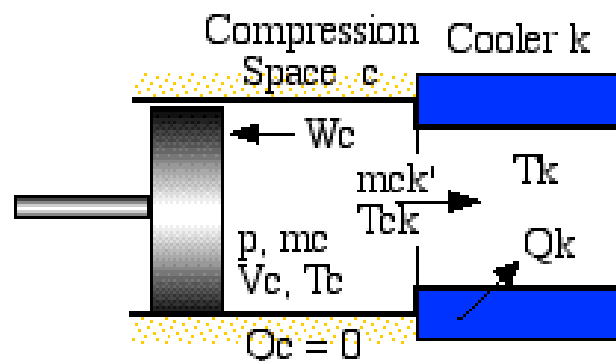
Thus,

$$\Delta m = \frac{\Delta p * m}{p} = \frac{\Delta p V}{RT} \quad (4.23)$$

By replacing in equation (21), we get:

$$\Delta m_c + \Delta m_e + \left(\frac{\Delta p}{R}\right) \left(\frac{V_k}{T_k} + \frac{V_r}{T_r} + \frac{V_h}{T_h}\right) = 0 \quad (4.24)$$

In order to obtain an explicit equation in  $\Delta p$ , we need to remove  $\Delta m_c$  and  $\Delta m_e$  from the above equation. Take the adiabatic compression space ( $\Delta Q_c = 0$ ):



Applying the above energy equation to this space we obtain:

$$-C_p T_{ck} m_{ck} = \Delta W_c + C_v \Delta(m_c T_c) \quad (4.25)$$

From continuity considerations the rate of accumulation of gas  $\Delta m_c$  is equal to the mass inflow of gas given by  $-m_{ck}'$ , and the work done  $\Delta W_c$  is given by  $p \Delta V_c$ , thus:

$$C_p T_{ck} \Delta m_c = p \Delta V_c + c_v \Delta(m_c T_c) \quad (4.26)$$

By substitute the ideal gas relations  $pV_c = m_c R T_c$ ,  $C_p - C_v = R$ , and  $C_p / C_v = \gamma$ , and simplifying[113]:

$$\Delta m_c = (p \Delta V_c + \frac{V_c \Delta p}{\gamma}) / (R T_{ck}) \quad (4.27)$$

In similar for the expansion space:

$$\Delta m_e = (p \Delta V_e + \frac{V_e \Delta p}{\gamma}) / (R T_{he}) \quad (4.28)$$

Now substituting value of  $d m_c$  and  $d m_e$  above and simplifying[118]:

$$\Delta p = \frac{-\gamma p \left( \frac{\Delta V_c}{T_{ck}} + \frac{\Delta V_e}{T_{he}} \right)}{\left[ \frac{V_c}{T_{ck}} + \gamma \left( \frac{V_K}{T_K} + \frac{V_r}{T_r} + \frac{V_h}{T_h} \right) + V_e / T_{he} \right]} \quad (4.29)$$

Applying the above energy equation (14) to each of the heat exchanger cells ( $dW = 0$ ,  $T$  is constant)

Also, substituting for the equation of state for a heat exchanger cell[119]:

$$\Delta m = \Delta p \frac{m}{p} = \left(\frac{\Delta p}{R}\right) V/T \quad (4.30)$$

Thus,

$$\Delta Q + (cp T_i m_i - cp T_o m_o) = cv T dm = V \Delta p cv/R \quad (4.31)$$

We get the following results for the three heat exchanger[120]:

$$\Delta Q_k = V_k \Delta p \frac{cv}{R} - cp(T_{ck} m_{ck} - T_{kr} m_{kr}) \quad (4.32)$$

$$\Delta Q_r = V_r \Delta p \frac{cv}{R} - cp(T_{kr} m_{kr} - T_{rh} m_{rh}) \quad (4.33)$$

$$\Delta Q_h = V_h \Delta p \frac{cv}{R} - cp(T_{rh} m_{rh} - T_{he} m_{he}) \quad (4.34)$$

It is noted that since the regenerator is ideal and the heat exchangers are isothermal, thus[121],

$$T_{kr} = T_k \text{ and } T_{rh} = T_h \quad (4.35)$$

Finally, the work done in the expansion and compression cells is given by[122]:

$$W = W_c + W_e \quad (4.36)$$

$$\Delta W = \Delta W_c + \Delta W_e \quad (4.37)$$

$$\Delta W_c = p \Delta V_c \quad (4.38)$$

$$\Delta W_e = p \Delta V_e \quad (4.39)$$

### 4.3.3 Simple analysis:

Once the ideal adiabatic analysis is simulated on a specific Stirling engine, the simple analysis also applied in order to evaluate the heat transfer and flow-friction effects of the three heat exchangers on the performance of the engine. This will

allow to perform a parametric sensitivity analysis, which is necessary for design optimization.

From the basic equation for convective heat transfer we obtain[123]:

$$Q = hA_{wg}(T_w - T) \quad (4.40)$$

Where, Q is the total heat transfer power (including the regenerator net enthalpy loss),  $A_{wg}$  refers to area of the heat exchanger surface, h is the convective heat transfer coefficient, T is the gas temperature, and  $T_w$  is the wall temperature. Now divide both sides by the frequency of operation to simplify the units of this equation to the net heat transferred over a single cycle Q (joules/cycle).

Thus,

$$Q_k - Q_{rloss} = h_k A_{wgk} (T_{wk} - T_k) / freq \quad (4.41)$$

$$Q_h - Q_{rloss} = h_h A_{wgh} (T_{wh} - T_h) / freq \quad (4.42)$$

The fluid friction associated with the flow through the heat exchangers will, in fact, cause a pressure drop across all of the heat exchangers, lowering the engine's power output. This is known as the "Pumping Loss". The pressure drop is calculated across the entire cycle of all three heat exchanger, and can determine the new value of work done and isolate the Pumping Loss term as follows[124]:

$$W = W_c + W_e = \oint p \Delta V_c + \oint (p - \sum \Delta p) \Delta V_e \quad (4.43)$$

Where the summation  $\sum \Delta P$  is taken over the three heat exchangers, thus[125]:

$$W = \oint p(\Delta V_c + \Delta V_e) - \oint \sum \Delta p \Delta V_e = W_i - \Delta W \quad (4.44)$$

Where,  $W_i$  is the ideal adiabatic work done per cycle, and  $\Delta W$  is the pressure drop loss or pumping loss per cycle.

#### 4.4 Numerical simulation and results:

As it can be seen from below diagram, the specific configuration must be identified before the any simulation can take place. Thus, the geometry of the engine, the working gas, the three heat exchangers and the operating conditions are specified. After that, the three levels of simulation: isothermal Schmidt analysis, ideal Adiabatic analysis, and Simple analysis of the Stirling engine are analysed and evaluated. The computer program was adopted from Israel Urieli; David M Berchowitz text book [69] which is written in the Matlab language as shown in the functional block diagram.

The main program **sea** (Stirling engine analysis) firstly defines the system to be simulated in terms of geometry and operation parameters of the engine which set up by the **define** function. It then perform either the function **simple** which does a Simple simulation to evaluate the effect of pressure drop and heat transfer, or the function **adiabatic** to do an ideal Adiabatic simulation. The **simple** set function includes four main functions which are **kolsim** and **hotsim** to respectively evaluate the cooler and heater fluid temperature, **worksim** to evaluate the pumping loss in the engine, and **regsim** to evaluate the regenerator effectiveness and obtain the enthalpy loss. The **reynum** function set to evaluate thermal conductivity, dynamic viscosity and Reynold number[72].

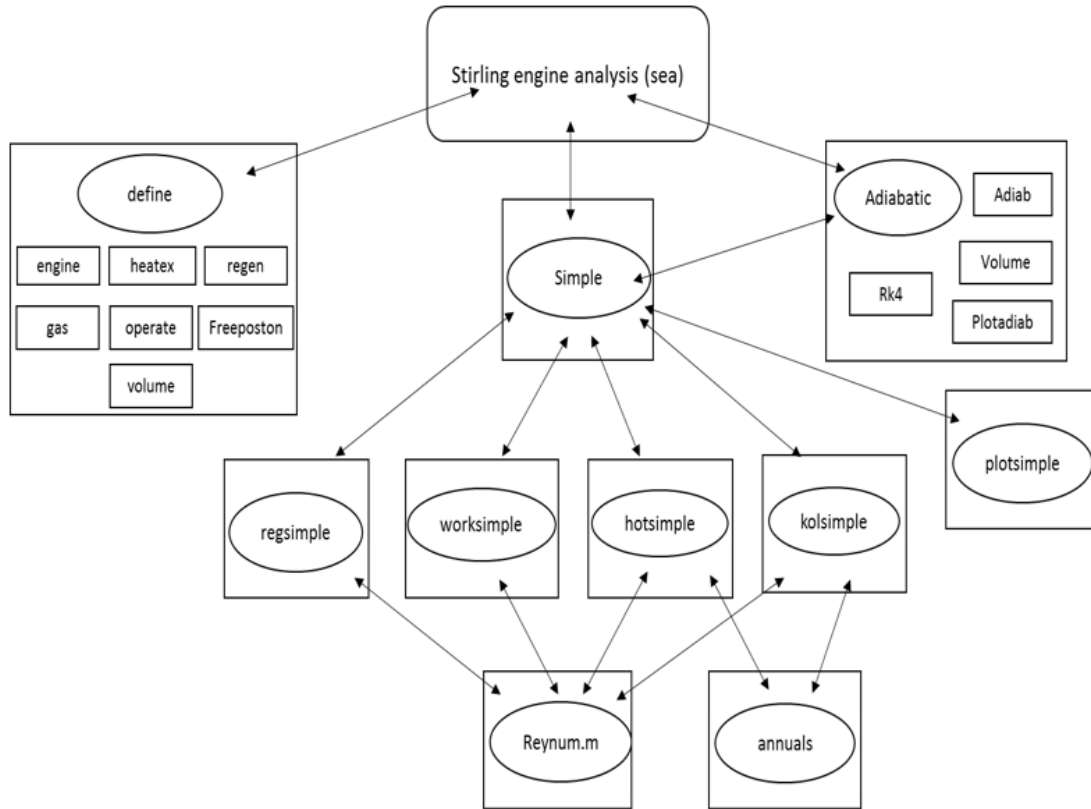


Figure 4.5: The progress function of the model simulation [72]

#### 4.5 Computer Model Results:

Table 4.1 shows the dimensions of the displacer and the power piston which were chosen based on the size of the bellow and availability off the shelf. The engine casing cylinder and the thickness was designed to be more withstand of the input heat.

Table 4.1: Dimensions of the parts engine

Part description	Part dimensions(mm)
Displacer (Diameter, Height, Thickness)	192* 250 * 1
Power piston (Bellows) (Diameter, Height, Thickness)	75 * 130* 1
Engine casing cylinder (Diameter, Height, Thickness)	198 * 300 * 1
Regenerator (Outer and inner diameter, Height)	197 * 188 * 120

The engine design shown in Figure 5.1 was analysed and simulated in order to validate and evaluate the output power with taking into consideration the pumping losses and imperfective heat exchanger. The computer model used a variety of operational parameters, however the values are provided in table 4.2 are suitable for meeting the engine's design and size in order to achieve output power at appropriate temperatures and atmospheric pressure.

Table 4.2: Operation parameters of the engine

<b>Variable</b>	<b>Value</b>
Hot side wall temperature	623K
Cold side wall temperature	298K
Operating frequency	9 to 17 Hz
Mean operating pressure	1 to 2 bar
Working gas	Air

Table 4.3 shows the numerical results that obtained from the Simple analysis simulation in terms of 11 Hz operating frequency and 1 bar mean pressure. It is found that the result of simple analysis was the most accurate result, because the heat losses and imperfect regeneration are considered as shown in the bottom of the table. Moreover, see appendices 4 for more result of all modelling analysis (Schmidt, Adiabatic, Simple).

Table 4.3: The numerical results from the computer analysis

Variable name	Value	Unit
Pressure phase angle (beta)	75.80	Degree
Total mass of air	0.375	g/mol
Cooler wall temperature ( $T_{wk}$ )	298.10	K
Heater wall temperature ( $T_{hk}$ )	573.10	K
Regenerator effectiveness (Simple analysis)	76.42	%
Number of transfer units NTU (Simple analysis)	3.2	–
Regenerator Net Enthalpy losses (Simple analysis)	89.99	W
Regenerator wall heat leakage (Simple analysis)	87.96	W
Heater gas temperature $T_{gh}$ (Simple analysis)	566.9	K
Heat transfer coefficient (Heater Simple analysis)	126.38	W/m <sup>2</sup> *K
Heat transfer to the heater (Heater Simple analysis)	2.63	J
Heat transfer coefficient (Cooler Simple analysis)	50.92	W/m <sup>2</sup> *K
Heat transferred from cooler (Cooler Simple analysis)	-1.61	J
Cooler gas temperature $T_{gk}$ (Simple analysis)	301	K
Work loss (Simple analysis)	4.67	W
Total power output (Simple analysis)	6.73	W
Efficiency (Simple analysis)	3.25	%

The program was run by applying equation 4.15 for every control volume, and it was assumed that the movement of the power piston and the displacer are sinusoids. The fluid type, the operating frequency, and the engine's geometry were specified. Before reaching the steady-state of the PV diagram, as shown in Figure 5.6, the program has gone through four processes: firstly, an isothermal expansion (heat

addition from the external source). Secondly, isothermal compression (heat rejection to the external sink). Thirdly, a rejection (internal heat transfer from the working fluid to the regenerator), and finally, heat addition (internal heat transfer from the regenerator back to the working fluid at constant volume).

It is obviously can be seen from Figure (4.6) that the enclosed PV diagram representing the power output from the engine. The highest pressure in Schmidt analysis is 1.18 bar at the end of the compression cycle, and the lowest is 0.85 bar, whereas the mean pressure is 1 bar. It is noticed that the value of highest pressure in Schmidt analysis is higher than in Simple analysis, which also noted that from the above table the calculated power output from Schmidt analysis is higher 14.32W and in Simple analysis is 6.73W, due to the imperfect regeneration and pumping losses are considered in Simple analysis.

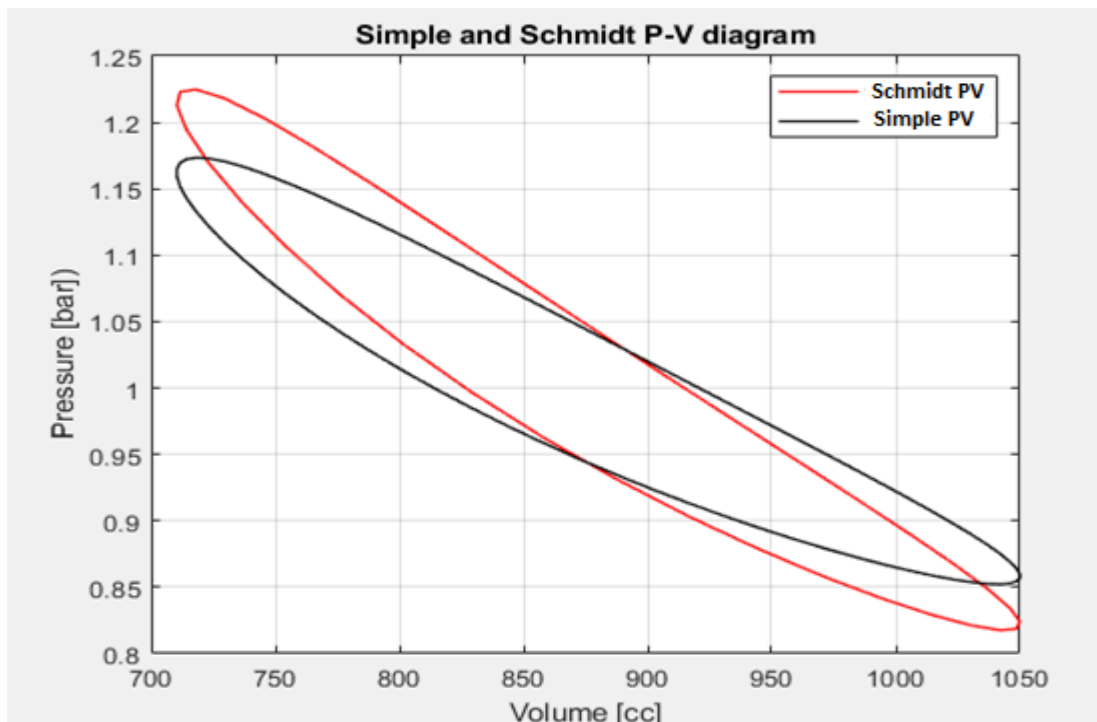


Figure 4.6: PV Diagram in the simulation

The temperature variations of the engine in Simple analysis are presented in Figure (4.7). It is noted that the temperature of compression ( $T_{comp}$ ) and expansion ( $T_{exp}$ ) space are lower and higher than regenerator temperature ( $T_r$ ), respectively. Whereas, the mean effective temperature (air temperature) for the real cooler ( $T_k$ ) and heater ( $T_h$ ) are higher and lower than the heat exchanger wall temperature ( $T_{wh}$ ) and ( $T_{wk}$ ). Therefore, the engine's power output is reduced in the actual operating temperature.

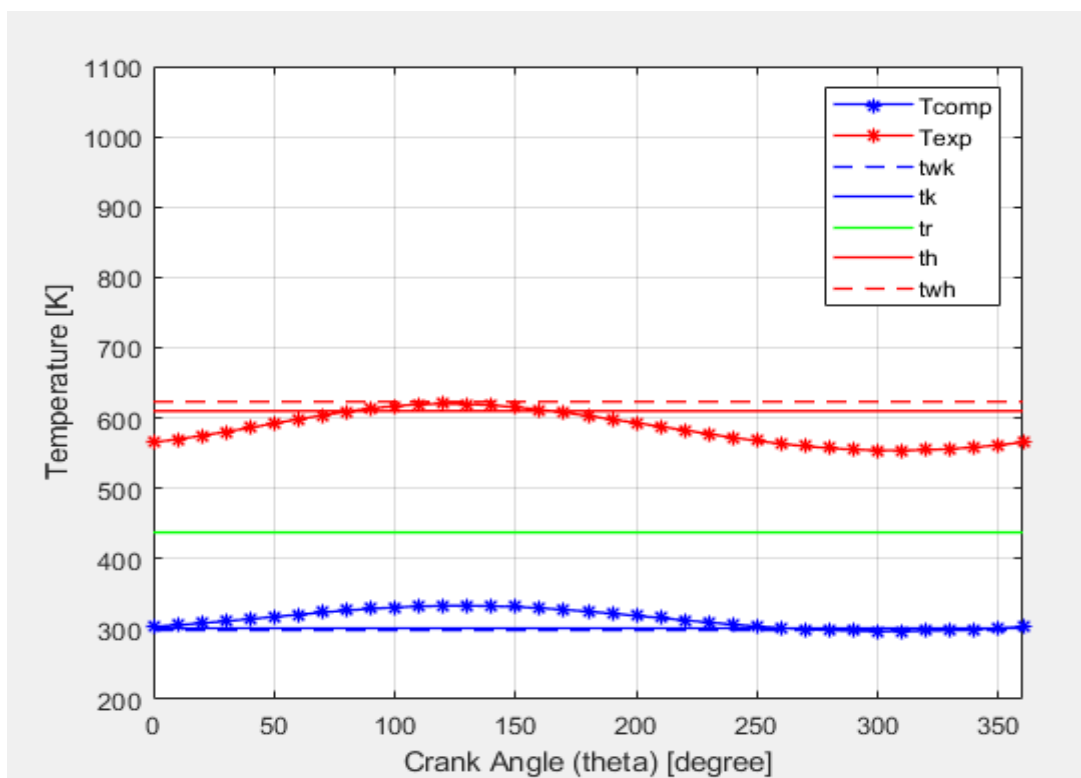


Figure 4.7: Temperature change in the engine parts in complete cycle

The heat transferred and work done over the cycle are described in the Figure (4.8). It is noted that the work done begins with the compression process and then the expansion space. Thus, the net work done at the end of the cycle is only 4 joules. Moreover, it is noted that the amount of heat transferred released in the regenerator ( $Q_r$ ) in the first half of the cycle is equal to the energy absorbed by the regenerator in

the second half of the cycle. Therefore, the net amount of heat transfer to the regenerator over the cycle is zero. Furthermore, the expansion work done ( $W_e$ ) equal to the value of heat transferred to the heater ( $Q_h$ ) at the end of the cycle. Similarly for the heat transferred to the cooler ( $Q_k$ ) and compression space work done ( $W_c$ ).

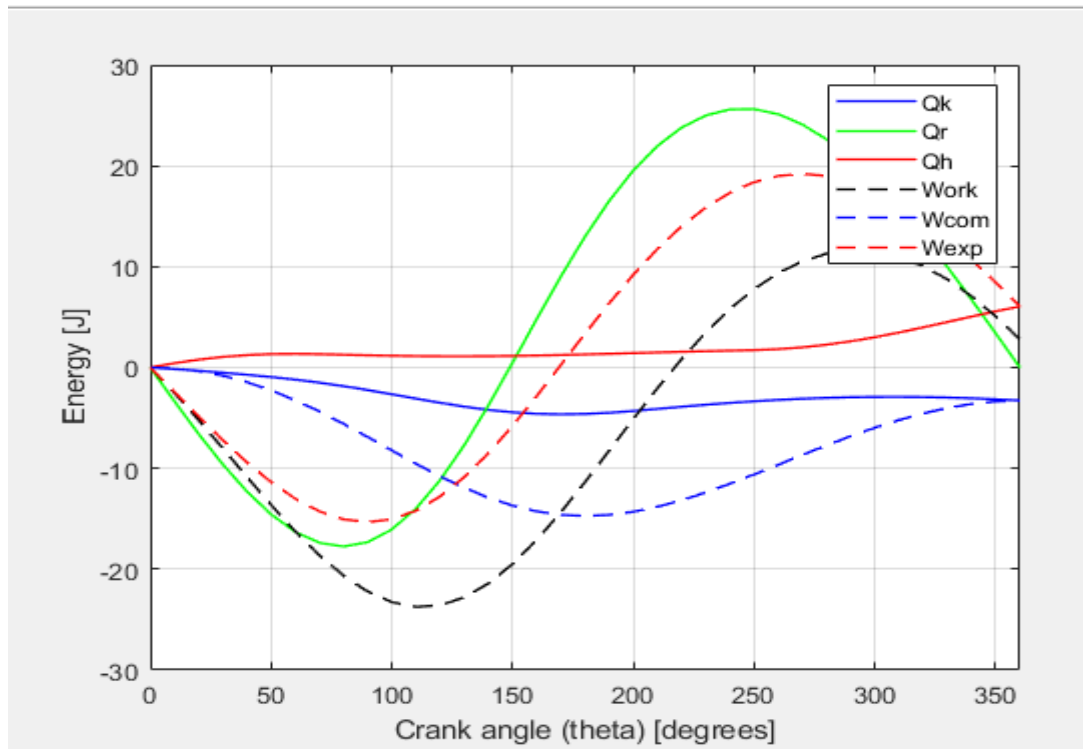


Figure 4.8: Diagram of energy and work in the engine cells over the cycle

Figure (4.9) shows the variations of pressure drop in the regenerator, cooler and heater. It is noted that the pressure drop in the regenerator is small comparing with the pressure drop in the heater and cooler. This is because of the regenerator cause the highest resistance for the mass flow air to move inside the regenerator.

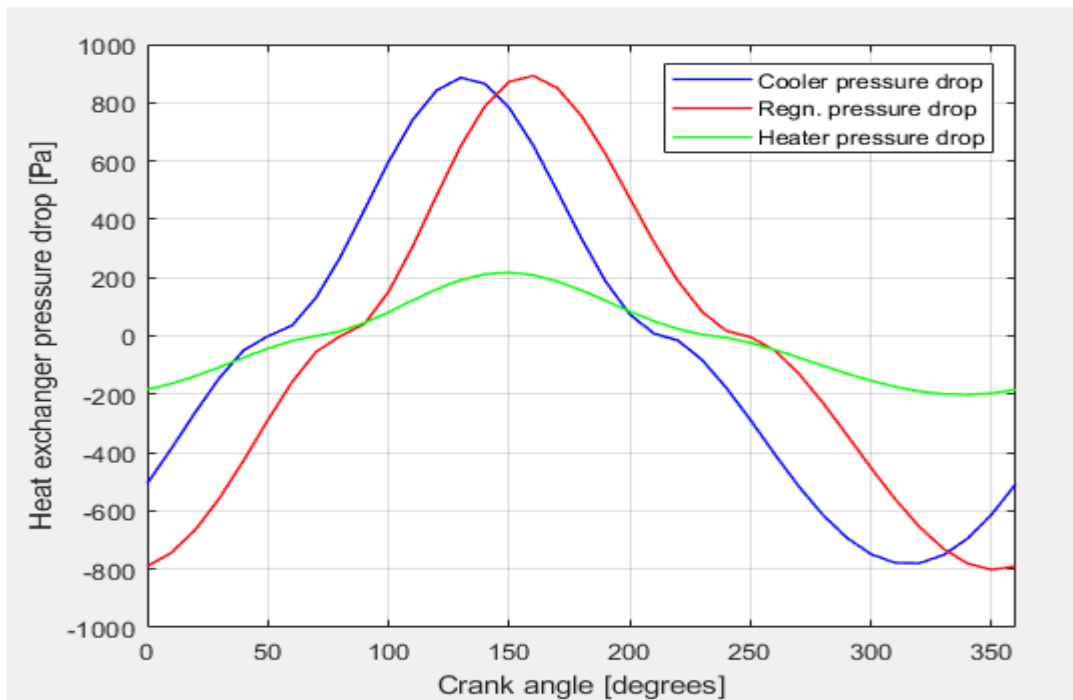


Figure 4.9: Pressure losses in heat exchanger over the cycle

Figure (4.10) presents the mass flow of air in and out of each chamber in the engine, the flow rate of the air swept between the displacer and power piston. The diagram indicates the air flow rate in the cooler which is blue, air flow rate in the regenerator which is green, air flow rate in the heater which is black and air flow rate in the expansion which is red. The assumption of quasi-steady is applied for mass calculation which the engine pressure is constant throughout the engine. The energy equation to the five cell is applied to obtain the mass flow rate within each cell depends on the direction of the flow.

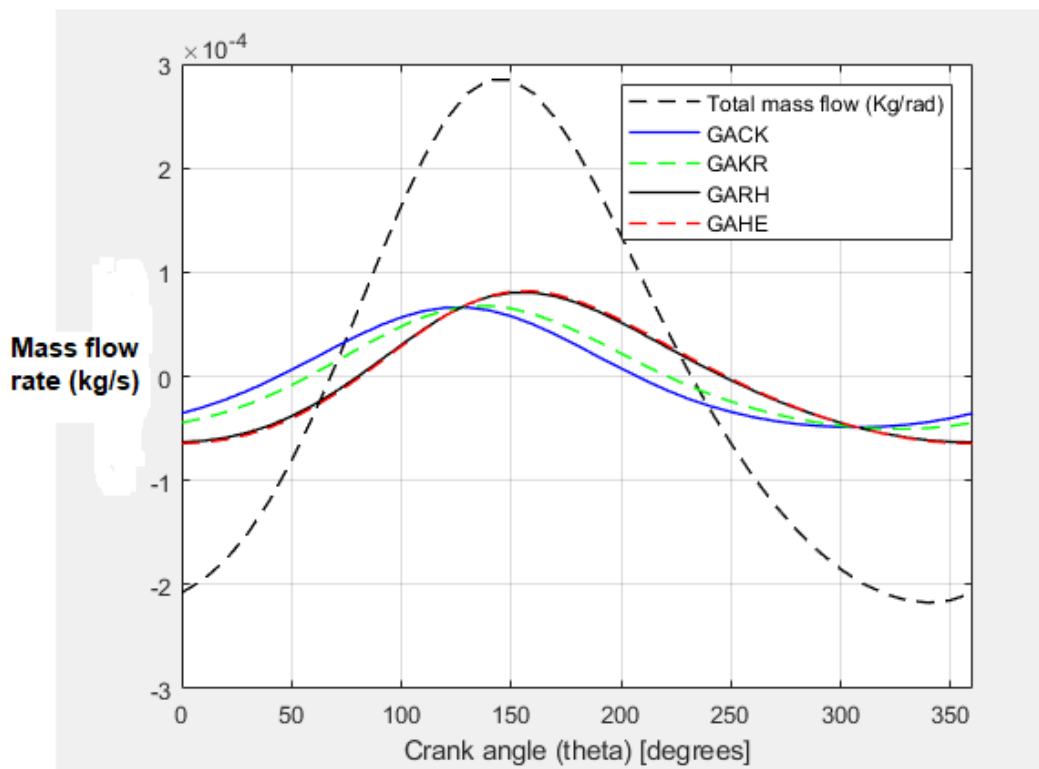


Figure 4.10: Mass flow rate in the working space over the cycle

#### 4.6 Consideration-variable frequency versus power output and efficiency:

In fact, the operating frequency is an essential parameter which affecting the performance of the engine. Consequently, the effect of operating frequency changes on the efficiency and power output is investigated. Figure (4.11) and (4.12) respectively describe the variations of operating frequency versus power output and efficiency of the engine in Schmidt analysis considering different external hot source temperatures ranging from 573K to 773K. It can be obviously seen that both figures, there is increasing of power output and efficiency, as the operating frequency of the

linear shaft increases. This is due to, the effectiveness of the regenerator in Schmidt analysis is assumed to be ideal and pressure losses is neglected.

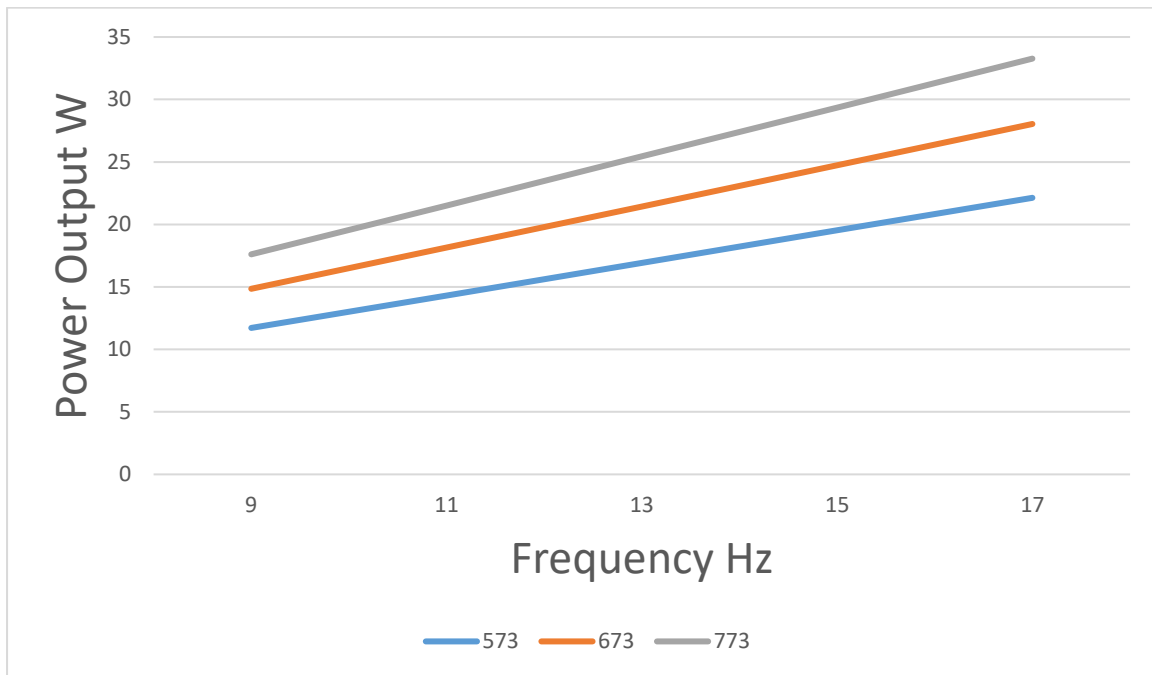


Figure 4.11: Engine Power output versus operating frequency for different values of external heat source temperature in Schmidt analysis

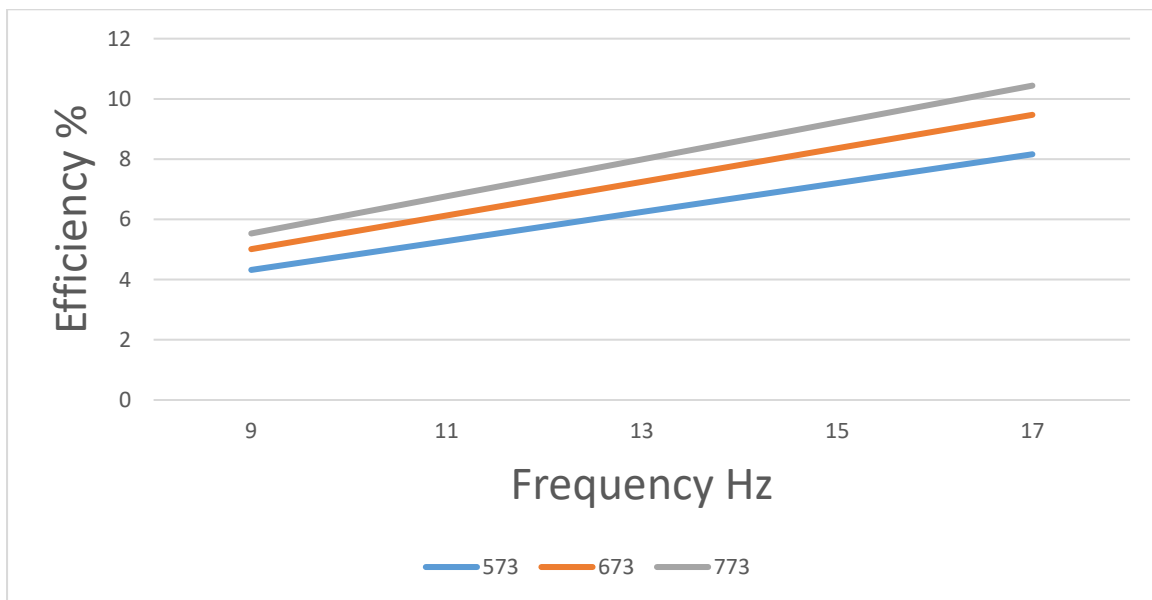


Figure 4.12: Engine Efficiency versus operating frequency for different values of external heat source temperature in Schmidt analysis

However, in figures (4.12) and (4.13) presents the result of power output and efficiency in Simple analysis. It is noted that the power output and efficiency of the engine start increasing to reach the peak point then begin to decrease rather than increasing. This is due to increasing the frequency lead to speed the air inside the engine. Therefore, as the speed of air increasing the heat losses in the engine will be increased. As mentioned before Simple analysis consider pressure drop in all heat exchanger, the power output of the engine expressed as:

$$\text{Output power} = W_{\text{power}} - \Delta p * \text{freq}$$

Where ( $\Delta p$ ) is the pressure drop in heat exchanger of the engine. Moreover, as it can be seen from figure (4.12) the optimum operation frequency at 573 k is 11 Hz which gives the highest power output. However, at heat in temperature of 773 k, the optimum operation frequency can be applied is 15 Hz. These indication can be used to design the engine in terms of operating frequency and temperature. It is concluded that Simple analysis is more realistic model to design the engine than Schmidt analysis which takes the heat losses in the system.

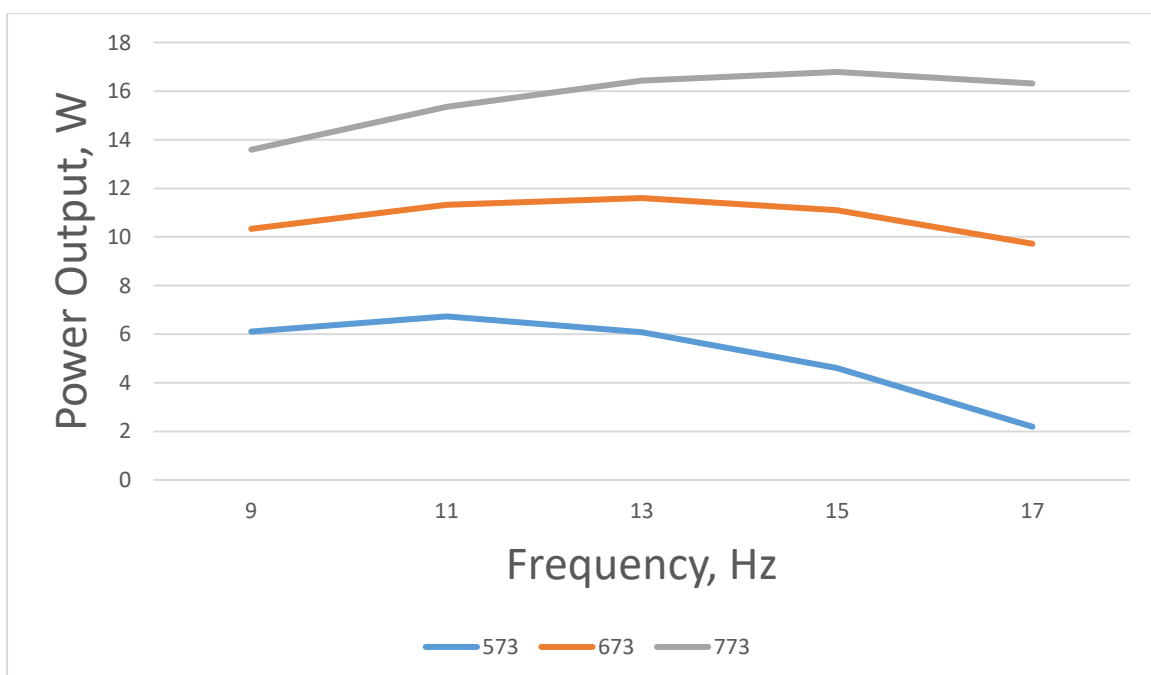


Figure 4.12: Engine Power output versus operating frequency for different values of external heat source temperature in Simple analysis

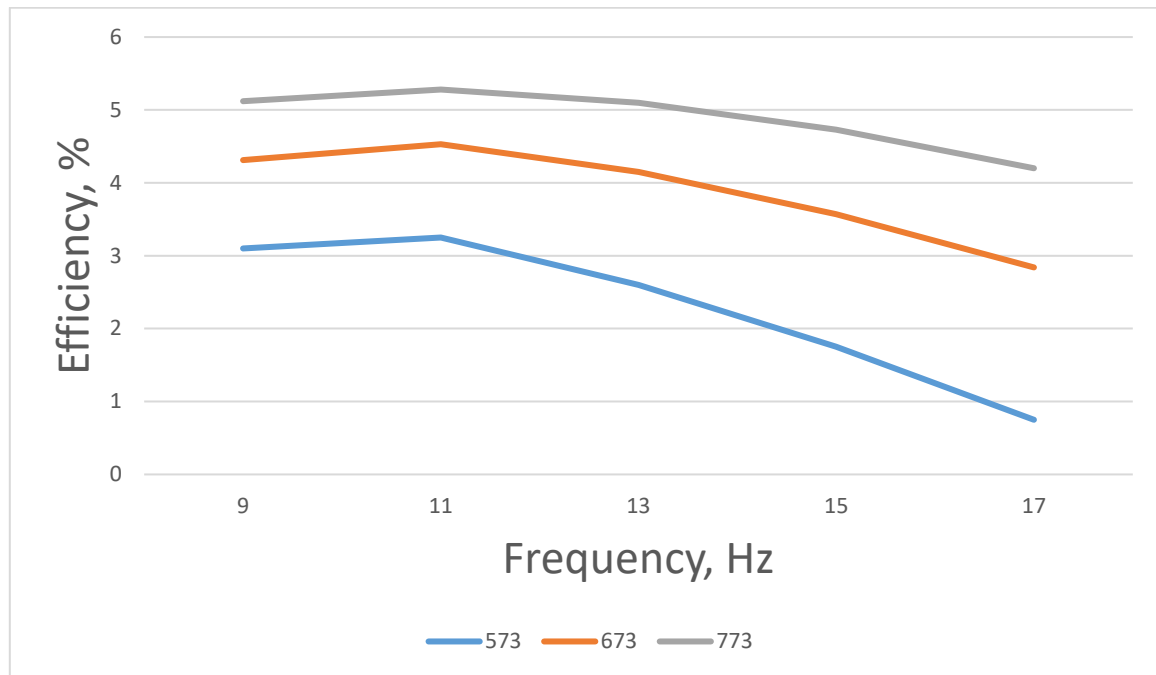


Figure 4.13: Engine Efficiency versus operating frequency for different values of external heat source temperature in Simple analysis

#### 4.7 Consideration-variable stroke versus power output and efficiency:

Figure (4.14) and (4.15) present the outcome of the power output and efficiency against increasing stroke of the engine in both analysis Schmidt and Simple modelling. The operating frequency and heat in have set up at 11 Hz and 573 K, respectively. It is obviously can be seen that the power output and efficiency increases, as the value of stroke increases. Increasing the stroke lead to increase the swept volume of the engine cylinder. Moreover, it is noted that the power output and efficiency of the engine in Simple analysis is less than Schmidt analysis, due to Simple analysis consider the heat losses in the engine as discussed before.

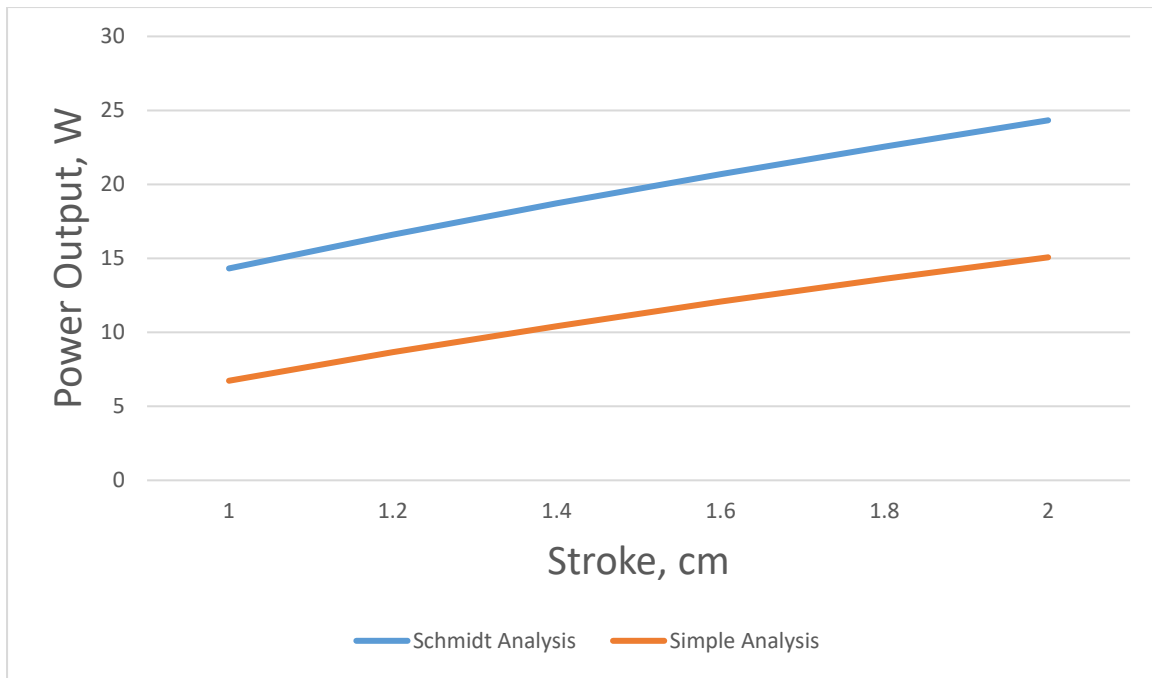


Figure 4.14: Engine Power output versus variable stroke in Schmidt and Simple analysis

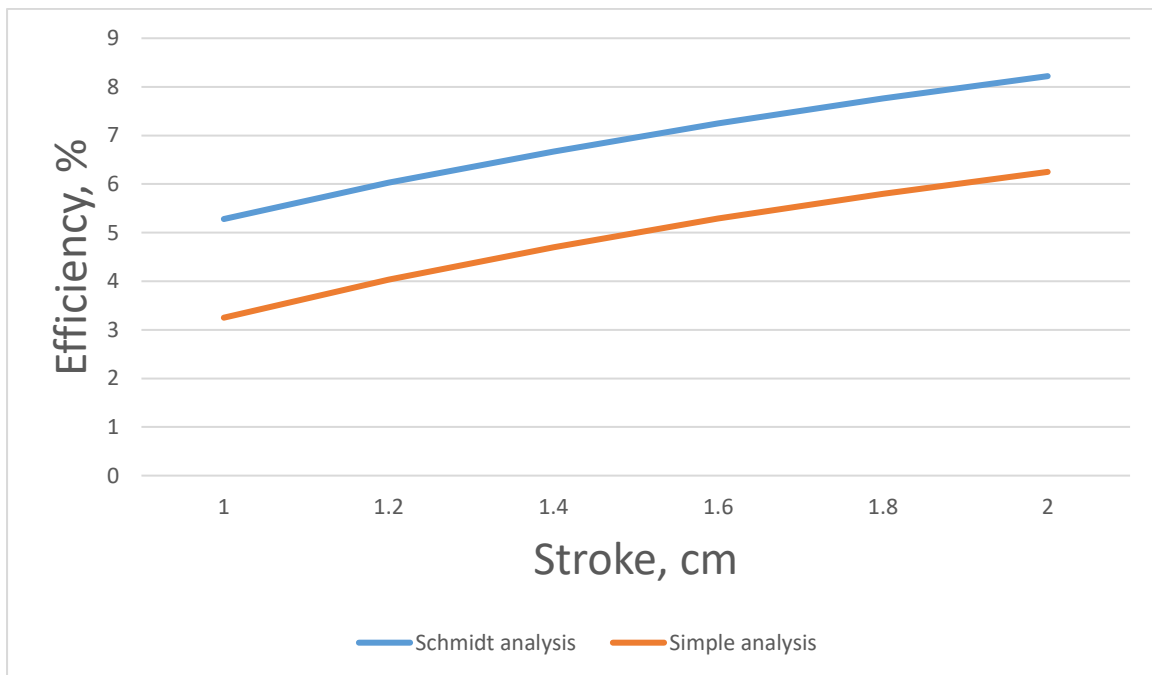


Figure 4.15: Engine efficiency versus variable stroke in Schmidt and Simple analysis

## 4.8 Consideration-variable pressure versus power output and efficiency:

Figure (4.16), (4.17) describe the variation of pressure inside the engine against power output and efficiency in Schmidt and Simple analysis. It is noted that the power output of the engine can be reached up to 10 W at 2 bar in Simple analysis. However, the pressure should not exceed the maximum range. Where the range of pressure between 1 to 2 bar will be applied in the experimental work.

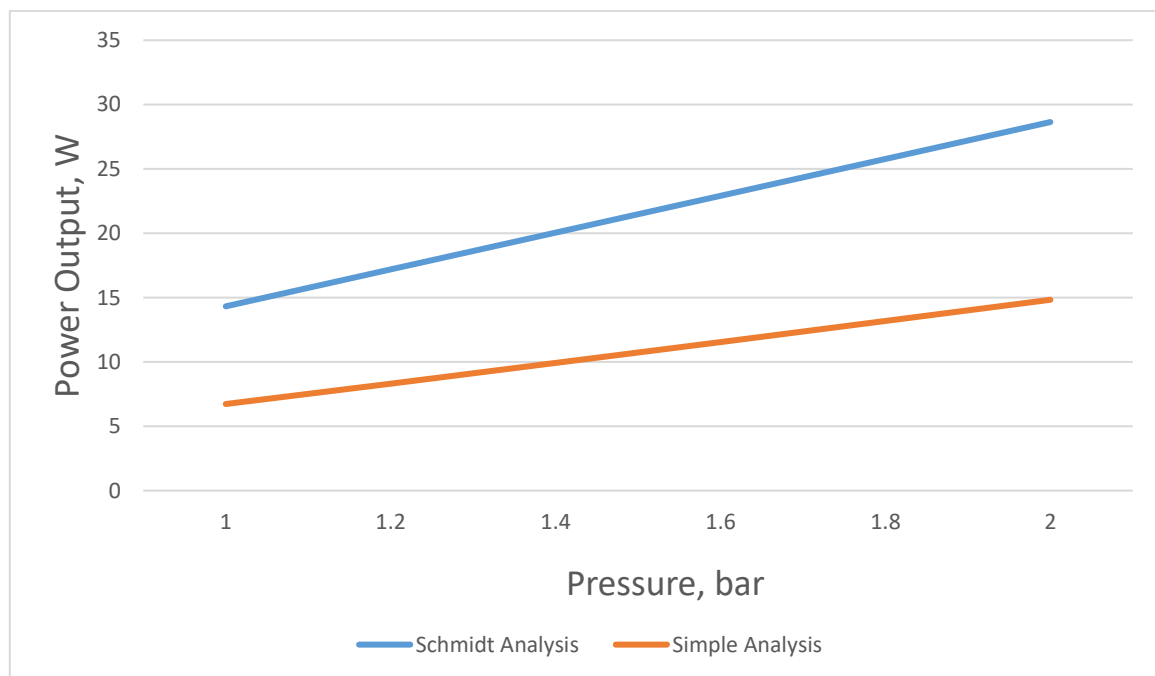


Figure 4.16: Engine Power output versus variable pressure in Schmidt and Simple analysis

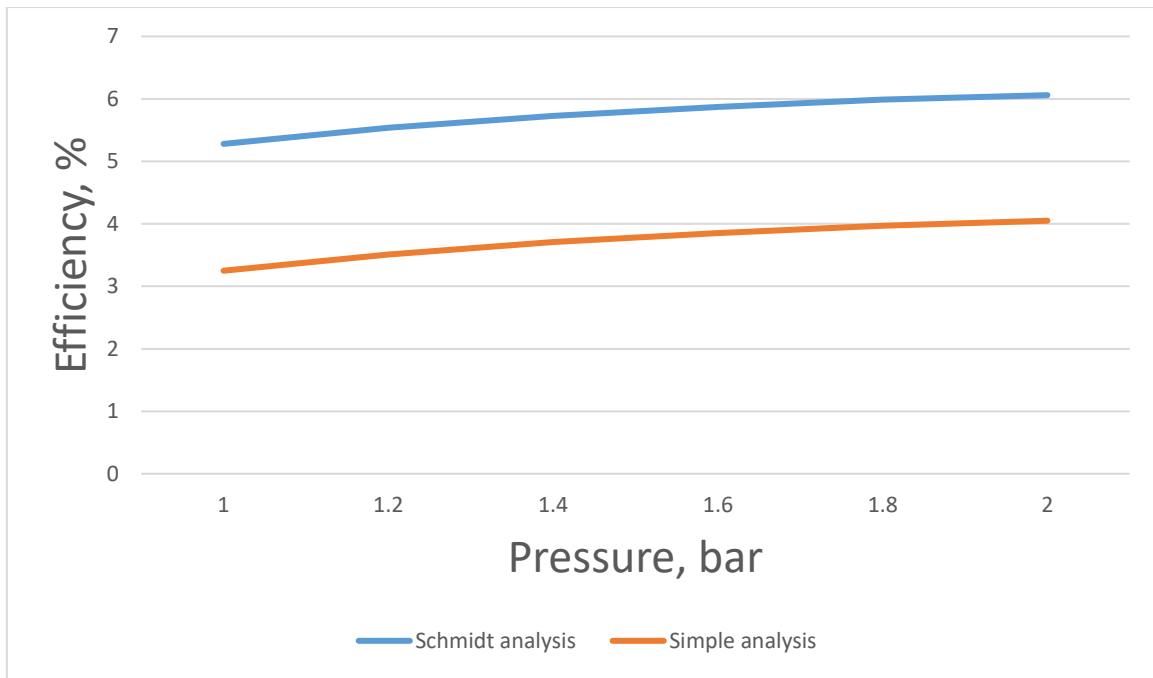


Figure 4.17: Engine efficiency versus variable pressure in Schmidt and Simple analysis

# Chapter 5:

## The proof of concept engine design, fabrication and assembly

### 5.1 Introduction:

The design of engine components and layout arrangements were manufactured to keep the production process simple and reduce component costs. The following factors were considered in the selection and size of the engine parts:

- Choose simple parts which make the assemble and dis-assemble easy for maintenance and experience testing.
- Follow a suitable manufacturing process with available tools in the workshop.
- Fabricate the design of components to be suitable for mathematical modelling.

The main challenge in this Free piston Stirling engine design was the pressure seals for the piston. The pressure seal was the weakest link in the engine's design as the thermal efficiency and the power output are proportional to both the mean engine pressure and the mass of the working fluid. Also, several layouts and structures of the dynamic components were considered and tested. However, all the parts are assembled into a functioning engine based on the parameters of computer model developed in Chapter 5.

The main design objectives of building the engine in terms of energy performance are:

- Make the displacer design as light as possible.

- Eliminate friction and mechanical seals between the displacer and the power piston.
- The displacer can be moved at atmospheric pressure.
- Operate the engine at low variant temperature.
- Reduce the air leakage from the expansion to compression space.
- Minimise the dead volume in the engine.

## 5.2 Engine design and configuration:

In this work, a simplified mechanical design of the displacer and power piston assembly and manufacture is proposed. The design mechanism is linear mechanical oscillation produced from a power piston and displacer in a housing cylinder without mechanical linkage. The novel design aims to present several of drawbacks associated with the engine, such as friction losses caused by moving parts, pressure losses in the power piston and heat losses. Moreover, the concept of novel design is proposed and installed to the FPSE, which aims to increase the engine's efficiency and apply output application such as water pumps and power generation.

The proposed design of the displacer component is integrated into mechanical support springs with long service life. However, two different designs for the power piston were considered and tested, using the flexure bellows and the rubber diaphragm. The prototype is manufactured as illustrated in Figure (5.1). The engine has two essential components which are the displacer and power piston. The displacer and its cylinder are fabricated from stainless steel material. The novelty of the design is based on using two helical springs installed inside the displacer to align the displacer reciprocating and for the use of power piston movement. The bellow represents the power piston which made from rubber, for low friction and durability.

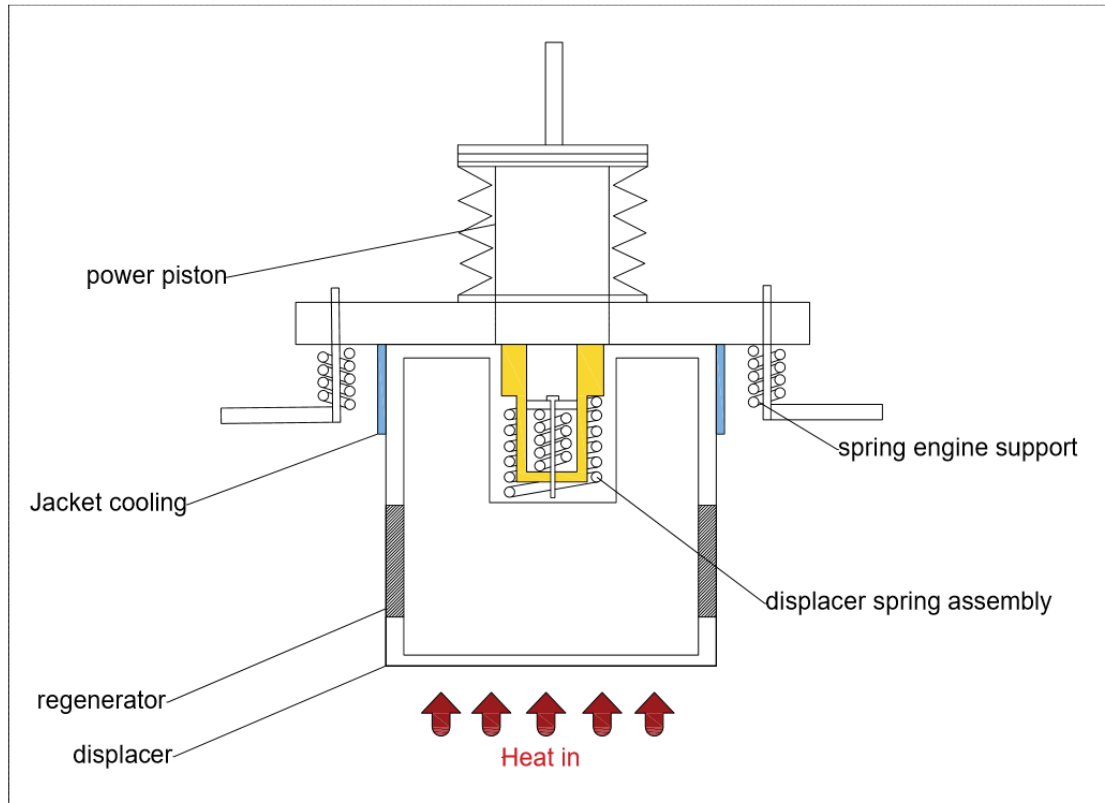


Figure 5.1: The main parts of the engine design

The working fluid used in this design is atmospheric air which must be sufficiently heated to expand and push the displacer outward the appropriate distance for the engine to operate. As shown in figure 5.1, the regenerator in the proposed design of FPSE works as an internal heat exchanger, located between the hot and cold parts of the engine. The working fluid (air) flows over it in both directions, storing heat from one cycle to be used in the next cycle. That mean, the regenerator is designed to recycle the heat within the FPSE.

### 5.3 Displacer assembly manufacturing:

The displacer is one of the essential component of the engine, the design has to be light in weight, high operating temperature material and utilise a low thermal conductivity. The design of displacer is a simple hermetically sealed cylinder. The

diameter of displacer cylinder and displacer is designed to be large and the stroke of the displacer is short, therefore, the swept volume ratio from displacer to power piston is large. Moreover, the effective heat transfer surfaces on the displacer cylinder's hot and cold end plates are large, and engine speed is low [126]. A cylinder cavity on the upper surface contains the displacer assembly that includes two springs. The mechanical spring consists of brass support and two helical springs. Moreover, both springs are installed under a pre-compressed position to maintain the proper position of the displacer and align the displacer's oscillation during negative and positive directions. The displacement of working fluid between hot and cold ends of the displacer is accomplished via holes bored across the displacer, see figure 6.3.

### **5.3.1 Mechanical spring selection:**

The displacer oscillations can be occurred in FPSE because of the mechanical spring movement. However, several spring forms can take, such as a planer, helical or flat springs. A coiled compression spring is used in the displacer design that withstands the axial compressive load and can be used in a pre-compression setting even when the engine is not working to keep the displacer in the correct location, as shown in Figure 5.2.



Figure 5.2: Inside the helical spring of the displacer

The displacer cylinder was made from stainless steel to resist high operating temperature and low thermal conductivity. The displacer's specification parameters, including the inner and outer diameter, and stiffness of the spring material, were obtained from the manufacturer's standard sizes and specification data sheet. The cylinder wall was designed to be 1 mm thick, which reduces its overall mass.

Figure (5.3) presents an unassembled displacer made of seven components. The novelty of the displacer design is based on using two outer and inner helical springs installed inside the displacer flange which made the displacer always pre-compressed.



Figure 5.3: The components of the displacer

- 1) Displacer cylinder
- 2) Cylinder flange
- 3) Displacer piston
- 4) Spacer
- 5) Outer spring
- 6) Innerspring
- 7) Pin connector

Figure (5.4) shows how the displacer parts are combined, and the whole displacer clamped to the engine body. The spacer disc has used to connect the engine body with the displacer. A fully assembled displacer block is ready to be fitted in the displacer cylinder. Cooling and heating are obtained by making the diameter of the displacer slightly less than that of the cylinder to create a small annulus of air to flow

between the expansion and compression spaces. This small annulus allows effective heat transfer between the wall and working fluid.



Figure 5.4: The combined displacer with the cylinder

#### 5.4 Power piston:

The power piston is the moving component made of rubber bellows, which converts the output power of the thermodynamic cycle into electricity. The bellows are made from a suitable rubber hardness to provide the required mechanical stroke and

minimise internal losses. The bellows were designed to achieve a specific displacer stroke and operating frequency.

#### **5.4.1 Design of Bellows and sizing:**

The expansion bellows are a cylindrical part with a corrugated wall with high pressure and torsion. The rubber bellows are both flexible and robust to pressure. The bellow has flexible axial, lateral and angular deformation due to the corrugations. Once properly constructed, the bellows is durable and will work safely for a long time without requiring maintenance. The bellow's flexibility and number of cycles, on the other hand, are determined by the material used and the load applied.

The size of the bellows is essential to maintain dynamic stability and life expectancy. The design considers outer and inner diameter, bellows length, stiffness, and several convolutions. The bellows is clamped directly on the top of the cylinder, while the top bellows is connected to the linear drive shaft for output, as shown in Figure 5.5. Moreover, a small magnet of weight was added to the output drive shaft to match the power piston's resonance frequency and the displacer's resonance frequency, which gives optimum operating frequency.

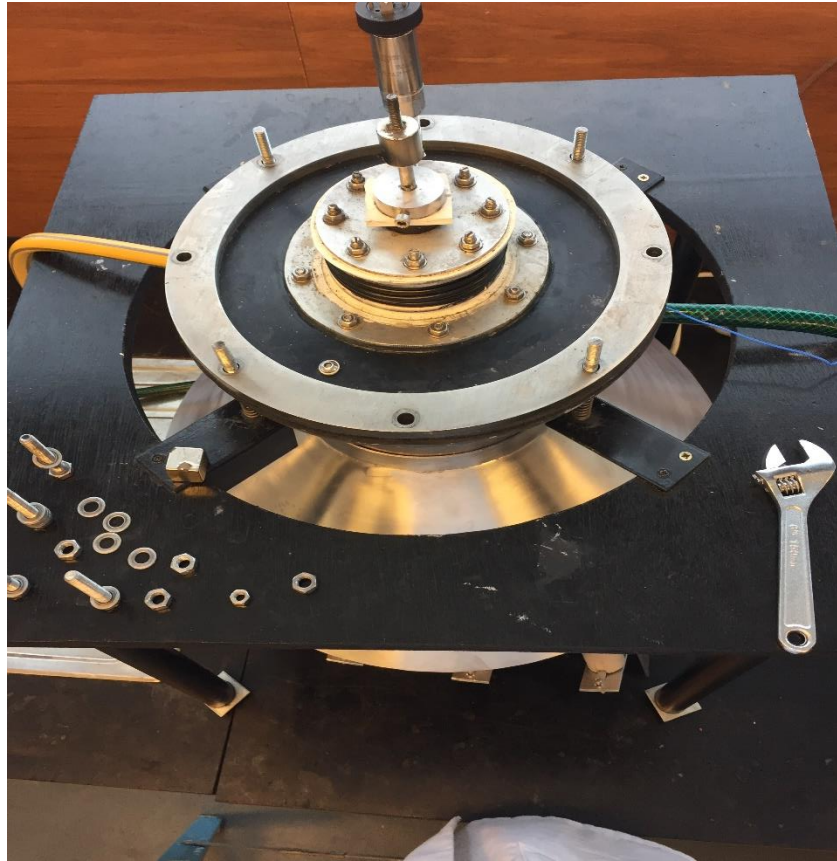


Figure 5.5: Power piston of bellows design

#### **5.4.2 Fabrication process:**

Two plate forming and seal welding operations are used to install the bellows on the top of the engine. The mechanical pressure and forming method formed bellows, known as convoluted bellows. There is a piston inside the bellows that is free of movement to compress the working fluid at the cold end temperature.

#### **5.4.3 Movement and Deflection:**

The bellows have a lot of deflection and movement. Axial, lateral, and angular motions are all included. To generate an axial deflection and supply the axial stroke, the bellows have been installed and tightened by eight screws and bolt from the top and the bottom, making the bellows compressed and expanded in an axial line. The inner piston of the bellows typically performs the compression and expansion

movement. Also, a stainless steel support guide is installed above the engine to prevent the power piston's sideways motion.

#### 5.4.4 The characteristics design of Bellows:

Several design aspects must be considered when contemplating bellows as a power piston. The essential design characteristics that must be regarded while selecting, sizing, and implementing bellows as a power piston in engineering applications are listed in Table 5.1:

**Table 5.1: The design characteristics of the bellows**

Properties	Description
Operating pressure	Consider the maximum pressure inside the bellows
Operating temperature	The maximum operating temperature is usually around 400C°
Axial movement	The number of convolutions determines the total axial movement, which gives dynamic stability.
Geometric limitation	It considers the bellows size restrictions such as the maximum length, outer and inner diameter.

#### 5.4.5 Diaphragm power piston manufacturing:

In the proof-of-concept prototype, a flat rubber diaphragm was designed as the power piston. The diaphragm has been made of rubber hardness to reduce internal losses and provide the requisite stroke. Two flanges are utilised to install the diaphragm across the prototype circumference, fastened with bolts. Figure 5.6 shows the design of the diaphragm, which is installed with the shaft loading to transfer the oscillation of the diaphragm to output power loading.



Figure 5.6: Diaphragm of engine power piston

### **5.5 Engine casing cylinder:**

The casing cylinder is designed to contain the displacer and the regenerator, where the regenerator is installed between the cylinder and the displacer. The bottom surface of the cylinder absorbs the heat supply and rejects the heat through the engine. The thickness of the cylinder is 1 mm, made of stainless steel sheet. The outer and inner diameters of the cylinder are 200 mm and 199 mm, respectively and 190 mm height.

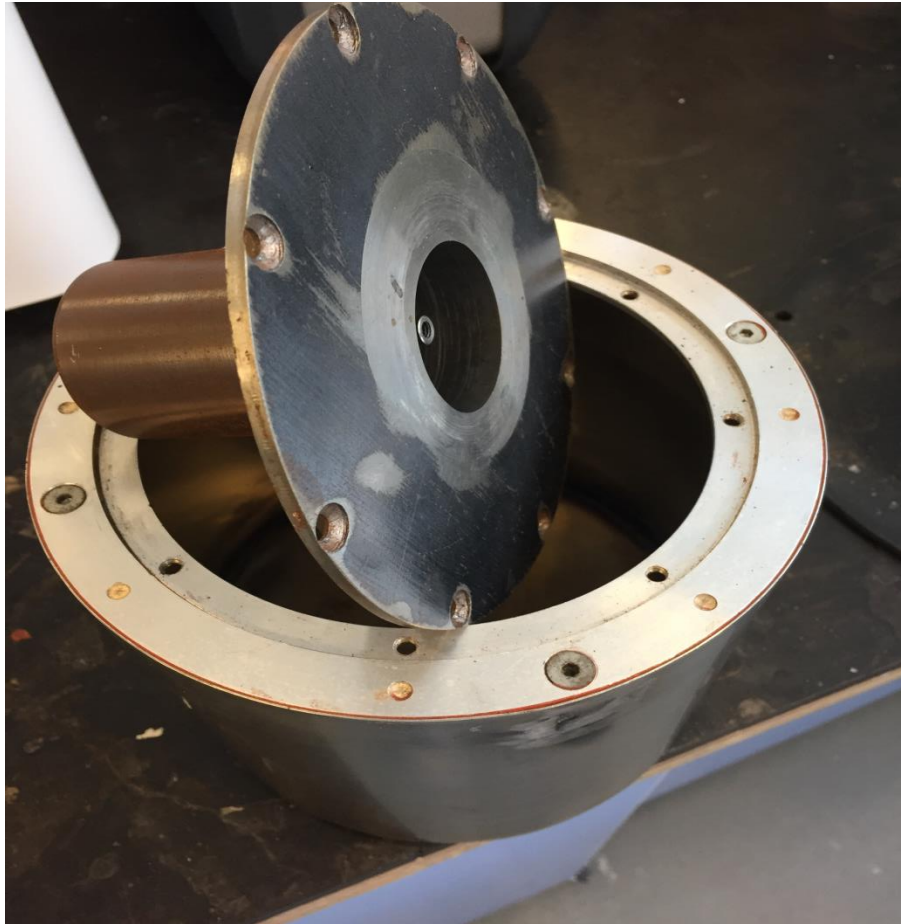


Figure5.7: The engine casing cylinder

## 5.6 Cooling coil:

The design of cooling coil made of nine copper loops with 10 mm diameter which cooled the half upper of the cylinder. However, the coiled design has limitations, where the tube is installed around the cylinder without welding, limiting the heat transfer. Moreover, the bottom two loops located around the expansion space which reduce the hot side temperature, as shown in figure (5.8).



Figure 5.8: Cooling coil design

## 5.7 Regenerator:

The regenerator made of a layer of stainless-steel blanket mesh that installed and filled 2 mm gap between the displacer and the cylinder. The heat is transferred from the simulator to the regenerator part and then transferred to the cold part does not happen simultaneously. During the first half of the thermodynamic cycle, the working fluid coming from the heater enters the regenerator at a hot temperature, ( $T_{h,in}$ ), and comes out at a very low temperature, ( $T_{h,out}$ ). In this process, the temperature of the regenerator is slightly lower than the temperature of the heater. Therefore, the regenerator absorbs some heat and stores it for the thermodynamic cycle's next half. After that in the second half of the cycle, the working fluid coming from the cooler enters the regenerator at low temperature,  $T_{k,in}$ . In this case, the regenerator temperature is slightly higher, allowing the regenerator material to return most of the stored heat and raise its outlet temperature  $T_{k,out}$ .

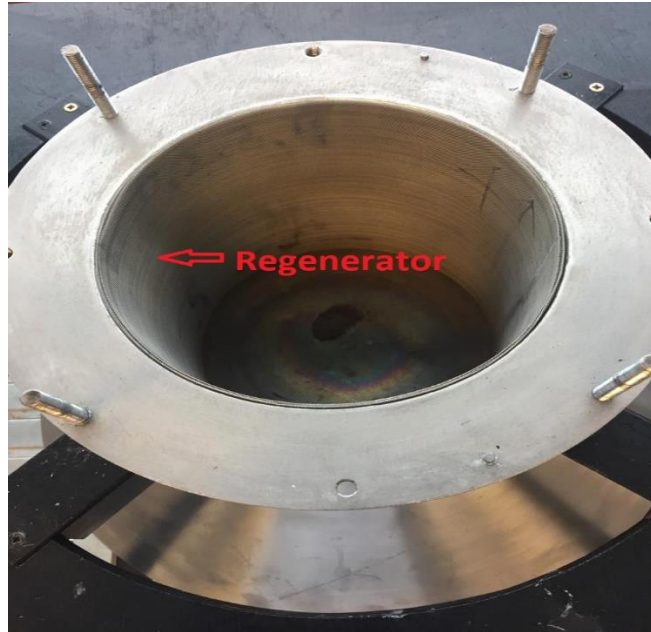


Figure 5.9: The regenerator inside the displacer cylinder

## 5.8 Solar simulator:

The solar simulator that used to heat the engine is 16 halogen bulbs with 100 W each. The simulator installed below the engine which simulate the dish reflector of solar rays. The spectrum of the light ray is 700 nm wavelength. Figure (5.10) presents the spectrum distribution of daylight comparing with several common bulb types. Therefore, it confirms that the spectrum of halogen bulb is the closest spectrum to the daylight.

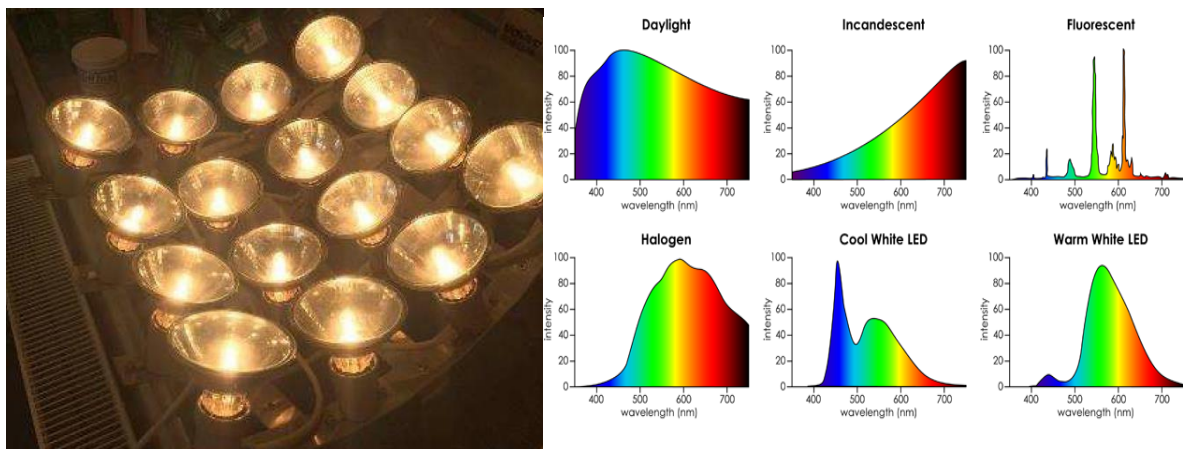


Figure 5.10: Solar simulator

In this project, the solar simulator performs as parabolic mirror concentrator that used for focusing the solar radiation into the receiver, then the radiation will reflect and focused at a focal point. Therefore, it is essential to consider the focal length or the distance of the focal point from the concentrator which can be calculated by using the below equation[126]:

$$\frac{f}{D_{co}} = \frac{1}{4\tan\left(\frac{\phi_{rim}}{2}\right)}$$

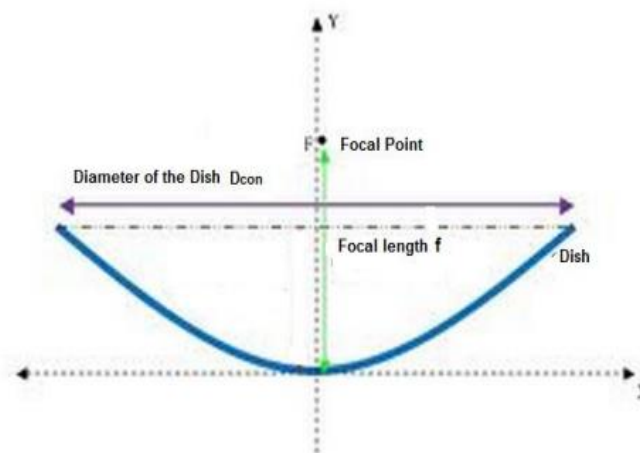


Figure 5.11: The focal point, diameter of concentrator and the focal length of concentrator

## 5.9 Cover Simulator:

The important feature of the solar simulator is to reflect as maximum as possible of energy to the working fluid with minimum loss. Therefore, the design of cover simulator with 190mm diameter and 45 degree shape has been installed around the Stirling cylinder, in order to increase the amount of solar radiation. Moreover, infrared camera is utilised to to ensure the thermal energy is delivered to the Stirling engine. The working fluid temperature also has increased from 350°C to 375°C with cover simulator.

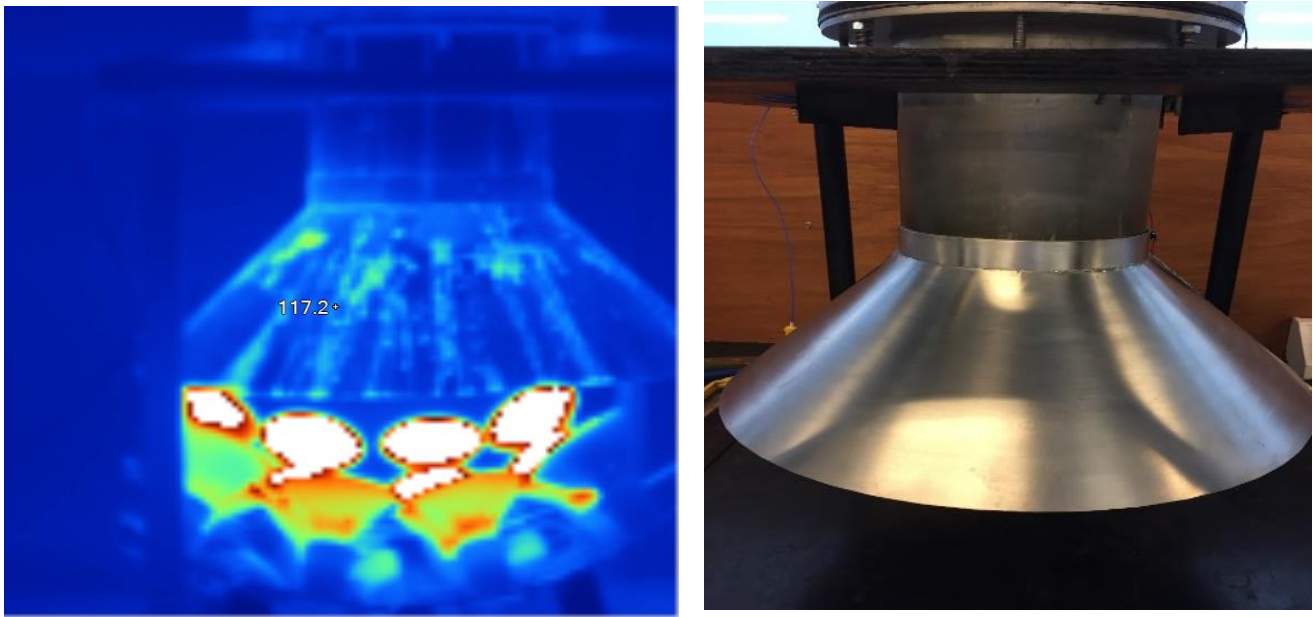


Figure 5.12: Cover simulator of the engine

### 5.10 Water jacket:

In order to keep the compression space area at low temperature, a water jacket with 192mm inside diameter was added to its outer surface. The water jacket was made by rolling sheet stainless steel metal with two inlet and outlet holes that welded on the cooler section. The two holes of the water jacket installed opposite each other and two tubes are connected over these holes which allow to supply the water through the water jacket, see figure (5.13).



Figure 5.13: Water jacket cooling design

### 5.11 Engine supporting frame:

The engine body was supported by a support frame comprised of a wood base plate and four threaded steel holes. The engine body is hanged by using four threaded rods with springs connected direct to the base plate, as shown in Figure 5.14.

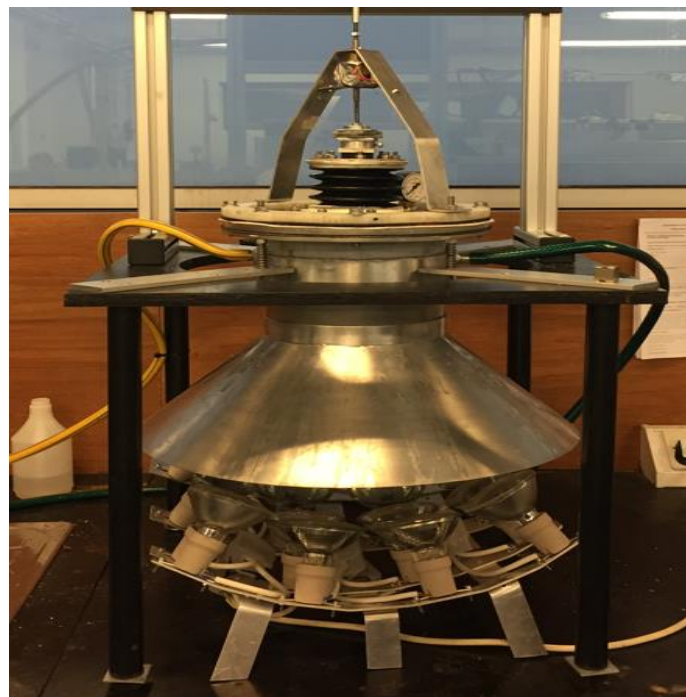


Figure 5.14: The support frame of the engine

## **5.12 Linear to rotary motion conversion mechanism:**

### **5.12.1 Introduction:**

The known mechanisms for converting linear motion to rotary motion have had one or more severe drawbacks up to this point. The most common applications of shaft with offset crank throws and connecting rods pivoted directly to a piston or a crosshead, are examples of such devices. Because of the angularity of the connecting rod or its equivalent part, most of them have varied thrust in one revolution. Moreover, the piston speed curve has a sinusoidal shape and the sine curve representing transmitted torque from the piston to the crankshaft due to the angularity of the connecting mechanism. However, the present design invention eliminates all thrust fluctuation by eliminating the angularity of the connecting mechanism between the piston and the shaft.

### **5.12.2 Advantages:**

This novel design relates to the mechanism for converting linear motion to rotary motion without using a crankshaft. There are several advantages of rotary motion compared with linear motion such as:

- Converting linear to rotational motion is useful in many different applications such as control systems.
- Rotary motion in any drive mechanism is always in an infinite loop, however, the drive initiation of linear motion must begin from where it left off.

## **5.13 Structural configuration of the prototype platform:**

Figure 5.15 presents the structural configuration of the prototype design based on the concept mentioned above. The prototype design consists of three principal units:

a linkage unit, where the bottom conrod part was connected with linear output shaft of the engine. Secondly, transfer unit that transfer the motion of linear output shaft to the final unit which is driving unit, where the unit has two (one way) bearing inside the lever housing.

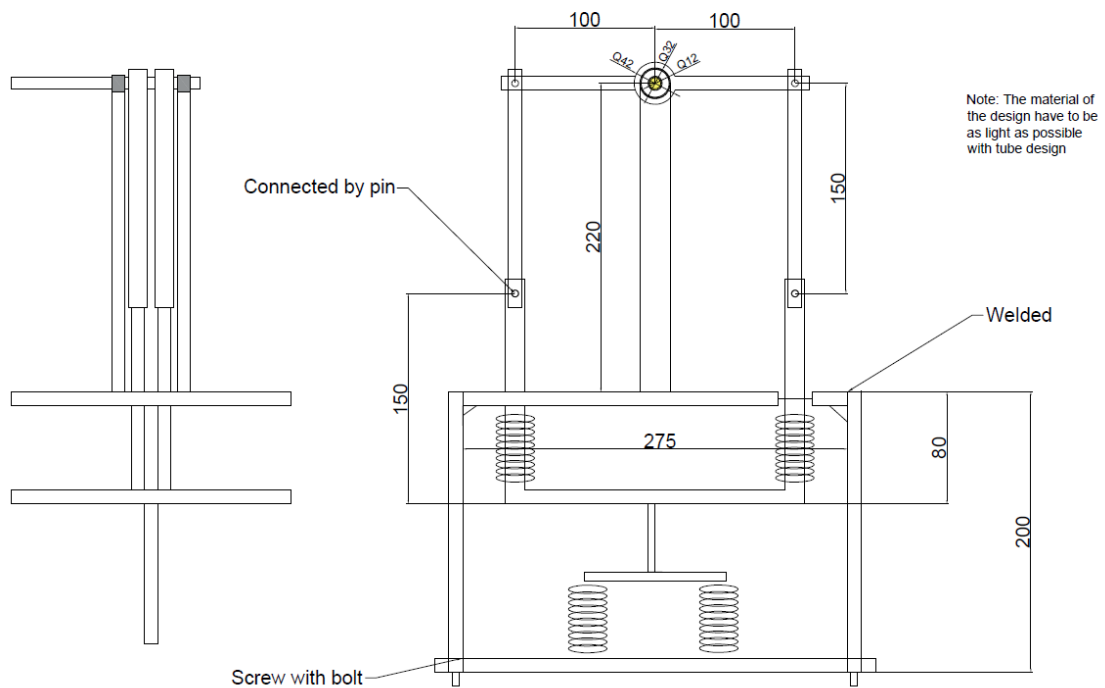


Figure 5.15: The diagram configuration of the prototype

#### 5.14 The purpose of the design:

The main aim of the design is to convert linear motion of the output shaft to rotary motion, which can be used for power generation or water pumping and increase the output and the efficiency of the engine. As it can be seen from the figure below:

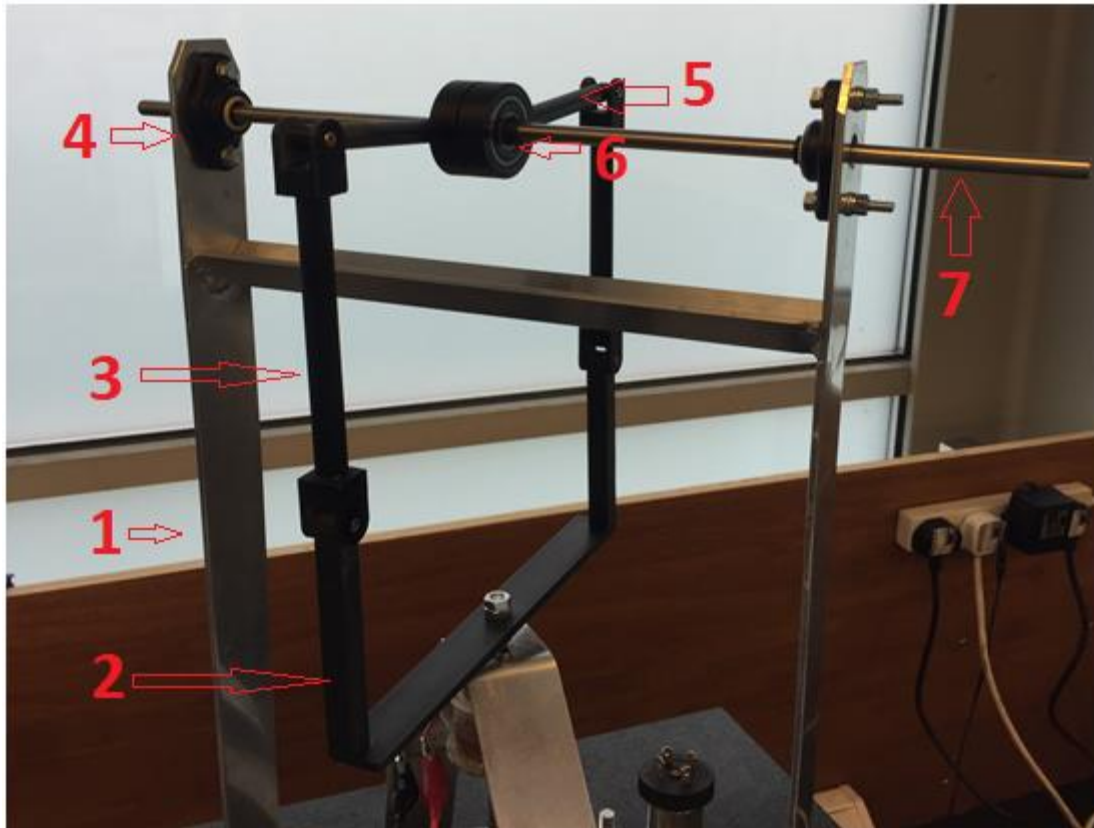


Figure 5.16: Two (one way bearing) design

1. Design support.
2. Conrod (1).
3. Conrod (2).
4. PTFE bearing.
5. Lever.
6. One way bearing.
7. Rotary shaft.

The key feature of the design that has two (one way bearing) which fixed in the same direction on the output shaft. The two bearings are connected by two levers and conrods. When the shaft of the rig goes up down, the output shaft turns in one direction.

### 5.15 The Lever design:

As shown in Figure 5.17, the two levers are designed to hold the one-way bearings on the shaft, where the conrods connect the levers. The lever is used to transfer forces between points. It transfers the motion from the linear shaft to the rotary shaft by means of joint connected to the small end of the lever.



Figure 5.17: The lever design

### 5.16 The Conrods design:

It is connected from the exist linear shaft of the engine to the lever of the design, also the conrods design constructed from two parts (compass design), due to the movement of the engine shaft is not exactly linear motion, so the design has a flexibility to convert linear motion to rotary motion without any friction.



Figure 5.18: The conrods design

## 5.17 Bearings:

The type of bearings are called Sprag clutch one way bearing with keyways (12\*32\*10 mm). The characterise is ability to turn in one direction only.

Table 5.2: Sprag clutch one way bearing specifications

Specification	Value	Unite
D	12	Mm
D	32	Mm
L	10	Mm
Torque	9.3	Nm
n max	10000	Rpm
Dynamic load	6.1	kN
Static load	2.77	Kn
Weight	0.04	Kg
Drag torque	0.7	Ncm



Figure 5.19: Sprag clutch one way bearing

### **5.18 Summary:**

In this chapter, the manufacturing and design of the proposed solar free piston Stirling engine using bellows or a rubber diaphragm as a power piston was discussed in detail. The selection and configuration of the engine parts as well as assembling of the engine components into a complete FPSE ready for experiment were fully described.

# Chapter 6:

## Experimental set up of assembled engine

The FPSE test and the procedures of experimental testing on the FPSE are presented in detail. Moreover, the measurement of operating parameters of the FPSE are shown. The fully-assembled engine and equipment with measuring instruments are presented in Figure (6.1).

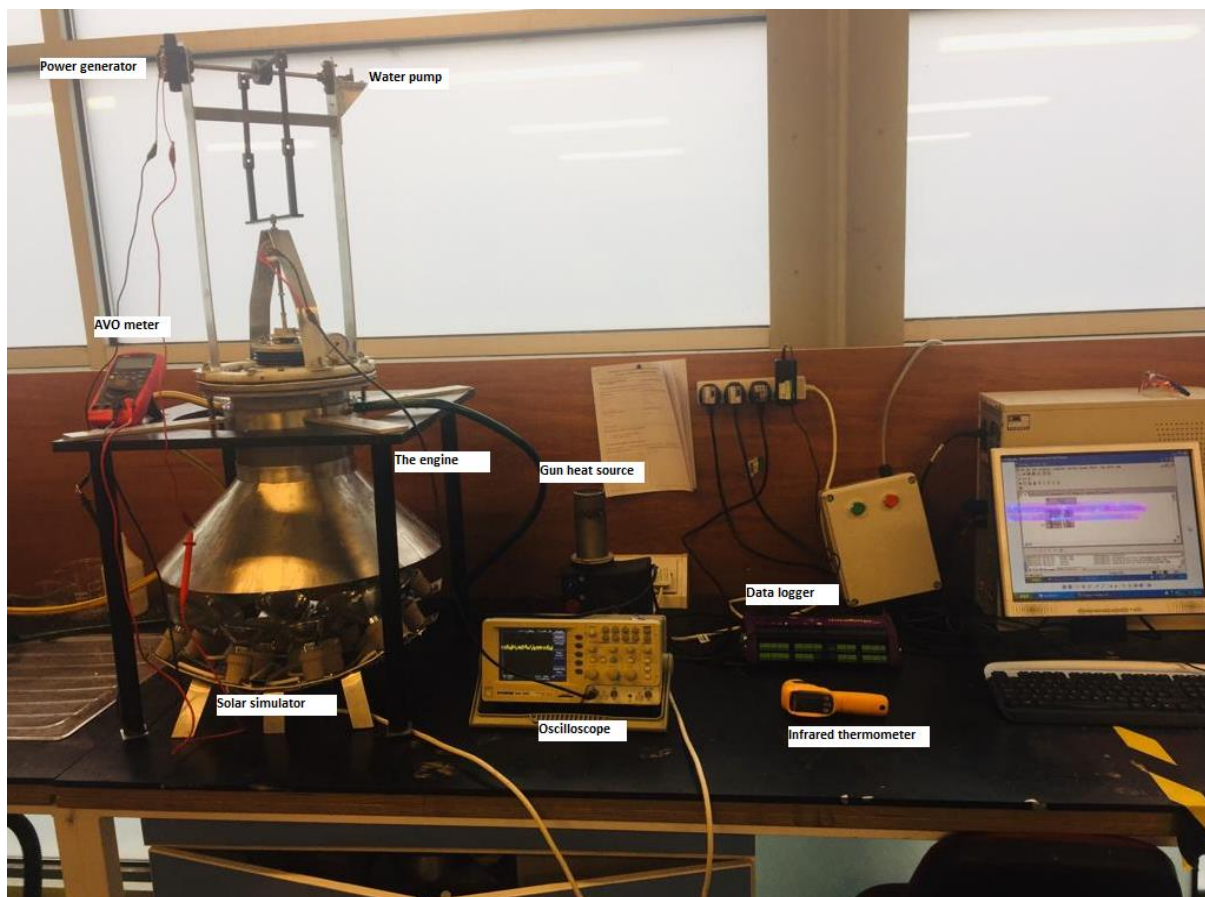


Figure 6.1: Instruments laboratory of the rig

To record the outcome and operating parameters of the engine, the FPSE is fully instrumented with a two-channel oscilloscope, data taker with thermocouple and AVO meter.

## 6.1 Instrument description:

The following sections describe the instruments used and installed on the engine to obtain the engine operating parameters below.

### 6.1.1 Thermocouple:

The working fluid temperature at the compression space is measured by utilising a k-technique thermocouple which is installed inside the compression space and linked to the data taker.

### 6.1.2 Data taker and data logger software:

The function of using data taker is the pressure transducer and thermocouple are connected to DT500 data taker. The data logger software then record and saves the data in excel files.



Figure 6.2: Data taker DT500

### 6.1.3 Infrared thermometer:

The type of infrared thermometer is Fluke 64 MAX that used to measure the cylinder temperature of the engine in hot side. The range of temperature can be measured between -30 to 600 °C with accuracy of  $\pm 1^{\circ}\text{C}$ .



Figure 6.3: Fluke 64 MAX infrared thermometer

#### 6.1.4 Oscilloscope:

GW-INSTEK digital storage oscilloscope was used to record the oscillation amplitude, frequency and the working fluid pressure variation.



Figure 6.4: GW-INSTEK oscilloscope

### 6.1.5 Pressure transducer:

The UNIK5000-PTX5072 pressure transducer is used and installed on the top of the engine at the expansion space. It has a range of -1 to 1.6 bar and the output is 4 to 20 mAmp.



Figure 6.5: The UNIK5000-PTX5072 pressure transducer

## 6.2 Engine start up procedures:

The testing procedures start by general check of all engine parts for any air leakage. Also, check the below (power piston) and springs of engine support are moving freely. Furthermore, make sure there is no water leak in the cooling jacket and tube connections. After ensuring that all components were appropriately assembled. The first step of operation starts by gradually adding the heat (Solar simulator) to the hot end (expansion space of the engine) and running the cooling water through the cooling jacket. The temperature at the displacer (hot side) is continuously measured by using infrared thermometer. It is recorded that the power piston has been started moving when the temperature reach  $220^{\circ}\text{C}$  at the hot side of the engine. However, the engine starts working and continue running when the expansion space temperature (hot side) was about  $350^{\circ}\text{C}$ , and the compression space temperature was  $26^{\circ}\text{C}$ .

### 6.3 Inspection and modification:

At this point in the project, all the works were focused on double-checking the assembly of engine components and operational parameters. The experiments of the engine went for a while, so the cooling, heating, checking the method of assembling engine parts and disassembling the engine were a daily routine. All these works were aim to more understand the mechanism of engine work and eliminate any evident failures in the design.

One of the most prevalent difficulties in the engine design is the seal gasket leak due to high temperature, vibration and contact with hot fluid over a period of time. Figure 6.6 presents improvement made to the cylinder hot end space of a high temperature gasket which avoid any air leak in the engine.



Figure 6.6: Resistance design high temperature gasket

Moreover, another modification on the design to minimise the friction and maintain the stability, the engine is connected to the support frame by four sets of flat plates and helical springs, in order to isolate the engine vibration from the frame. The studs of the engine are designed to pass through the hole in the flat plates without any connection as shown in Figure 6.7.

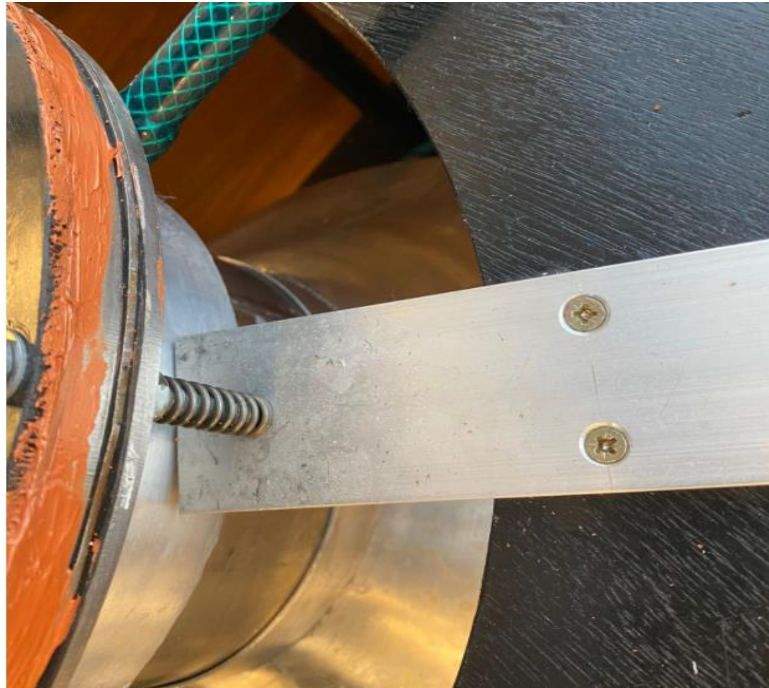


Figure 6.7: One of the four sets of flat plates with springs

#### **6.4 Power piston operating frequency tuning:**

After establishing a functional basis on which the engine can maintain its oscillation, the next stage is to improve the engine's performance by optimising the operating frequency of the engine. The major goal is to validate the simulation model's design parameters. The power piston working frequency was one of the first parameters to be tuned. It is stated [69] that the free piston Stirling engine can achieve an optimum operating frequency when the oscillating components (the power piston and displacer) have similar resonance frequencies. Since the resonance frequency of the displacer cannot change without changing the stiffness of the spring or the mass of the displacer, the power piston resonance frequency on the other hand can be modified by attaching a magnet lump weight to the bellows output shaft, as indicated in Figure 6.8.

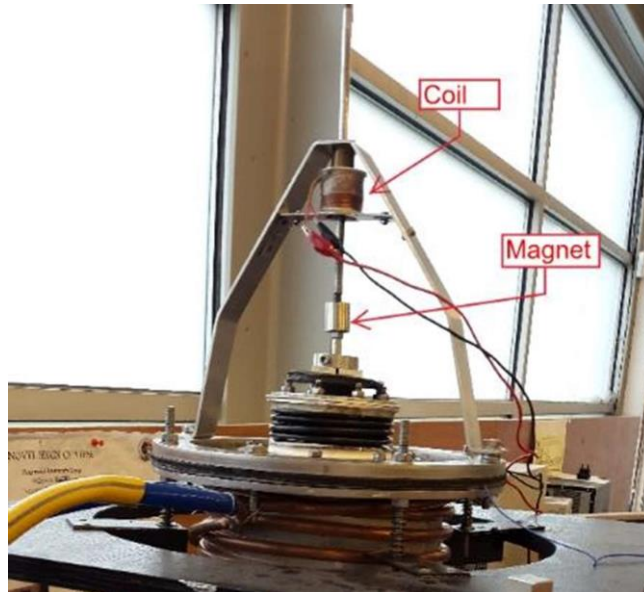


Figure 6.8: A magnet lump weight and coil transducer

The tuning of the power piston resulted in an excellent start-up of the engine and an increase in pressure variation and oscillation amplitude. Variant weight was tested with the shaft output. It was discovered that a mass of 80g produced the resonance frequency closest to the design frequency of 11 Hz, which was 10.42 Hz at hot end temperature of 350 C° and compression space temperature of 35 C°. The power piston oscillation amplitude reached 18 mm, which a simple ruler measured. The effective swept volume is calculated and found to be approximately  $\approx 70$  cc.

#### **6.4 Steady state operation results:**

The maintained below (power piston) has resulted in a good engine start-up and raised the pressure variation and oscillation amplitude. At the expansion, hot end temperature was maintained at 350 °C and the compression space temperature at 28 °C, the power piston gave the record operation frequency 10.42Hz, as shown in Figure 6.9.

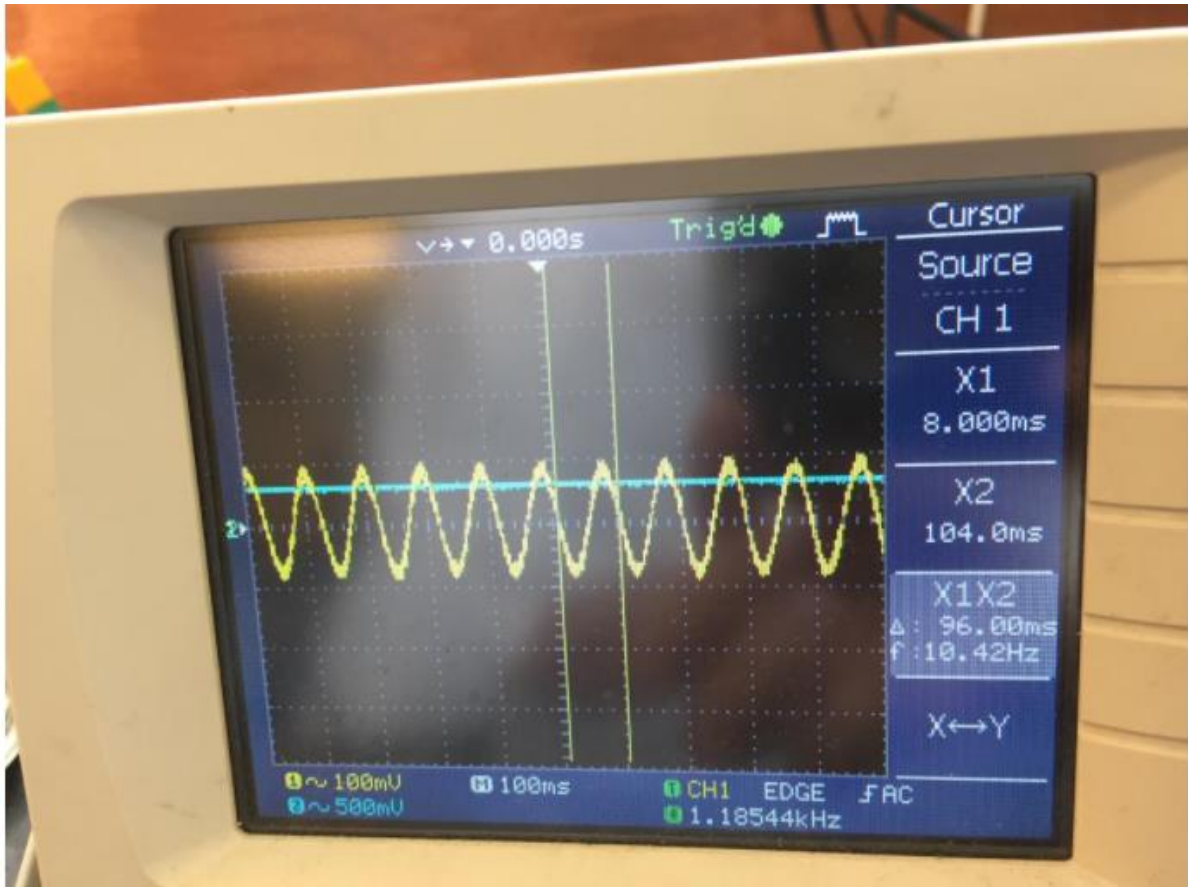


Figure 6.9: The operation frequency diagram

Moreover, Figure 6.10 given below shows a graph of an AC voltage output which obtained from the engine. The channel was operating with wave frequency of 10.48Hz. The full scale voltage range of the channel is 116mv to -100mv. This data presented were taken at input heat temperature of 350C°.

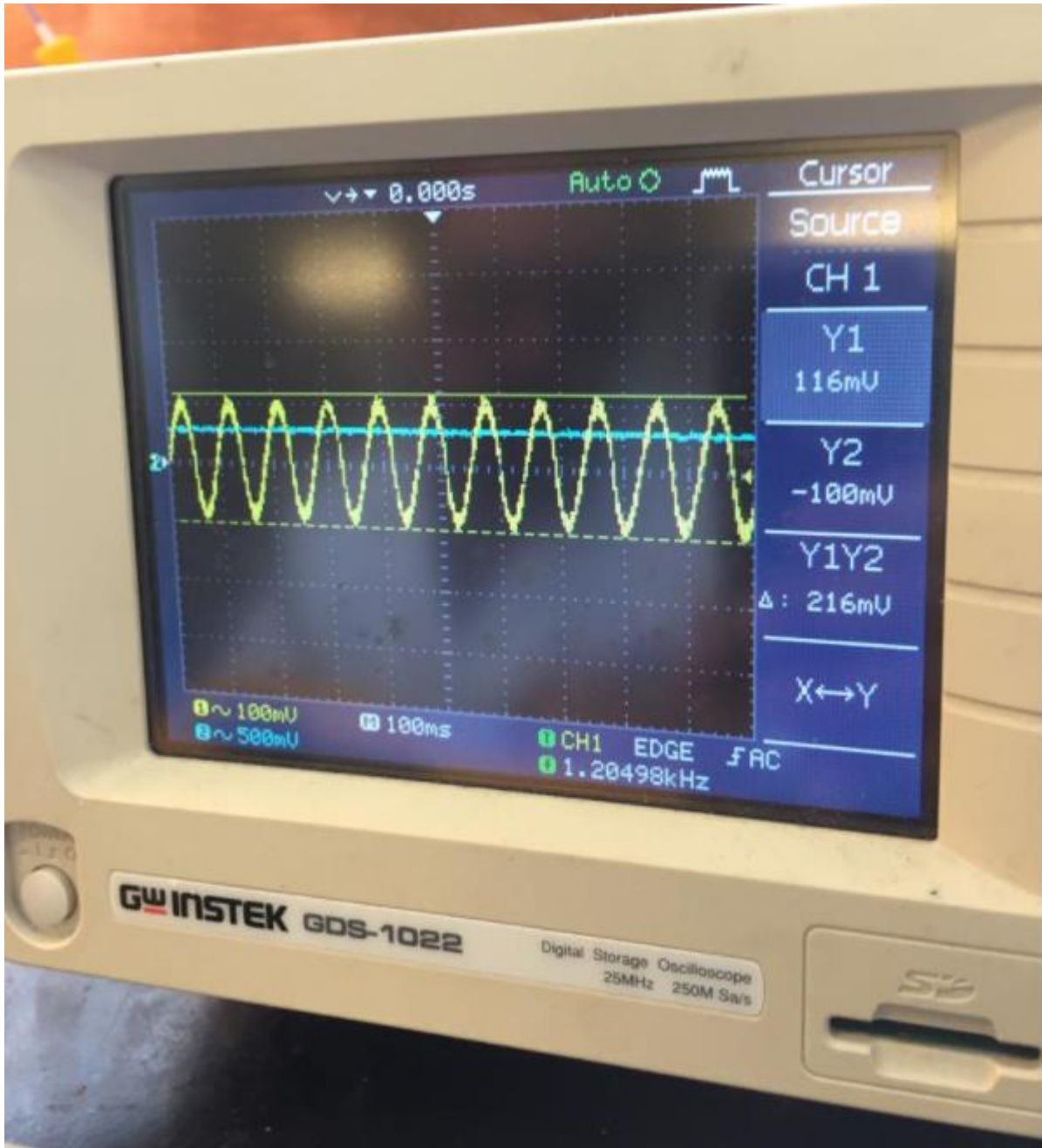


Figure 6.10: The operation voltage output diagram

### 6.5 Water pump output:

To evaluate the performance of rotary water micro pump, the output rotary shaft was connected to the motor of the pump. The pump is powered by a frequency drive from linear shaft of 10 Hz with speed of 120rpm records on the rotary shaft. Experimental

tests were performed first with pump load, the test record that the pump can suck the water from 550mm deep height and flow 260ml of water per minute.

Therefore, the power of pump can be expressed as:

$$P = \delta g h v$$

Where,  $P$  is pump output power (W),  $\delta$  is density of water ( $\text{kg/m}^3$ ),  $g$  is the gravitational constant ( $\text{m/sec}^2$ ),  $h$  is total developed head in meter, and  $v$  is the flow rate ( $\text{m}^3/\text{sec}$ ).

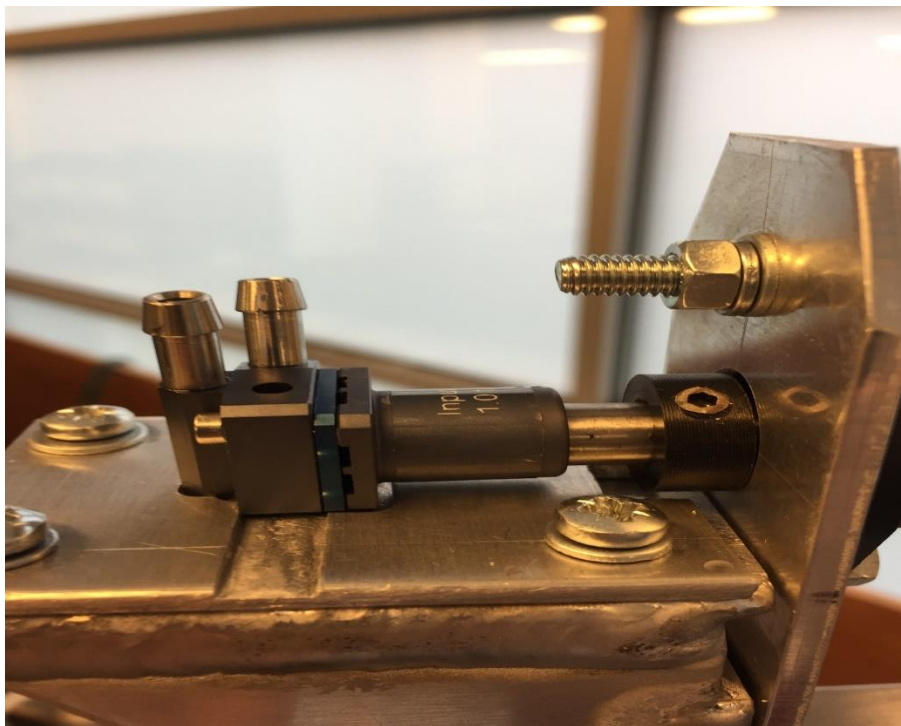


Figure 6.11: Water pump installed on the rotary output shaft

## 6.6 Power generation output:

The generator of micro-hydro water turbine is utilised to evaluate the performance of the rotary electric generator. The inside rotary generator was installed to the output

rotary shaft, as shown in Figure 6.12 The experimentally measured generator terminal voltage and load voltages profiles.

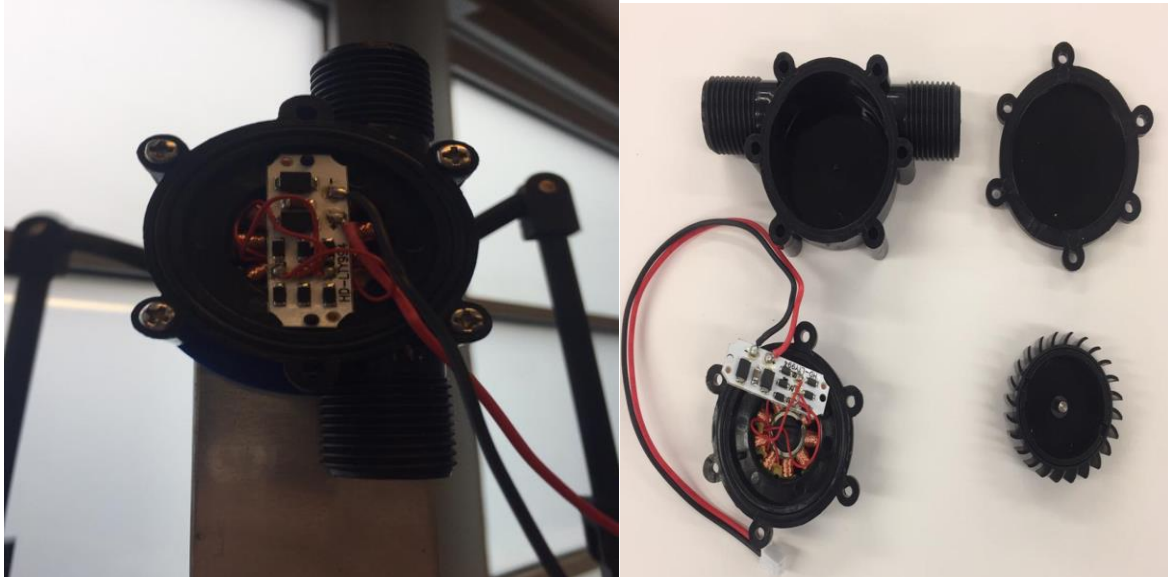


Figure 6.12: Small power generation installed on the rotary output shaft

The test was done with electrical load to determine the output of the electric generator and frequency operation of the engine. The hot end temperature range was between 300 to 350 C°. It is found that the electric generator produced low power output.



Figure 6.13: Power output from electric generator

### 6.7 Engine lifting capacity:

Before conducting tests, the engine was run under several working conditions.. After the successful start-up of the engine and reaching the steady state operation of continuous running for about 20 minutes. The engine was able to lift up to 1.2 kg by rotary motion design.



Figure 6.14: The rotary shaft of engine lifting amount of weight

## 6.8 Summary of the experiment result compared to modelling result:

The experimental result show that FPSE has a successful operated at input modelling hot and cold end temperature, which also give a very close operation frequency compared to the simulation result. However, the indicated power output is much lower in comparison with modelling result.

Table 6.1 comparison of experimental result and modelling result at 300 C° heat in:

Data	Experimental result	Modelling result
$T_{hot}$	300 C°	300C°
$T_{cold}$	25 C°	25 C°
Operation frequency	10.47 Hz	11 Hz
Average pressure	1 bar	1 bar
Indicated power	0.69 W	6.73 W

# Chapter 7:

## Conclusion and future work

After a detailed study in the literature review, it is found that the Stirling engine is a developing technology for converting thermal energy to mechanical power in terms of solar technology, particularly for small scale power. Considering that the solar to thermal energy conversion is a mature technology, the primary purpose of this research was to understand the process of the Stirling thermodynamic cycle. The developed mathematical model of the free-piston Stirling engine was a predictable approach to numerical simulation of the engine operation. The model provides results of Schmidt, adiabatic and Simple thermodynamic analysis, to predict the novel design's performance. The model's equations consider the mass conversion in each part of the engine. The simple model analysis allows taking a range of heat losses, which provides a high accuracy prediction of the engine performance. The model predicts a lower than 10% thermal efficiency at input heat temperatures up to 300C°, where the indicated power output record 6.73W.

The proof of concept engine prototype was designed and fabricated as part of the research work. This prototype incorporates a bellows working as a power piston which is actuated independently from the displacer; hence the name is free-piston. The experimental test setup and the results were provided. The main purpose of this experimental engine was to present a validation of the simulation model and contribution for further study and development. The test results showed a successful operation of the engine at a frequency of 10.42Hz for the hot side 300C° and the cold side of 25C°, however, the indicated power output was 0.69 W which is lower comparing to simulation result.

## **7.1 Contribution to the development of FPSE design and Novelty of the research:**

- Introducing a strong basis for the design of using two pre-compressed springs in the displacer design that could be a potential candidate for commercial utilization.
- Incorporating the flexible bellows for the power piston and considering the combination with the displacer to a new engine configuration.
- Develop a new design for simple installation and dismantling of the engine parts.
- Developed a mathematical modelling which can be useful and contribute in the optimization of advancing FPSE design.
- Building and apply a novel design of converting linear motion to rotary motion in FPSE design.

## **7.2 Recommendation for future work:**

Without a doubt, building a concept-proof of free piston Stirling engine working by solar thermal system is the most important task in pursuing the proposed technology. The following recommendations suggest some research areas that can help improve the engine design and the performance.

- To improve further accuracy of the developed approach in mathematical modelling of engine performance, it is recommended to investigate a dynamic analysis model of the engine.
- It is recommended to consider increasing the engine's working pressure, which can improve the power output of the engine.
- More work is required for the variant design of the solar simulator.

- Finally, it is recommended to carry out further analysis in the heat exchanger part to optimise the engine's heat transfer.

## REFERENCES:

- [1] John Stringer, *Basic Research Needs to Assure A Secure Energy Future*. 2003.
- [2] Gaynor, P.T., R.Y. Webb, and C.C. Lloyd, *Low Enthalpy Heat Stirling Engine Based Electric Power Generation: A Research Design*. 2009 *International Conference on Clean Electrical Power*. 2009. 615-618.
- [3] Clean Edge, 2007. "Clean-Energy Trends" Available at: [www.cleaneedge.com](http://www.cleaneedge.com)
- [4] O. Ogunmodimu and E. Okoroigwe, "Concentrating solar power technologies for solar thermal grid electricity in Nigeria: A review", *Renewable and Sustainable Energy Reviews*, vol. 90, pp. 104-119, 2018.
- [5] P. Ng and N. Mithraratne, "Lifetime performance of semi-transparent building-integrated photovoltaic (BIPV) glazing systems in the tropics", *Renewable and Sustainable Energy Reviews*, vol. 31, pp. 736-745, 2014.
- [6] E. Saretta, P. Caputo and F. Frontini, "A review study about energy renovation of building facades with BIPV in urban environment", *Sustainable Cities and Society*, vol. 44, pp. 343-355, 2019.
- [7] Zhou, B., Pei, J., Nasir, D. and Zhang, J., 2021. A review on solar pavement and photovoltaic/thermal (PV/T) system. *Transportation Research Part D: Transport and Environment*, 93, p.102753.
- [8] International Energy Agency IEA, 2014. Solar photovoltaic energy. Technol Roadmap 60. [https://doi.org/10.1007/SpringerReference\\_7300](https://doi.org/10.1007/SpringerReference_7300).
- [9] Ali, H., 2020. Recent advancements in PV cooling and efficiency enhancement integrating phase change materials based systems – A comprehensive review. *Solar Energy*, 197, pp.163-198.
- [10] Gul M, Kotak Y, Muneer T. Review on recent trend of solar photovoltaic technology. *Energy Exploration & Exploitation*. 2016;34(4):485-526.

- [11] Zhang HL, Baeyens J, Degreve J, Cacéres G. Concentrated solar power plants: review and design methodology. *Renew Sustain Energy Rev* 2013;22:466–81.
- [12] Leitner A, Owens B. Brighter than a hundred suns: solar power for the Southwest. USA: National Renewable Energy Laboratory Colorado; 2003.
- [13] E. González-Roubaud, D. Pérez-Osorio and C. Prieto, "Review of commercial thermal energy storage in concentrated solar power plants: Steam vs. molten salts", *Renewable and Sustainable Energy Reviews*, vol. 80, pp. 133-148, 2017. Available: 10.1016/j.rser.2017.05.084.
- [14] Fernández-García, A., et al., *Parabolic-trough solar collectors and their applications*. *Renewable and Sustainable Energy Reviews*, 2010. 14(7): p. 1695-1721.
- [15] Ali H. Recent advancements in PV cooling and efficiency enhancement integrating phase change materials based systems – A comprehensive review. *Solar Energy*. 2020;197:163-198.
- [16] Batuecas E, Mayo C, Díaz R, Pérez F. Life Cycle Assessment of heat transfer fluids in parabolic trough concentrating solar power technology. *Solar Energy Materials and Solar Cells*. 2017;171:91-97.
- [17] Mokhtar, G., B. Boussad, and S. Noureddine, *A linear Fresnel reflector as a solar system for heating water: Theoretical and experimental study*. *Case Studies in Thermal Engineering*, 2016. 8: p. 176-186.
- [18] Kalogirou SA. Solar thermal collectors and applications. *Prog Energy Combust Sci* 2004;30:231–95.
- [19] Breeze P. Parabolic Trough and Fresnel Reflector Solar Power Plants. In: Breeze P, ed. *Solar Power Generation*. PP: 25-34.

(<https://www.sciencedirect.com/science/article/pii/B978012804004100004X>).  
Accessed January 8, 2022.

- [20] Collado FJ, Guallar J. A review of optimized design layouts for solar power tower plants with campo code. *Renew Sustain Energy Rev* 2013;20:142–54.
- [21] Ávila-Marín AL. Volumetric receivers in Solar Thermal Power Plants with Central Receiver System technology: a review. *Sol Energy* 2011;85. [891–10].
- [22] Alexopoulos, S. and B. Hoffschmidt, *Solar tower power plant in Germany and future perspectives of the development of the technology in Greece and Cyprus*. *Renewable Energy*, 2010. 35(7): p. 1352-1356.
- [23] Alnaimat F, Rashid Y. Thermal Energy Storage in Solar Power Plants: A Review of the Materials, Associated Limitations, and Proposed Solutions. *Energies (Basel)*. 2019;12(21):4164.
- [24] Noor N, Muneer S. Concentrating Solar Power (CSP) and Its Prospect in Bangladesh. In 2009 Proceedings of the 1st International Conference on the Developments in Renewable Energy Technology (ICDRET), Date 17-19 Dec. Doi: 10.1109/ICDRET.2009.5454207; 2009.
- [25] Hafez, A.Z., et al., *Solar parabolic dish Stirling engine system design, simulation, and thermal analysis*. *Energy Conversion and Management*, 2016. 126: p. 60-75.
- [26] Mancini T, Heller P, Butler B, Osborn B, Schiel W, Goldberg V, et al. Dish-stirling systems: an overview of development and status. *J Sol Energy Engineer* 2003;125(2):135–5.
- [27] Karabulut H, Yücesu HS, Çınar C, Aksoy F. An experimental study on the development of a b-type Stirling engine for low and moderate temperature heat sources. *Appl Energy* 2009;86(1):68–73.

- [28] Wu S, Xiao L, Cao Y, Li Y. A parabolic dish/AMTEC solar thermal power system and its performance evaluation. *Appl Energy*. 2010;87(2):452-462.2009.
- [29] Bonnet S, Alaphilippe M, Stouffs P. Thermodynamic solar energy conversion: reflections on the optimal solar concentration ratio. *Int J Energy Environ Econ* 2006;12(3):141–52.
- [30] R.J. Meijer, Stirling Thermal Motors Inc, assignee, Solar powered Stirling engine, United States patent US 4,707,990, 1987 Nov 24.
- [31] Singh, U.R. Kumar, A., *Review on solar Stirling engine: Development and performance*, Thermal Science and Engineering Progress, 2018. 8: p. 244-256.
- [32] Reve, "Tessera Solar and Stirling Energy Systems unveil world's first commercial-scale SunCatcher plant | REVE", *Evwind.es*, 2019. [Online]. Available: <https://www.evwind.es/2010/01/25/tessera-solar-and-stirling-energy-systems-unveil-worlds-first-commercial-scale-suncatcher-plant/3616>. [Accessed: 09- Apr- 2019].
- [33] R. Beltran, N. Velazquez, A.C. Espericueta, D. Saucedo, G. Perez, *Mathematical model for the study and design of a solar dish collector with cavity receiver for its application in Stirling engines*, *J. Mech. Sci. Technol.* 26 (2012) 3311–3321.
- [34] A.C. Ferreira, S. Teixeira, J.C. Teixeira, L.B. Martins, Design optimization of a solardish collector for its application with Stirling engines, in: ASME 2015 International Mechanical Engineering Congress and Exposition 2015, pp.V06AT07A033–V06AT07A033.
- [35] T. Srinivas, B.V. Reddy, R. Natarajan, S. Sriram, *Thermodynamic and heat transfer studies on solar Stirling engine*, in: Energy Efficient Technologies for Sustainability (ICEETS) 2013, pp. 7–13.
- [36] D.J. Shendage, S.B. Kedare, S.L. Bapat, *Numerical investigations on the Dish-Stirling engine system*, *Int. J. Ambient Energy* (2017) 1–11.

- [37] K. Sookramoon, P. Bunyawanichakul, B. Kongtragool, Experimental Study of a 2-stage Parabolic dish-Stirling Engine in Thailand, *Walailak J. Sci. Technol. (WJST)*13 (2015) 579–594.
- [38] J. Coventry and C. Andraka, "Dish systems for CSP", *Solar Energy*, vol. 152, pp. 140-170, 2017.
- [39] Lopez CW, Stone K, W. Performance of the Southern California Edison Company Stirling Dish, 1264 Sandia National Laboratories, 1993.
- [40] Andraka CE, Powell M. Dish Stirling development for utility-scale commercialization. In: 14th 1272 SolarPACES conference. 2008. Las Vegas.
- [41] A. Hafez, A. Soliman, K. El-Metwally and I. Ismail, "Solar parabolic dish Stirling engine system design, simulation, and thermal analysis", *Energy Conversion and Management*, vol. 126, pp. 60-75, 2016.
- [42] Caughley, A., Sellier, M., Gschwendtner, M. and Tucker, A. (2016). *A free-piston Stirling cryocooler using metal diaphragms*. *Cryogenics*, 80, pp.8-16.
- [43] T. Mancini et al., "Dish-Stirling Systems: An Overview of Development and Status", *Journal of Solar Energy Engineering*, vol. 125, no. 2, p. 135, 2003.
- [44] J. Garrido, W. Wang, M. Nilsson, B. Laumert, A detailed radiation heat transfer study of a dish-Stirling receiver: the impact of cavity wall radiation properties and cavity shapes, *AIP Conf. Proc.* 1734 (1) (2016).
- [45] M. Cucumo, V. Ferraro, D. Kaliakatsos, M. Mele, Analysis of the performances of a dish-Stirling system equipped with hot chamber, *Int. J. Heat Technol.* 33 (4)(2015) 125–136.
- [46] R. Gil, C. Monné, N. Bernal, M. Muñoz and F. Moreno, "Thermal Model of a Dish Stirling Cavity-Receiver", *Energies*, vol. 8, no. 2, pp. 1042-1057, 2015.
- [47] L.S. Castellanos, G.E. Caballero, V.R. Cobas, E.E. Lora, A.M. Reyes, Mathematical modelling of the geometrical sizing and thermal performance of a Dish/Stirling system for power generation, *Renewable Energy* 107 (2017) 23–35.

- [48] Q. Yang, G. Bao, B. Zhang, Design of cylindrical linear magnetic gear generator for Sterling solar power generate system, in: Magnetics Conference (INTERMAG) IEEE2015, p. 1.
- [49] L. Mendoza Castellanos et al., "Experimental analysis and numerical validation of the solar Dish/Stirling system connected to the electric grid", *Renewable Energy*, vol. 135, pp. 259-265, 2019. Available: 10.1016/j.renene.2018.11.095.
- [50] D. Llamas, "Infinia begins commissioning 1.5 MW dish Stirling solar Concentrating Solar Power plant in Utah", *HELIO SCSP*, 2019. [Online]. Available: <http://helioscsp.com/infinia-begins-commissioning-1-5-mw-Dish-Stirling-solar-concentrating-solar-power-plant-in-utah/>. [Accessed: 12- Apr-2019].
- [51] M. Abbas, B. Boumeddane, N. Said, A. Chikouche, Dish Stirling technology: a 100MW solar power plant using hydrogen for Algeria, *Int. J. Hydrogen Energy* 36 (7)(2011) 4305–4314.
- [52] G.C. Bakos, C. Antoniadou, Techno-economic appraisal of a dish/Stirling solar power plant in Greece based on an innovative solar concentrator formed by elastic film, *Renewable Energy* 60 (2013) 446–453.
- [53] Wazed, S.M, Hughes, B.R. Connor, A. Calautit, J.K., *A review of sustainable solar irrigation systems for Sub-Saharan Africa*. *Renewable and Sustainable Energy Reviews*, 2018. 81: p. 1206-1225.
- [54] A. Saini, "SOLAR POWERED STIRLING ENGINE DRIVEN WATER PUMP", *International Journal of Research in Engineering and Technology*, vol. 02, no. 11, pp. 615-620, 2013. Available: 10.15623/ijret.2013.0211094.
- [55] R. K. Bumataria and N. K. Patel, "Review of Stirling Engines for Pumping Water using Solar Energy as a source of Power", *International Journal of Engineering Research and Applications (IJERA)*, vol. 3, no. 1, pp. 864-868, 2013.
- [56] T. Gadelkareem, A. EldeinHussin, G. Hennes and A. El-Ehwany, "Stirling cycle for hot and cold drinking water dispenser", *International Journal of Refrigeration*, vol. 99, pp. 126-137, 2019. Available: 10.1016/j.ijrefrig.2018.11.033.

- [57] A. Al-Dafaie, M. Dahdolan and M. Al-Nimr, "Utilizing the heat rejected from a solar dish Stirling engine in potable water production", *Solar Energy*, vol. 136, pp. 317-326, 2016. Available: 10.1016/j.solener.2016.07.007.
- [58] G. T. R. a. C. Hooper, *Stirling Engines*: E&F N Spon, 1991.
- [59] Leben. *Stirling Engine*. Available: [http://www.wikiwand.com/de/Robert Stirling](http://www.wikiwand.com/de/Robert_Stirling)
- [60] C. M. Hargreaves, *The Philips Stirling Engine*. Amsterdam: Elsevier Science Publishers B.V., 1991.
- [61] Anonymous, "California Unions for Reliable Energy Partners with K Road Calico Solar Project," in *Business Wire*, ed. New York:Business Wire, 2011.
- [62] I. Urieli, "The Regenerator and the Stirling Engine," *Proceedings of the Institution of Mechanical Engineers*, vol. 212, p. 531, 1998.
- [63] A. J. Organ and T. Finkelstein, *Air engines*. London: Professional Engineering Pub, 2001.
- [64] Graham Walker, G.R., Owen R. Fauvel and Edward R. Bingham, *The Stirling Alternative Power systems, refrigerants and Heat Pumps*. 1994, OPA Amsterdam: Gordon and Breach Science Publishers.
- [65] Senft, G.W.a.J.R., *Free Piston Stirling Engine*. Lecture Notes in Engineering, ed. C.A.B.a.S.A. Orszag. Vol. 12. 1985, Berlin Heidelberg, Germany: Springer Berlin Heidelberg. 23-99.
- [66] Senft, G.W.a.J.R., *Lecture Notes in Engineering, Free Piston Stirling Engines*. Lecture Notes in Engineering, ed. C.A.B.a.S.A. Orszag. 1985, Berlin, Heidelberg, New York, Tokyo: Springer. 284.
- [67] Hooper, G.T.R.a.C., *Stirling engines*. 1983, USA: E. & F. N. Spon.
- [68] Organ, A.J., *The regenerator and the Stirling engine*. 1997, UK: Mechanical engineering publications limited.

- [69] Urieli, I.a.B.D.M., *Stirling Cycle Engine Analysis*. 1984, Bristol, Great Britain: Adam Hilger Ltd.
- [70] Walker G. *Stirling engines*. Oxford: Clarendon Press; 1980.
- [71] S. Alfarawi, R. AL-Dadah and S. Mahmoud, "Enhanced thermodynamic modelling of a gamma-type Stirling engine", *Applied Thermal Engineering*, vol. 106, pp. 1380-1390, 2016. Available: 10.1016/j.applthermaleng.2016.06.145.
- [72] Israel Urieli, Ohio University, "Stirling Cycle Machine Analysis," 2012.
- [73] Boucher, J., F. Lanzetta, and P. Nika, *Optimization of a dual free piston Stirling engine*. *Applied Thermal Engineering*, 2007. 27(4): p. 802-811.
- [74] Lange, R. and Carroll, W. (2008). Review of recent advances of radioisotope power systems. *Energy Conversion and Management*, 49(3), pp.393-401.
- [75] Universe Today. (2019). *NASA Halts Work on its New Nuclear Generator for Deep Space Exploration - Universe Today*. [Online] Available at: <https://www.universetoday.com/106604/nasa-halts-work-on-its-new-nuclear-generator-for-deep-space-exploration/> [Accessed 25 Mar. 2019].
- [76] Formosa, F., *Coupled thermodynamic–dynamic semi-analytical model of free piston Stirling engines*. *Energy Conversion and Management*, 2011. 52(5): p. 2098-2109.
- [77] GEA, "Green Energy Africa", *Green Energy Africa*, 2019. [Online]. Available: <https://greenenergyafrica.net/forums/what-is-solar-power>. [Accessed: 16- Apr- 2019].
- [78] Microgen-engine.com. (2019). *Technology - Microgen*. [online] Available at: <https://www.microgen-engine.com/technology/technology/> [Accessed 27 Mar. 2019].
- [79] Griffin, N.C.J.C.a.P., *A review of Stirling Engine Mathematical Models*. 1983, Ridge National Laboratory: USA.

- [80] G. Walker, Fauvel G.R., Reader and E.R. Bingham, "*The Stirling alternative Power systems, refrigerants and Heat Pumps*" 1994.
- [81] Kongtragool, B. and S. Wongwises, *Investigation on power output of the gamma-configuration low temperature differential Stirling engines*. *Renewable Energy*, 2005. 30(3): p. 465-476.
- [82] M. Güven, H. Bedir and G. Anlaş, "Optimization and application of Stirling engine for waste heat recovery from a heavy-duty truck engine", *Energy Conversion and Management*, vol. 180, pp. 411-424, 2019.
- [83] Chahartaghi, M. and Sheykhi, M. ,*Energy and exergy analyses of beta-type Stirling engine at different working conditions*. *Energy Conversion and Management*, 2018. 169, pp.279-290.
- [84] K. Bataineh, "Numerical thermodynamic model of alpha-type Stirling engine", *Case Studies in Thermal Engineering*, vol. 12, pp. 104-116, 2018. Available: 10.1016/j.csite.2018.03.010.
- [85] W. Uchman, L. Remiorz, K. Grzywnowicz and J. Kotowicz, "Parametric analysis of a beta Stirling engine – A prime mover for distributed generation", *Applied Thermal Engineering*, vol. 145, pp. 693-704, 2018. Available: 10.1016/j.applthermaleng.2018.09.088.
- [86] K. Chong, W. Tan, C. Wong, T. Yew, M. Tan and B. Lim, "Theoretical Analysis of Hybrid Dense-Array Concentrator Photovoltaic and Stirling Engine System", *Energy Procedia*, vol. 158, pp. 284-290, 2019. Available: 10.1016/j.egypro.2019.01.090.
- [87] Urieli I, Berchowitz DM. *Stirling Cycle Engine Analysis*. Bristol: Adam Hilger LTD;1984.
- [88] M. Ahmadi, M. Ahmadi and F. Pourfayaz, "Thermal models for analysis of performance of Stirling engine: A review", *Renewable and Sustainable Energy Reviews*, vol. 68, pp. 168-184, 2017.

- [89] S. Toghyani, A. Kasaeian and M. Ahmadi, "Multi-objective optimization of Stirling engine using non-ideal adiabatic method", *Energy Conversion and Management*, vol. 80, pp. 54-62, 2014.
- [90] C. Cheng, H. Yang and L. Keong, "Theoretical and experimental study of a 300-W beta-type Stirling engine", *Energy*, vol. 59, pp. 590-599, 2013. Available: 10.1016/j.energy.2013.06.060.
- [91] Senft JR. Mechanical efficiency of kinematic heat engines. *Journal of the Franklin Institute* 1987;324(2):273-90.
- [92] H. Karabulut, M. Okur, S. Halis and M. Altin, "Thermodynamic, dynamic and flow friction analysis of a Stirling engine with Scotch yoke piston driving mechanism", *Energy*, vol. 168, pp. 169-181, 2019. Available: 10.1016/j.energy.2018.11.078.
- [93] M. Babaelahi and H. Sayyaadi, "Simple-II: A new numerical thermal model for predicting thermal performance of Stirling engines", *Energy*, vol. 69, pp. 873-890, 2014. Available: 10.1016/j.energy.2014.03.084.
- [94] Finkelstein T. Computer analysis of Stirling engines. *Adv Cryog Eng*, United States 1975; 20.
- [95] S. Abdullah, B. Yousif and K. Sopian, "Design consideration of low temperature differential double-acting Stirling engine for solar application", *Renewable Energy*, vol. 30, no. 12, pp. 1923-1941, 2005. Available: 10.1016/j.renene.2004.11.011.
- [96] S. Toghyani, A. Kasaeian, S. Hashemabadi and M. Salimi, "Multi-objective optimization of GPU3 Stirling engine using third order analysis", *Energy Conversion and Management*, vol. 87, pp. 521-529, 2014. Available: 10.1016/j.enconman.2014.06.066.
- [97] Chen CL, Chia-En H, Yau HT. Performance analysis and optimization of a solarpowered Stirling engine with heat transfer considerations. *Energies* 2012;5(9):3573–85.
- [98] Kraitong K, Mahkamov K. Optimization of low temperature difference solar

Stirling engines using genetic algorithm. In: World renewable energy congress, Sweden; 2011.

- [99] K. Sim and D. Kim, "Development and Performance Measurements of a Beta-Type Free-Piston Stirling Engine Along With Dynamic Model Predictions", *Journal of Engineering for Gas Turbines and Power*, vol. 139, no. 11, p. 112806, 2017. Available: 10.1115/1.4036967.
- [100] Beale WT. Free piston Stirling- some model tests and simulation. International Automotive Engineering Congress Detroit, Mich. January 13e17, No 690230. Society of Automotive Engineers Inc.; 1969.
- [101] Benvenuto G, De Monte F, Farina F. Dynamic behaviour prediction of freepiston Stirling engine. Proceedings of the Intersociety Energy Conversion Engineering Conference; 1990;5;346e351.
- [102] Redlich RW, Berchowicz DM. Linear dynamics of free-piston Stirling engine. Proceedings of the Institution of Mechanical Engineers 1985;199:203e13.
- [103] Rogdakis ED, Bormpilas NA, Koniakos Ik. A Thermodynamic study for the optimization of stable operation of free piston Stirling engines. *Energy Conversion and Management* 2004;45:575e93.
- [104] Boucher J, Lanzetta F, Nika P. Optimization of a dual free piston Stirling engine. *Applied Thermal Engineering* 2007;27:802e11.
- [105] Walker G, Senft JR. Free piston Stirling engines. Berlin: Springer-Verlag; 1985.
- [106] S. Zare and A. Tavakolpour-Saleh, "Frequency-based design of a free piston Stirling engine using genetic algorithm", *Energy*, vol. 109, pp. 466-480, 2016.
- [107] Hofacker M, Barth E. A Lumped-Parameter Dynamic Model of a Thermal Regenerator for Free-Piston Stirling Engines. *researchgate*. 2009.
- [108] H. Karabulut, "Dynamic analysis of a free piston Stirling engine working with closed and open thermodynamic cycles", *Renewable Energy*, vol. 36, no. 6, pp. 1704-1709, 2011. Available: 10.1016/j.renene.2010.12.006.

- [109] H. Chen, C. Lin and J. Longtin, "Dynamic modeling and parameter optimization of a free-piston Vuilleumier heat pump with dwell-based motion", *Applied Energy*, vol. 242, pp. 741-751, 2019. Available: 10.1016/j.apenergy.2019.03.077.
- [110] J. Mou, W. Li, J. Li and G. Hong, "Gas action effect of free piston Stirling engine", *Energy Conversion and Management*, vol. 110, pp. 278-286, 2016. Available: 10.1016/j.enconman.2015.12.020.
- [111] A. Tavakolpour-Saleh, S. Zare and A. Omidvar, "Applying perturbation technique to analysis of a free piston Stirling engine possessing nonlinear springs", *Applied Energy*, vol. 183, pp. 526-541, 2016. Available: 10.1016/j.apenergy.2016.09.009.
- [112] D. Thombare and S. Verma, "Technological development in the Stirling cycle engines", *Renewable and Sustainable Energy Reviews*, vol. 12, no. 1, pp. 1-38, 2008.
- [113] I. Urieli, "Stirling Cycle Machine Analysis (updated 3/21/2016)", *Ohio.edu*, 2019. [Online]. Available: <https://www.ohio.edu/mechanical/stirling/>. [Accessed: 09- Apr- 2019].
- [114] Snyman H, Harms T, Strauss J. Design analysis methods for Stirling engines. *Journal of Energy in Southern Africa*. 2008;19(3):4-19.
- [115] Dobre C, Grosu L, Costea M, Constantin M. Beta Type Stirling Engine. Schmidt and Finite Physical Dimensions Thermodynamics Methods Faced to Experiments. *Entropy*. 2020;22(11):1278.
- [116] Gaponenko A, Kagramanova A. Analysis of the Stirling engine in the Schmidt approximation. *Journal of Physics: Conference Series*. 2018; 1111:012019.
- [117] Ghozzi S, Boukhanouf R. Computer Modeling of a Novel Mechanical Arrangement of a Free-Piston Stirling Engine. *Journal of Clean Energy Technologies*. 2015;3(2):140-144.

- [118] Urieli I, Berchowitz DM. Stirling Cycle Engine Analysis. Bristol: Adam Hilger LTD; 1984.
- [119] L. Mendoza Castellanos et al., "Experimental analysis and numerical validation of the solar Dish/Stirling system connected to the electric grid", *Renewable Energy*, vol. 135, pp. 259-265, 2019.
- [120] Korlu M, Pirkandi J, Maroufi A. Thermodynamic analysis of a gas turbine cycle equipped with a non-ideal adiabatic model for a double acting Stirling engine. *Energy Convers Manag.* 2017;147:120-134.
- [121] Parlak N, Wagner A, Elsner M, Soyhan H. Thermodynamic analysis of a gamma type Stirling engine in non-ideal adiabatic conditions. *Renew Energy.* 2009;34(1):266-273.
- [122] Torres García M, Carvajal Trujillo E, Vélez Godiño J, Sánchez Martínez D. Thermodynamic Model for Performance Analysis of a Stirling Engine Prototype. *Energies (Basel).* 2018;11(10):2655.
- [123] Yang H, Cheng C, Ali M. Performance and operating modes of a thermal-lag Stirling engine with a flywheel. *Appl Therm Eng.* 2022;205:118061.
- [124] Ahadi F, Azadi M, Biglari M, Madani S. Study of coating effects on the performance of Stirling engine by non-ideal adiabatic thermodynamics modeling. *Energy Reports.* 2021;7:3688-3702.
- [125] Bataineh K, Maqableh M. A new numerical thermodynamic model for a beta-type Stirling engine with a rhombic drive. *Thermal Science and Engineering Progress.* 2021;28:101071.
- [126] Rosnani Affandi et al, R., "Development of Design Parameters for the Concentrator of Parabolic Dish (PD) Based Concentrating Solar Power (CSP) under Malaysia Environment", *Journal of Applied Science and Agriculture*, vol. 11, pp. 42-48, 2014.
- [127] Ghozzi S, Boukhanouf R. Computer Modeling of a Novel Mechanical Arrangement of a Free-Piston Stirling Engine. *Journal of Clean Energy Technologies.* 2015;3(2):140-144.

## Appendices 1:

The equations of Schmidt analysis:

From the diagram in Figure (3.4), the sinusoidal volume variation of the compression and expansion space are expressed as follows:

$$V_c = V_{clc} + \frac{V_{swc}(1+\cos\theta)}{2} \quad (3.13)$$

$$V_e = V_{cle} + \frac{V_{swe}(1+\cos(\theta+\alpha))}{2} \quad (3.14)$$

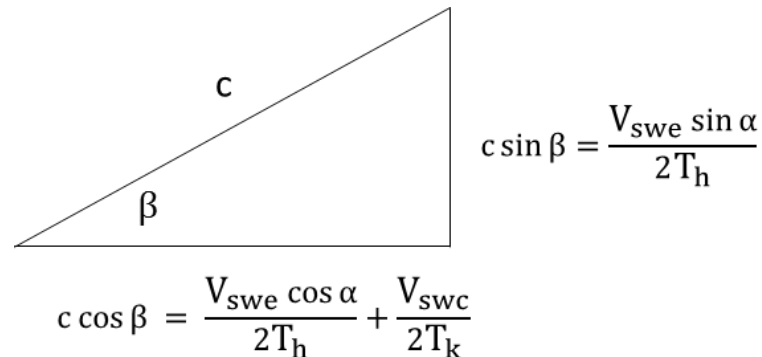
Where  $V_{sw}$  and  $V_{cl}$  are the swept and clearance volume respectively in ( $m^3$ ), and  $\Theta$  is the cycle angle. By substituting equation (3.13) and (3.14) in the pressure equation (3.8) which can be expressed as follows:

$$P = \frac{MR}{\left[ S + \left( \frac{V_{swc}}{2T_k} + \frac{V_{swe} \cos \alpha}{2T_h} \right) \cos \theta - \left( \frac{V_{swe} \sin \alpha}{2T_h} \right) \sin \theta \right]} \quad (3.15)$$

Where:

$$S = \left[ \frac{V_{swc}}{2T_k} + \frac{V_{clc}}{T_k} + \frac{V_k}{T_k} + \frac{V_r \ln\left(\frac{T_h}{T_k}\right)}{(T_h - T_k)} + \frac{V_h}{T_h} + \frac{V_{swe}}{2T_h} + \frac{V_{clc}}{T_h} \right] \quad (3.16)$$

In order to simplify the above pressure equation, Trigonometric calculation is considered by substituting  $\beta$  and  $c$  which defined as right-angle triangle.



Therefore,

$$\beta = \tan^{-1} \left( \frac{\frac{V_{swe} \sin \alpha}{T_h}}{\frac{V_{swe} \cos \alpha}{T_h} + \frac{V_{swc}}{T_k}} \right) \quad (3.17)$$

And,

$$c = \frac{1}{2} \sqrt{\left(\frac{V_{swe}}{T_h}\right)^2 + 2 \frac{V_{swe}}{T_h} \frac{V_{swc}}{T_k} \cos \alpha + \left(\frac{V_{swc}}{T_k}\right)^2} \quad (3.18)$$

By substituting  $\beta$  and  $c$  in the above pressure equation (3.15) and simplifying pressure at working spaces:

$$P = \frac{MR}{S(1 + b \cos \varphi)} \quad (3.19)$$

Where,

$$\varphi = \theta + \beta$$

$$b = c/S$$

The minimum and maximum values of the pressure can now be estimated for the extreme value of  $\cos \varphi$  and expressed as:

$$P_{\min} = \frac{MR}{S(1 + b)} \quad (3.20)$$

$$P_{\max} = \frac{MR}{S(1 - b)} \quad (3.21)$$

The average pressure over the cycle is expressed as:

$$P_{\text{mean}} = \frac{MR}{2\pi S} \int_0^{2\pi} \frac{1}{(1 + b \cos \varphi)} d\varphi \quad (3.22)$$

According to integrals tables, the equation can be as:

$$P_{\text{mean}} = \frac{MR}{(S\sqrt{1 - b^2})} \quad (3.23)$$

Therefore, the network of the engine is the sum work done by the expansion and compression space over complete cycle and can be expressed as:

$$W_c = \int_0^{2\pi} \left( P \frac{dV_c}{d\theta} \right) d\theta \quad (3.24)$$

$$W_e = \int_0^{2\pi} \left( P \frac{dV_e}{d\theta} \right) d\theta \quad (3.25)$$

The volumes derivatives can be obtained as:

$$\frac{dV_c}{d\theta} = -\frac{1}{2} V_{swc} \sin \theta \quad (3.26)$$

$$\frac{dV_e}{d\theta} = -\frac{1}{2} V_{swe} \sin(\theta + \alpha) \quad (3.27)$$

By substituting the equations (3.26) and (3.27) in the equations (3.24) and (3.25) respectively,

$$W_c = -\frac{V_{swc} M R}{2s} \int_0^{2\pi} \frac{\sin \theta}{1 + b \cos(\beta + \theta)} d\theta \quad (3.28)$$

$$W_e = -\frac{V_{swe} M R}{2s} \int_0^{2\pi} \frac{\sin(\theta + \alpha)}{1 + b \cos(\beta + \theta)} d\theta \quad (3.29)$$

The solution of these equations requires use of integrals tables which is done by Urieli and Berchowitz and obtained:

$$W_c = \pi V_{swc} P_{mean} \sin \beta \frac{(\sqrt{1 - b^2} - 1)}{b} \quad (3.30)$$

$$W_e = \pi V_{swe} P_{mean} \sin(\beta - \alpha) \frac{(\sqrt{1 - b^2} - 1)}{b} \quad (3.31)$$

Therefore, the overall efficiency can be found as [41]:

$$\eta = \frac{W}{Q_e} = 1 - \frac{T_k}{T_h} \quad (3.32)$$

## Appendices 2:

The equations of Adiabatic analysis:

The differential equation of mass balance from equation (3.36) is expressed as:

$$Dm_c + Dm_k + Dm_r + Dm_h + Dm_e = 0 \quad (3.37)$$

Assuming the constant volume and temperature of the heat exchanger, equation (3.35) can be written as equation (3.38):

$$\frac{Dp}{P} = \frac{Dm}{m} \quad (3.38)$$

By substituting equation (3.38) into equation (3.37), we obtain:

$$Dm_c + Dm_e + Dp \left( \frac{m_k}{p} + \frac{m_r}{p} + \frac{m_h}{p} \right) = 0 \quad (3.39)$$

However, equation (3.33) can be expressed for compression space as followings:

$$DQ_c + C_p T_{ck} gA_{ck} = DW_c + C_v D(m_c T_c) \quad (3.40)$$

As the compression space is assumed to be adiabatically, hence  $DQ_c=0$ , and the done work is:

$$DW_c = pDV_c \quad (3.41)$$

According to the mass conservation law, the control volume of the input mass ( $-gA_{ck}$ ) is equal to the working fluid accumulation rate ( $Dm_c$ ).

$$C_p T_{ck} Dm_c = p DV_c + C_v D(m_c T_c) \quad (3.42)$$

Therefore, the accumulation rates of the fluid in the compression space and expansion space are expressed as:

$$Dm_c = pDV_c + \left(\frac{V_c Dp}{\gamma}\right)/RT_{ck} \quad (3.43)$$

$$Dm_e = pDV_e + \left(\frac{V_e Dp}{\gamma}\right)/RT_{he} \quad (3.44)$$

By substituting equation (3.43) and (3.44) in equation (3.39), we can obtain the pressure differential [39]:

$$Dp = \frac{-\gamma p \left(\frac{DV_c}{T_{ck}} + \frac{DV_e}{T_{he}}\right)}{\left(\frac{V_c}{T_{ck}} + \gamma \left(\frac{V_k}{R_k} + \frac{V_r}{T_r} + \frac{V_h}{T_h}\right) + \frac{V_e}{T_{he}}\right)} \quad (3.45)$$

The changes in the volume of the expansion and compression spaces are stated as follows:

$$V_e = 0.5 * V_{sc} * (1 + \cos\phi) + V_{de} \quad (3.46)$$

$$V_c = 0.5 * V_{se} * (1 - \cos\phi) + 0.5 * V_{sc} * (1 + \cos(\phi - \theta)) + V_{dc} \quad (3.47)$$

Where,  $V_{se}$  is the expansion swept volume,  $V_{sc}$  is the compression swept volume and  $V_{de}$ ,  $V_{dc}$  are expansion and compression dead volume, respectively. Also, the total output work of the engine can be calculated as summation of the work done in the compression and expansion spaces:

$$DW = p(DV_c + DV_e) \quad (3.48)$$

The relative volumes in heat exchanger are constant, thus the following energy equations of heat transferred to the working gas for cooler, heater and regenerator can be written as [39]:

$$DQ_k = V_k Dp C_v / R - C_p (T_{ck} m_{ck} - T_{kr} m_{kr}) \quad (3.49)$$

$$DQ_r = V_r Dp C_v / R - C_p (T_{kr} m_{kr} - T_{rh} m_{rh}) \quad (3.50)$$

$$DQ_h = V_h Dp C_v / R - C_p (T_{rh} m_{rh} - T_{he} m_{he}) \quad (3.51)$$

### Appendices 3: Matlab Computer Modelling (functions):

% sea (stirling engine analysis) - main program

% Row indices of the var, dvar arrays:

TC = 1; % Compression space temperature (K)  
 TE = 2; % Expansion space temperature (K)  
 QK = 3; % Heat transferred to the cooler (J)  
 QR = 4; % Heat transferred to the regenerator (J)  
 QH = 5; % Heat transferred to the heater (J)  
 WC = 6; % Work done by the compression space (J)  
 WE = 7; % Work done by the expansion space (J)  
 W = 8; % Total work done (WC + WE) (J)  
 P = 9; % Pressure (Pa)  
 VC = 10; % Compression space volume (m^3)  
 VE = 11; % Expansion space volume (m^3)  
 MC = 12; % Mass of gas in the compression space (kg)  
 MK = 13; % Mass of gas in the cooler (kg)  
 MR = 14; % Mass of gas in the regenerator (kg)  
 MH = 15; % Mass of gas in the heater (kg)  
 ME = 16; % Mass of gas in the expansion space (kg)  
 TCK = 17; % Conditional temperature compression space / cooler (K)  
 THE = 18; % Conditional temperature heater / expansion space (K)  
 GACK = 19; % Conditional mass flow compression space / cooler (kg/rad)  
 GAKR = 20; % Conditional mass flow cooler / regenerator (kg/rad)  
 GARH = 21; % Conditional mass flow regenerator / heater (kg/rad)  
 GAHE = 22; % Conditional mass flow heater / expansion space (kg/rad)  
 V = 23; % Total volume (m^3)

% Size of var(ROWV,COL), dvar(ROWD,COL)

ROWV = 23; % number of rows in the var matrix  
 ROWD = 16; % number of rows in the dvar matrix  
 COL = 37; % number of columns in the matrices (every 10 degrees)

%=====

global tk % cooler temperatures [K]  
 global tr % regen temperatures [K]  
 global th % heater temperatures [K]  
 global vk % cooler void volume [m^3]

```

global vr % regen void volume [m^3]
global vh % heater void volume [m^3]
global freq % operating frequency [Hz]

display('start sim')

define;
% choice = 'x';
% while(~strncmp(choice,'q',1))
% fprintf('Choose simulation:\n');
% choice = input('a)diabatic, s)imple q)uit: ','s');
% if(strncmp(choice,'a',1))
% [var,dvar] = adiabatic;
% else if(strncmp(choice,'s',1))

[var,dvar] = simple;

fprintf('quitting simulation...\n');

function [var,dvar] = adiab

% ideal adiabatic model simulation
% Returned values:
% var(23,37) array of variable values every 10 degrees (0 - 360)
% dvar(16,37) array of derivatives every 10 degrees (0 - 360)

% Row indices of the var, dvar matrices, and the y,dy variable vectors:
TC = 1; % Compression space temperature (K)
TE = 2; % Expansion space temperature (K)
QK = 3; % Heat transferred to the cooler (J)
QR = 4; % Heat transferred to the regenerator (J)
QH = 5; % Heat transferred to the heater (J)
WC = 6; % Work done by the compression space (J)
WE = 7; % Work done by the expansion space (J)
W = 8; % Total work done (WC + WE) (J)
P = 9; % Pressure (Pa)
VC = 10; % Compression space volume (m^3)
VE = 11; % Expansion space volume (m^3)
MC = 12; % Mass of gas in the compression space (kg)
MK = 13; % Mass of gas in the cooler (kg)
MR = 14; % Mass of gas in the regenerator (kg)
MH = 15; % Mass of gas in the heater (kg)
ME = 16; % Mass of gas in the expansion space (kg)
TCK = 17; % Conditional temperature compression space / cooler (K)
THE = 18; % Conditional temperature heater / expansion space (K)
GACK = 19; % Conditional mass flow compression space / cooler (kg/rad)
GAKR = 20; % Conditional mass flow cooler / regenerator (kg/rad)
GARH = 21; % Conditional mass flow regenerator / heater (kg/rad)
GAHE = 22; % Conditional mass flow heater / expansion space (kg/rad)
V = 23; % Total volume (m^3)

% Size of var(ROWV,COL), y(ROWV), dvar(ROWD,COL), dy(ROWD)
ROWV = 23; % number of rows in the var matrix
ROWD = 16; % number of rows in the dvar matrix
COL = 37; % number of columns in the matrices (every 10 degrees)

```

```

global tk % cooler temperatures [K]
global th % heater temperatures [K]

% *****

fprintf('===== The Ideal Analysis =====\n')

fprintf('Cooler temperature: Tk = %.1f (K)\n', tk);
fprintf('Heater temperatuer: Th = %.1f (K)\n\n', th);

fprintf('*****\n\n');

epsilon = 0.1; % Allowable error in temperature (K)
max_iteration = 20; % Maximum number of iterations to convergence
ninc = 360; % number if integration increments (every degree)
step = ninc/36; % for saving values in var, dvar matrices
dtheta = 2.0*pi/ninc; % integration increment (radians)

% Initial conditions:
y(THE) = th;
y(TCK) = tk;
y(TE) = th;
y(TC) = tk;

iter = 0;
t_error = 10*epsilon; % Initial error to enter the loop

% Iteration loop to cyclic convergence
while ((t_error >= epsilon)&(iter < max_iteration))

% cyclic initial conditions
tc0 = y(TC);
te0 = y(TE);
theta = 0;
y(QK) = 0;
y(QR) = 0;
y(QH) = 0;
y(WC) = 0;
y(WE) = 0;
y(W) = 0;

fprintf('iteration %d: y(TC) = %.1f(K) & y(TE) = %.1f(K)\n\n',iter,y(TC),y(TE));

for i = 1:1:ninc

[theta,y,dy] = rk4('dadiab',7,theta,dtheta,y);

end

t_error = abs(tc0 - y(TC)) + abs(te0 - y(TE));
iter = iter + 1;

end

if (iter >= max_iteration)

```

```

fprintf('No convergence within %d iteration\n',max_iteration);

end

% Initial var and dvar matrix
var = zeros(23,37);
dvar = zeros(16,37);

% a final cycle, to fill the var, dvar matrices
theta = 0;
y(QK) = 0;
y(QR) = 0;
y(QH) = 0;
y(WC) = 0;
y(WE) = 0;
y(W) = 0;

[var,dvar] = Filmatrix(1,y,dy,var,dvar);

for i = 2:1:COL
for j = 1:1:step

[theta,y,dy] = rk4('dadiab',7,theta,dtheta,y);

end

[var,dvar] = Filmatrix(i,y,dy,var,dvar);

end

end

function define

% define the stirling engine geometric and operational parameters

% The set of global variables defined are:

% engine % Free Piston Stirling Engine (FPSE)
global vclc % compression clearance vols [m^3]
global vcle % expansion clearance vols [m^3]
global vswc % compression swept volumes [m^3]
global vswe % expansion swept volumes [m^3]
global alpha % phase angle advance of expansion space [radians]
% global dpp % diameter of power pistons [m]
% global ddcomp % diameter of displacer at compression side [m]
% global ddexp % diameter of displacer at expansion side [m]
% global app % area of power pistons [m^2]
% global adcomp % area of displacer at compression side [m^2]
% global adexp % area of displacer at expansion side [m^2]
% global ypp % maximum power piston vertical displacement [m]
% global yd % maximum displacer vertical displacement [m]

% heatex/cooler
global dk % cooler hydraulic diameter [m]
global lk % cooler effective length [m]
global ak % cooler internal free flow area [m^2]

```

```

global vk % cooler void volume [m^3]
global awgk % cooler internal wetted area [m^2]

% heatex/heater
global dh % heater hydraulic diameter [m]
global lh % heater effective length [m]
global ah % heater internal free flow area [m^2]
global vh % heater void volume [m^3]
global awgh % heater internal wetted area [m^2]

% heatex/regenerator
global dr % regen hydraulic diameter [m]
global lr % regenerator effective length [m]
global ar % regen internal free flow area [m^2]
global vr % regen void volume [m^3]
global awgr % regen internal wetted area [m^2]
global cqwr % regenerator housing thermal conductance [W/K]
global awgr0 % no matrix regenerator wetted area [m^2]

% gas
global rgas % gas constant [J/kg.K]
global cp % specific heat capacity at constant pressure [J/kg.K]
global cv % specific heat capacity at constant volume [J/kg.K]
global gama % ratio: cp/cv
global mu0 % dynamic viscosity at reference temp t0 [kg.m/s]
global t0 % reference temp. [K]
global t_suth % Sutherland constant [K]
global prandtl% Prandtl number

% operat
global tk % cooler temperatures [K]
global tr % regenerator temperatures [K]
global th % heater temperatures [K]
global pmean % mean (charge) pressure [Pa]
global freq % cycle frequency [Hz]
global omega % cycle frequency [rads/s]
global mgas % total mass of gas in engine [kg]

% new data file
global new fid

new = input('Create a new data file? (y/n)', 's');

if strcmp(new, 'y', 1)

    filename = input('enter new filename: ', 's');
    fid = fopen(filename, 'w');

else

    fid = 0;

    while fid < 1

```

```

        filename = input('open filename: ','s');
        [fid, message] = fopen(filename,'r');

        if fid == -1

                display(message)
        display('press ^C to exit')

        end

    end

end

engine;
heatex;
gas;
operat;
% status =
fclose(fid);

end

function engine

% Define the free piston engine configuration geometric parameters.

% global engine_type % free piston type)
global new fid % new data file

freepiston;

% *****

function freepiston

% New Free-Piston Stirling Engine design (FPSE)
% Ghozzi 13/02/2014

global vclc % compression clearance vols [m^3]
global vcle % expansion clearance vols [m^3]
global vswc % compression swept volumes [m^3]
global vswe % expansion swept volumes [m^3]
global alpha % phase angle advance of expansion space [radians]

% global dcomp dexp % diameter of compression/expansion pistons [m]
% global acomp aexp % area of compression/expansion pistons [m^2]
% global yminc % minimum piston vertical displacement [m]
% global ymaxc % maximum piston vertical displacement [m]
% global ymine % minimum displacer vertical displacement [m]
% global ymaxe % maximum displacer vertical displacement [m]
% global new fid % new data file

fprintf('===== FPSE Data configuration =====\n\n');

if(strcmp(new,'y',1))

```

```

vclc = input('enter compression space clearance volume (vclc) [m^3]: ');
vswc = input('enter compression space swept volume (vswc) [m^3]: ');
vcle = input('enter expansion space clearance volume (vcle) [m^3]: ');
vswe = input('enter expansion space swept volume (vswe) [m^3]: ');
phase = input('enter expansion phase angle advance (alpha) [degrees]: ');

alpha = phase * pi/180;

fprintf(fid, '%.3e\n', vclc);
    fprintf(fid, '%.3e\n', vswc);
    fprintf(fid, '%.3e\n', vcle);
    fprintf(fid, '%.3e\n', vswe);
    fprintf(fid, '%.3f\n', alpha);

else

    vclc = fscanf(fid,'%e',1);
    vswc = fscanf(fid,'%e',1);
    vcle = fscanf(fid,'%e',1);
    vswe = fscanf(fid,'%e',1);
    alpha = fscanf(fid, '%f',1);

end

fprintf('==== free piston stirling engine data summary =====\n');
fprintf(' compression clearance volume: vclc = %.1f (cc)\n', vclc*1e6);
fprintf(' compression swept volume: vswc = %.1f (cc)\n', vswc*1e6);
fprintf(' expansion clearance volume: vcle = %.1f (cc)\n', vcle*1e6);
fprintf(' expansion swept volume: vswe = %.1f (cc)\n', vswe*1e6);
fprintf(' expansion phase angle advance: alpha = %.1f (rad)\n\n', alpha);
fprintf('*****\n\n');

end

end
function gas

% specifies the working gas properties (he, h2, air)
global cp % specific heat capacity at constant pressure [J/kg.K]
global cv % specific heat capacity at constant volume [J/kg.K]
global gama % ratio: cp/cv
global rgas % gas constant [J/kg.K]
global mu0 % dynamic viscosity at reference temp t0 [kg.m/s]
global t0 % reference temperature [K]
global t_suth % Sutherland constant [K]
global prandtl % Prandtl number
global new fid % new data file

gas_type = 'un';

while(strncmp(gas_type,'un',2))

    if(strncmp(new,'y',1))

        fprintf('Available gas types are:\n');
        fprintf(' hy)drogen)\n');

```

```

        fprintf(' helium\n');
        fprintf(' air\n');
        gas_type = input('enter gas type: ','s');
        gas_type = [gas_type(1), gas_type(2)];
        fprintf(fid, '%s\n', gas_type);

    else

        fscanf(fid, '%c',1); % bypass the previous newline character
        gas_type = fscanf(fid, '%c',2);

    end

    if(strncmp(gas_type,'hy',2))

        fprintf('gas type is hydrogen\n')
        gama = 1.4;
        rgas = 4157.2;
        mu0 = 8.35e-6;
        t_suth = 84.4;

        elseif(strncmp(gas_type,'he',2))

            fprintf('gas type is helium\n')
            gama = 1.67;
            rgas = 2078.6;
            mu0 = 18.85e-6;
            t_suth = 80.0;

            elseif(strncmp(gas_type,'ai',2))

                fprintf('gas type is air\n')
                gama = 1.4;
                rgas = 287.0;
                mu0 = 17.08e-6;
                t_suth = 112.0;

            else

                fprintf('gas type is undefined\n\n')
                gas_type = 'un';

            end

        end

    cv = rgas/(gama - 1);
    cp = gama*cv;
    t0 = 273;
    prandtl = 0.71;

    end

function heatex

% Specify heat exchanger geometric parameters

```

```

cooler;
heater;
regen;

%*****

function cooler

% Specify cooler geometric parameters

global vk % cooler void volume [m^3]
global ak % cooler internal free flow area [m^2]
global awgk % cooler internal wetted area [m^2]
global dk % cooler hydraulic diameter [m]
global lk % cooler effective length [m]
global new fid % new data file

fprintf('===== Available cooler type is smooth annulus =====\n\n');

    [vk,ak,awgk,dk,lk] = annulus;

fprintf('===== cooler data summary =====\n');
fprintf(' cooler void volume: vk = %.2f (cc)\n', vk*1e6);
fprintf(' cooler free flow area: ak = %.2f (cm^2)\n', ak*1e4);
fprintf(' cooler wetted area: awgk = %.2f (cm^2)\n', awgk*1e4);
fprintf(' cooler hydraulic diameter: dk = %.2f (mm) \n', dk*1e3);
fprintf(' cooler length: lk = %.2f (cm)\n\n', lk*1e2);
fprintf('*****\n\n');

end

%*****

function heater

% Specify heater geometric parameters

global vh % heater void volume [m^3]
global ah % heater internal free flow area [m^2]
global awgh % heater internal wetted area [m^2]
global dh % heater hydraulic diameter [m]
global lh % heater effective length [m]
global new fid % new data file

fprintf('===== Available heater type is smooth annulus =====\n\n');

    [vh,ah,awgh,dh,lh] = annulus;

fprintf('===== heater data summary =====\n');
fprintf(' heater void volume: vh = %.2f (cc)\n', vh*1e6);
fprintf(' heater free flow area: ah = %.2f (cm^2)\n', ah*1e4);
fprintf(' heater wetted area: awgh = %.2f (cm^2)\n', awgh*1e4);
fprintf(' heater hydraulic diameter: dh = %.2f (mm)\n', dh*1e3);
fprintf(' heater length:lh = %.2f (cm)\n\n', lh*1e2);
fprintf('*****\n\n');

end

```

```

%*****

function [v,a,awg,d,len] = annulus

% annular gap heat exchanger

global new fid % new data file

% fprintf(' annular gap heat exchanger\n');

if(strncmp(new,'y',1))

    dout = input('enter annular gap outer diameter (dout) [m] : ');
    din  = input('enter annular gap inner diameter (din) [m] : ');
    len  = input('enter heat exchanger length (len) [m] : ');

    fprintf(fid, '%.3e\n', dout);
    fprintf(fid, '%.3e\n', din);
    fprintf(fid, '%.3e\n', len);

else

    dout = fscanf(fid,'%e',1);
    din  = fscanf(fid,'%e',1);
    len  = fscanf(fid,'%e',1);

end

a = pi*(dout*dout - din*din)/4;
v = a*len;
awg = pi*dout*len;
d = dout - din;

end

%*****

% function [v,a,awg,d,len] = pipes
% % homogeneous smooth pipes heat exchanger

% global new fid % new data file
%
% fprintf('INTERCAMBIADOR DE TUBOS\n')
% if(strncmp(new,'y',1))
% d = input('ingrese el diametro del tubo [m] : ');
% l = input('ingrese el diametro promedio del intercambiador [m] : ');
% num = input('ingrese el numero de vueltas : ');
% fprintf(fid, '%.3e\n', d);
% fprintf(fid, '%.3e\n', l);
% fprintf(fid, '%d\n', num);
% else
% d = fscanf(fid,'%e',1);
% l = fscanf(fid,'%e',1);
% num = fscanf(fid,'%d',1);
% end

```

```

%
% dout = 0.65 + d/2;
% din = 0.65 - d/2;
% len=pi*I;
% a = pi*(0.63*0.63 - 0.6*0.6)/4 - pi*(dout*dout - din*din)/4; % area de paso es el area total
menos la
% cantidadd de tubos en la primero fila, de 3.
% v = num*pi*d*d/4*len;
% awg = num*pi*d*len;

% end

```

```

% *****

```

```

% function [v,a,awg,d,len] = slots
% % slots heat exchanger
%
% global new fid % new data file
%
% fprintf(' slots heat exchanger\n')
% if(strncmp(new,'y',1))
% w = input('enter width of slot [m] : ');
% h = input('enter height of slot [m] : ');
% len = input('enter heat exchanger length [m] : ');
% num = input('enter number of slots : ');
% fprintf(fid, '%.3e\n', w);
% fprintf(fid, '%.3e\n', h);
% fprintf(fid, '%.3e\n', len);
% fprintf(fid, '%d\n', num);
% else
% w = fscanf(fid,'%e',1);
% h = fscanf(fid,'%e',1);
% len = fscanf(fid,'%e',1);
% num = fscanf(fid,'%d',1);
% end
%
% a = num*w*h;
% v = a*len;
% awg = num*2*(w + h)*len;
% d = 4*v/awg;

% end

```

```

end

```

```

function tgh = hotsimple(var,twh)

```

```

% evaluate heater average heat transfer performance
% Arguments:
% var(23,37) array of variable values every 10 degrees (0 - 360)
% twh - heater wall temperature [K]
% Returned values:
% tgh - heater average gas temperature [K]

```

```

% Row indices of the var array:
TC = 1; % Compression space temperature [K]

```

```

TE = 2; % Expansion space temperature [K]
QK = 3; % Heat transferred to the cooler [J]
QR = 4; % Heat transferred to the regenerator [J]
QH = 5; % Heat transferred to the heater [J]
WC = 6; % Work done by the compression space [J]
WE = 7; % Work done by the expansion space [J]
W = 8; % Total work done (WC + WE) [J]
P = 9; % Pressure [Pa]
VC = 10; % Compression space volume [m^3]
VE = 11; % Expansion space volume [m^3]
MC = 12; % Mass of gas in the compression space [kg]
MK = 13; % Mass of gas in the cooler [kg]
MR = 14; % Mass of gas in the regenerator [kg]
MH = 15; % Mass of gas in the heater [kg]
ME = 16; % Mass of gas in the expansion space [kg]
TCK = 17; % Conditional temperature compression space / cooler [K]
THE = 18; % Conditional temperature heater / expansion space [K]
GACK = 19; % Conditional mass flow compression space / cooler [kg/rad]
GAKR = 20; % Conditional mass flow cooler / regenerator [kg/rad]
GARH = 21; % Conditional mass flow regenerator / heater [kg/rad]
GAHE = 22; % Conditional mass flow heater / expansion space [kg/rad]
V = 23; % Total volume [m^3]

```

```

%*****

```

```

global th % heater temperature [K]
global dh % heater hydraulic diameter [m]
global ah % heater internal free flow area [m^2]
global awgh % heater internal wetted area [m^2]
global freq % cycle frequency [Hz]
global omega % cycle frequency [rads/s]
global qrloss % Regenerator net enthalpy loss

```

```

% Calculating the Reynolds number over the cycle
for i = 1:1:37
%
%   freq = 5:5:185;
%   omega = 2*pi*freq(i);

```

```

gah(i) = (var(GARH,i) + var(GAHE,i))*omega/2;
gh = gah(i)/ah;

```

```

[mu,kgas,re(i)] = reynum(th,gh,dh);

```

```

end

```

```

% Average and maximum Reynolds number
sumre=0;
remax=re(1);

```

```

for i = 1:1:36

```

```

sumre=sumre + re(i);

```

```

if(re(i) > remax)

```

```

remax = re(i);

end

end

reavg = sumre/36;

[ht,fr] = pipefr(dh,mu,reavg); % Heat transfer coefficient

tgh = twh - (var(QH,37))*freq/(ht*awgh); % Heater gas temperature [K]

qh = var(QH,37);

fprintf('===== Heater Simple analysis =====\n');
fprintf(' Average Reynolds number: reavg = %.1f\n',reavg);
fprintf(' Maximum Reynolds number: remax = %.1f\n',remax);
fprintf(' Heat transfer coefficient: ht = %.2f (W/m^2*K)\n',ht);
fprintf('Heat transferred to the heater: qh = %.2f (J)\n',qh);
fprintf('heater wall temperatures: Twh = %.1f (K)\n',twh);
fprintf('heater gas temperatures: Tgh = %.1f (K)\n\n',tgh);
fprintf('*****\n\n');

end

function tgtk = kolsimple(var,twk)

% evaluate cooler average heat transfer performance
% Arguments:
% var(23,37) array of variable values every 10 degrees (0 - 360)
% twk - cooler wall temperature [K]
% Returned values:
% tgtk - cooler average gas temperature [K]

% Row indices of the var array:
TC = 1; % Compression space temperature [K]
TE = 2; % Expansion space temperature [K]
QK = 3; % Heat transferred to the cooler [J]
QR = 4; % Heat transferred to the regenerator [J]
QH = 5; % Heat transferred to the heater [J]
WC = 6; % Work done by the compression space [J]
WE = 7; % Work done by the expansion space [J]
W = 8; % Total work done (WC + WE) [J]
P = 9; % Pressure [Pa]
VC = 10; % Compression space volume [m^3]
VE = 11; % Expansion space volume [m^3]
MC = 12; % Mass of gas in the compression space [kg]
MK = 13; % Mass of gas in the cooler [kg]
MR = 14; % Mass of gas in the regenerator [kg]
MH = 15; % Mass of gas in the heater [kg]
ME = 16; % Mass of gas in the expansion space [kg]
TCK = 17; % Conditional temperature compression space / cooler [K]
THE = 18; % Conditional temperature heater / expansion space [K]
GACK = 19; % Conditional mass flow compression space / cooler [kg/rad]
GAKR = 20; % Conditional mass flow cooler / regenerator [kg/rad]
GARH = 21; % Conditional mass flow regenerator / heater [kg/rad]
GAHE = 22; % Conditional mass flow heater / expansion space [kg/rad]

```

V = 23; % Total volume ([m^3])

%\*\*\*\*\*

global tk % cooler temperature [K]  
global freq % cycle frequency [Hz]  
global omega % cycle frequency [rads/s]  
global ak % cooler internal free flow area [m^2]  
global awgk % cooler internal wetted area [m^2]  
global dk % cooler hydraulic diameter [m]  
global qrloss % Regenerator net enthalpy loss

% Calculating the Reynolds number over the cycle  
for i = 1:1:37

% freq = 5:5:185;  
% omega = 2\*pi\*freq(i);

gak(i) = (var(GACK,i) + var(GAKR,i))\*omega/2;  
gk = gak(i)/ak;

[mu,kgas,re(i)] = reynum(tk,gk,dk);

end

% Average and maximum Reynolds number  
sumre=0;  
remax=re(1);

for i = 1:1:36

sumre=sumre + re(i);

if(re(i) > remax)

remax = re(i);

end

end

reavg = sumre/36;

[ht,fr] = pipefr(dk,mu,reavg); % Heat transfer coefficient

tgk = twk - (var(QK,37))\*freq/(ht\*awgk); % Cooler gas temperature [K]

qk = var(QK,37);

% tgk = twk - (var(QK,37)-qrloss)\*freq/(ht\*awgk); % Cooler gas temperature [K]

fprintf('=====  
Cooler Simple analysis  
=====\n')

fprintf(' Average Reynolds number: reavg = %.1f\n',reavg)

fprintf(' Maximum Reynolds number: remax = %.1f\n',remax)

fprintf(' Heat transfer coefficient: ht = %.2f (W/m^2\*K)\n',ht)

fprintf('Heat transferred from the cooler: qk = %.2f (J)\n',qk);

fprintf('cooler wall temperatures: Twk = %.1f (K)\n',twk);

```

fprintf('cooler gas temperatures: Tk = %.1f (K)\n\n',tgk);
fprintf('*****\n\n');

end

function operat

% Determine operating parameters

global pmean % mean (charge) pressure [Pa]
global tk tr th % cooler, regenerator, heater temperatures [K]
global freq omega % cycle frequency [herz], [rads/s]
global new fid % new data file

if(strncmp(new,'y',1))

    pmean = input('enter mean pressure (Pa) : ');
    tk = input('enter cold sink temperature (tk) in [K] : ');
    th = input('enter hot source temperature (th) in [K] : ');
    freq = input('enter operating frequency in (freq) in [Hz] : ');

    fprintf(fid, '%.1f\n', pmean);
    fprintf(fid, '%.1f\n', tk);
    fprintf(fid, '%.1f\n', th);
    fprintf(fid, '%.1f\n', freq);

else

    pmean = fscanf(fid,'%f',1);
    tk = fscanf(fid,'%f',1);
    th = fscanf(fid,'%f',1);
    freq = fscanf(fid,'%f',1);

end

tr = (th - tk)/log(th/tk);

% for i = 1:1:37
%
% freq = 5:5:185;
omega = 2*pi*freq;

% end

%save('freq.mat','freq');
%save('omega.mat','omega');

fprintf('*****\n\n');
fprintf('===== operating parameters ===== \n');
fprintf(' mean pressure: pmaen = %.3f (kPa) \n',pmean*1e-3);
fprintf(' cold sink temperature: tk = %.1f (K) \n',tk);
fprintf(' hot source temperature: th = %.1f (K) \n',th);
fprintf(' effective regenerator temperature: tr = %.1f (K) \n',tr);
fprintf(' operating frequency: freq = %.1f (Hz)\n\n',freq);
fprintf('*****\n\n');

```

Schmidt;

end

%\*\*\*\*\*

function Schmidt

% Schmidt analysis

global vclc % compression clearance volume [m<sup>3</sup>]

global vcle % expansion clearance volume [m<sup>3</sup>]

global vswc % compression swept volume [m<sup>3</sup>]

global vswe % expansion swept volume [m<sup>3</sup>]

global vk % cooler volumes [m<sup>3</sup>]

global vr % regenerator volumes [m<sup>3</sup>]

global vh % heater volumes [m<sup>3</sup>]

global tk % cooler temperatures [K]

global tr % regen temperatures [K]

global th % heater temperatures [K]

global pmean % mean (charge) pressure [Pa]

global mgas % total mass of gas in engine [kg]

global rgas % gas constant [J/kg.K]

global freq % cycle frequency [Hz]

global omega % cycle frequency [rads/s]

global alpha % phase angle advance of expansion space [radians]

global vtot % total Schmidt volume

global p % pressure

%\*\*\*\*\*

% Schmidt analysis

c = (((vswe/th)<sup>2</sup> + (vswc/tk)<sup>2</sup> + 2\*(vswe/th)\*(vswc/tk)\*cos(alpha))<sup>0.5</sup>)/2;

s = (vswc/2 + vclc + vk)/tk + vr/tr + (vswe/2 + vcle + vh)/th;

b = c/s;

sqrtb = (1 - b<sup>2</sup>)<sup>0.5</sup>;

bf = (1 - 1/sqrtb);

beta = atan(vswe\*sin(alpha)/th/(vswe\*cos(alpha)/th + vswc/tk));

fprintf(' pressure phase angle: (beta) = %.1f(degrees)\n\n',beta\*180/pi);

% total mass of working gas in engine

mgas = pmean\*s\*sqrtb/rgas;

fprintf(' total mass of gas: (mgas) = %.3f(gm)\n\n',mgas\*1e3);

% work output

wc = (pi\*vswc\*mgas\*rgas\*sin(beta)\*bf/c);

we = (pi\*vswe\*mgas\*rgas\*sin(beta - alpha)\*bf/c);

w = (wc + we);

% for i = 1:1:37

% freq = 5:5:185;

power = w\*freq;

eff = power /we; % qe = we

% end

save('effecincy.mat','eff');

% power = w\*freq;

% eff = w/we; % qe = we

```

% figure;
% plot(freq,eff,'k-', 'LineWidth',2);
% grid on
% xlabel('frequency [Hz]');
% ylabel('Effecincy [%]');
% Printout Schmidt analysis results
fprintf('*****\n\n');
fprintf('===== Schmidt analysis =====\n');
fprintf(' Work: w = %.3e (joules)\n', w);
fprintf(' Power: power = %.3e (Watts)\n',power);
fprintf(' Heat removed from compression space: qc = wc = %.3e (joules)\n',wc);
fprintf(' Heat added to the expansion space: qe = we = %.3e (joules) \n', we);
fprintf(' Schmidt efficiency: eff = %.2f\n\n', eff);
fprintf('*****\n\n')

% Plot Schmidt analysis pv and p-theta diagrams
theta = 0:5:360;
vc = vclc + 0.5*vswc*(1 + cos(theta*pi/180));
ve = vcle + 0.5*vswe*(1 + cos(theta*pi/180 + alpha));
p = mgas*rgas./(vc/tk + vk/tk + vr/tr + vh/th + ve/th)*1e-5; % conversion to [bar]
vtot = (vc + vk + vr + vh + ve)*1e6; % conversion to [cc]

% fprintf('*****\n\n')

% Plot Alan Organ's particle mass distribution in Natural Coordinates
% fprintf('Do you want particle mass distribution plot\n');
% choice = input('yes or n)o: ','s');
% if(strncmp(choice,'y',1))
% plotmass
% end
end

%=====
=

function regen

% Specifies regenerator geometric and thermal properties

global lr % regenerator effective length [m]
global cqwr % regenerator housing thermal conductance [W/K]
global awgr0 % no matrix regenerator wetted area [m^2]
global new fid % new data file

fprintf('=== Available regenerator is anuular nomatrix regenerator ===\n\n');

if(strncmp(new,'y',1))

    dout = input('enter housing external diameter (dout) [m]: ');
    din = input('enter housing internal diameter (din) [m]: ');
    dimat = input('enter matrix internal diameter (dimat) [m]: ');
    lr = input('enter regenerator length (lr) [m]: ');

```

```

        fprintf(fid, '%.3e\n', dout);
        fprintf(fid, '%.3e\n', din);
        fprintf(fid, '%.3e\n', dimat);
        fprintf(fid, '%.3e\n', lr);

    else

        dout = fscanf(fid, '%e', 1);
        din  = fscanf(fid, '%e', 1);
        dimat = fscanf(fid, '%e', 1);
        lr   = fscanf(fid, '%e', 1);

    end

    num = 1;
    awgr0 = pi*(dimat + din)*lr;
    amat = num*pi*(din*din - dimat*dimat)/4; % regen matrix area
    awr  = num*pi*(dout*dout - din*din)/4; % regen housing wall area

    kwr = 25; % thermal conductivity for stainless steel, which depends on temp. [W/m/K]
    cqwr = kwr*awr/lr; % regen wall thermal conductance [W/K]

    nomatrix(amat);

    % note that stainless steel thermal conductivity is temp dependent
    % 25 W/m/K for normal engine conditions,
    % 6 W/m/K for cryogenic coolers.

    % matrix(amat);

end

%*****

function nomatrix(amat)

% Specifies conditions for no regenerator matrix
global dr % regen hydraulic diameter [m]
global vr % regen void volume [m^3]
global ar % regen internal free flow area [m^2]
global awgr % regen internal wetted area [m^2]
global awgr0 % no matrix regenerator wetted area [m^2]
global lr % regenerator effective length [m]

ar = amat;
vr = ar*lr;
awgr = awgr0;
dr = 4*vr/awgr;

fprintf('===== regenerator data summary =====\n');
fprintf(' regenerator hydraulic diam: dr = %.3f (mm)\n', dr*1e3);
fprintf(' regenerator total wetted area: awgr = %f (sq.m)\n', awgr);
fprintf(' regenerator void volume: vr = %.2f (cc)\n\n', vr*1e6);
fprintf('*****\n\n');

end
function qrloss = regsimple(var)

```

```

% Evaluate the effectiveness and performance of the regenerator
% Arguments:
% var(22,37) array of variable values every 10 degrees (0 - 360)
% Returned value:
% qrgloss - regenerator net enthalpy loss [J]

% Row indices of the var array:
TC = 1; % Compression space temperature [K]
TE = 2; % Expansion space temperature [K]
QK = 3; % Heat transferred to the cooler [J]
QR = 4; % Heat transferred to the regenerator [J]
QH = 5; % Heat transferred to the heater [J]
WC = 6; % Work done by the compression space [J]
WE = 7; % Work done by the expansion space [J]
W = 8; % Total work done (WC + WE) [J]
P = 9; % Pressure [Pa]
VC = 10; % Compression space volume [m^3]
VE = 11; % Expansion space volume [m^3]
MC = 12; % Mass of gas in the compression space [kg]
MK = 13; % Mass of gas in the cooler [kg]
MR = 14; % Mass of gas in the regenerator [kg]
MH = 15; % Mass of gas in the heater [kg]
ME = 16; % Mass of gas in the expansion space [kg]
TCK = 17; % Conditional temperature compression space / cooler [K]
THE = 18; % Conditional temperature heater / expansion space [K]
GACK = 19; % Conditional mass flow compression space / cooler [kg/rad]
GAKR = 20; % Conditional mass flow cooler / regenerator [kg/rad]
GARH = 21; % Conditional mass flow regenerator / heater [kg/rad]
GAHE = 22; % Conditional mass flow heater / expansion space [kg/rad]
V = 23; % Total volume ([m^3]

% *****

% global matrix_type % mesh or foil %% No matrix
% global tr1 % regen1 temperature [K]
% global tr2 % regen2 temperature [K]
global tr % regen temperature [K]
global dr % regen hydraulic diameter [m]
global ar % regen internal free flow area [m^2]
global awgr % regen internal wetted area [m^2]
global freq % cycle frequency [Hz]
global omega % cycle frequency [rads/s]

% Reynolds number over the cycle
for i = 1:1:37

    gar(i) = (var(GAKR,i) + var(GARH,i))*omega/2;

    gr = gar(i)/ar;

    [mu,kgas,re(i)] = reynum(tr,gr,dr);

end

% average and maximum Reynolds number

```

```

sumre = 0;
remax = re(1);

for i = 1:1:36

    sumre = sumre + re(i);

    if(re(i) > remax)

        remax = re(i);

    end

end

reavg = sumre/36;

[st,fr] = matrixfr(reavg); %%% No matrix

ntu = st*awgr/(2*ar);

effect = ntu/(ntu + 1);

% Calculate qrloss
for i = 1:1:37

    qreg(i) = var(QR,i);

end

qrmin = min(qreg);
qrmax = max(qreg);
qrloss = (1 - effect)*(qrmax - qrmin);

% Regenerator Simple Analysis Results:
fprintf('===== Regenerator simple analysis =====\n');
fprintf('Average Reynolds number: reavg = %.1f\n', reavg);
fprintf('Maximum Reynolds number: remax = %.1f\n', remax);
fprintf('Stanton number(Average Re): st = %.3f\n',st);
fprintf('Number of transfer units: ntu = %.1f\n',ntu);
fprintf('Regenerator effectiveness = %.3f%\n\n',effect*100);
fprintf('*****\n\n');

end

function [mu,kgas,re] = reynum(t,g,d)

% evaluate dynamic viscosity, thermal conductivity, Reynolds number
% Arguments:
% t - gas temperature [K]
% g - mass flux [kg/m^2.s]
% d - hydraulic diameter [m]
% Returned values:
% mu - gas dynamic viscosity [kg.m/s]
% kgas - gas thermal conductivity [W/m.K]

```

```

% re - Reynolds number

global cp % specific heat capacity at constant pressure [J/kg.K]
global mu0 % dynamic viscosity at reference temp t0 [kg.m/s]
global t0 % reference temperature [K]
global t_suth % Sutherland constant [K]
global prandtl % Prandtl number

mu = mu0*(t0 + t_suth)/(t + t_suth)*(t/t0)^1.5;
kgas = cp*mu/prandtl;
re = abs(g)*d/mu;

if(re < 1)

    re = 1;

end

end

function [x, y, dy] = rk4(deriv,n,x,dx,y)

%Classical fourth order Runge-Kutta method
%Integrates n first order differential equations
%dy(x,y) over interval x to x+dx

x0 = x;
y0 = y;

[y,dy1] = feval(deriv,x0,y);

for i = 1:n

    y(i) = y0(i) + 0.5*dx*dy1(i);

end

xm = x0 + 0.5*dx;

[y,dy2] = feval(deriv,xm,y);

for i = 1:n

    y(i) = y0(i) + 0.5*dx*dy2(i);

end

[y,dy3] = feval(deriv,xm,y);

for i = 1:n

    y(i) = y0(i) + dx*dy3(i);

end

x = x0 + dx;

[y,dy] = feval(deriv,x,y);

```

```

for i = 1:n

dy(i) = (dy1(i) + 2*(dy2(i) + dy3(i)) + dy(i))/6;
y(i) = y0(i) + dx*dy(i);

end

end
function [var,dvar] = simple

% Simple Analysis- including heat transfer and pressure drop effects
% Returned values:
% var(23,37) array of variable values every 10 degrees (0 - 360)
% dvar(16,37) array of derivatives every 10 degrees (0 - 360)

% Row indices of the var, dvar arrays:
TC = 1; % Compression space temperature [K]
TE = 2; % Expansion space temperature [K]
QK = 3; % Heat transferred to the cooler [J]
QR = 4; % Heat transferred to the regenerator [J]
QH = 5; % Heat transferred to the heater [J]
WC = 6; % Work done by the compression space [J]
WE = 7; % Work done by the expansion space [J]
W = 8; % Total work done (WC + WE) [J]
P = 9; % Pressure [Pa]
VC = 10; % Compression space volume [m^3]
VE = 11; % Expansion space volume [m^3]
MC = 12; % Mass of gas in the compression space [kg]
MK = 13; % Mass of gas in the cooler [kg]
MR = 14; % Mass of gas in the regenerator [kg]
MH = 15; % Mass of gas in the heater [kg]
ME = 16; % Mass of gas in the expansion space [kg]
TCK = 17; % Conditional temperature compression space / cooler [K]
THE = 18; % Conditional temperature heater / expansion space [K]
GACK = 19; % Conditional mass flow compression space / cooler [kg/rad]
GAKR = 20; % Conditional mass flow cooler / regenerator [kg/rad]
GARH = 21; % Conditional mass flow regenerator / heater [kg/rad]
GAHE = 22; % Conditional mass flow heater / expansion space [kg/rad]
V = 23; % Total volume ([m^3]

% Size of var(ROWV,COL), dvar(ROWD,COL)
ROWV = 23; % number of rows in the var matrix
ROWD = 16; % number of rows in the dvar matrix
COL = 37; % number of columns in the matrices (every 10 degrees)

%*****

global tk % cooler temperatures [K]
global tr % regen temperatures [K]
global th % heater temperatures [K]
global cqwr % regenerator housing thermal conductance [W/K]
global freq % cycle frequency [Hz]

%*****

twk = tk; % Cooler wall temp - equal to initial cooler gas temp

```

```

twh = th; % Heater wall temp - equal to initial heater gas temp
epsilon = 1; % allowable temperature error bound for cyclic convergence
t_error = 10*epsilon; % Initial temperature error (to enter loop)

while (t_error > epsilon)

    [var,dvar] = adiab;

    qrlloss = regsimple(var);
    tgh = hotsimple(var,twh); % new heater gas temperature
    tgk = kolsimple(var,twk); % new cooler gas temperature

    t_error = abs(th - tgh) + abs(tk - tgk);

    th = tgh;
    tk = tgk;
    tr = (th-tk)/log(th/tk);

end

fprintf('===== converged heater and cooler mean temperatures =====\n');
fprintf('heater wall temperatures: Twh = %.1f (K)\n',twh);
fprintf('heater gas temperatures: Th = %.1f (K)\n',th);
fprintf('cooler wall temperatures: Twk = %.1f (K)\n',twk);
fprintf('cooler gas temperatures: Tk = %.1f (K)\n\n',tk);
fprintf('*****\n\n');

%===== Print out Ideal Adiabatic analysis results =====
% for i = 1:1:37
%
% eff(i) = var(W,i)/var(QH,i); % engine thermal efficiency
%
% end

% for i = 1:1:37
% freq = 5:5:185;
Qkpower = var(QK,COL)*freq; % Heat transferred to the cooler (W)
Qrpower = var(QR,COL)*freq; % Heat transferred to the regenerator (W)
Qhpower = var(QH,COL)*freq; % Heat transferred to the heater (W)
Wpower = var(W,COL)*freq; % Total power output (W)
eff = Wpower/Qhpower; % engine thermal efficiency
% eff(i) = var(W,i)/var(QH,i); % engine thermal efficiency
% end
% eff = var(W,COL)/var(QH,COL); % engine thermal efficiency
save('Wpower.mat','Wpower');
save('Qhpower.mat','Qhpower');

% Efficiency;
% for i = 1:1:37
% eff(i) = Wpower(i)/Qhpower(i); % engine thermal efficiency
% end

% for i = 1:1:37
% freq = 5:5:185;
% power(i) = var(W,37)*freq(i);
% heatadd(i) = var(QH,37)*freq(i);
% eff(i) = power / heatadd;

```

```
%
% end
```

```
fprintf('===== Ideal Adiabatic analysis results =====\n');
fprintf('Heat transferred to the cooler: Qkpower = %.3f (W)\n\n', Qkpower);
fprintf('*****\n\n');
fprintf('Heat transferred to the regen.: Qrpower = %.3f (W)\n\n', Qrpower);
fprintf('*****\n\n');
fprintf('Heat transferred to the heater: Qhpower = %.3f (W)\n\n', Qhpower);
fprintf('*****\n\n');
fprintf(' Total power output: Wpower = %.3f (W)\n\n', Wpower);
fprintf('*****\n\n');
fprintf(' Ideal Adiabatic Thermal efficiency: eff = %.3f(%%)\n\n', eff*100);
fprintf('*****\n\n');
```

```
% save('thermal_efficiency.mat','eff');
```

```
fprintf('===== REGENERATOR ANALYSIS RESULTS =====\n\n');
```

```
% qrloss = regquasi(var);
fprintf(' **** Regenerator Net Enthalpy Losses (qrloss) ****\n');
```

```
fprintf(' qrloss = %.3f (W)\n\n', qrloss*freq);
```

```
fprintf('*****\n\n');
```

```
fprintf(' **** Regenerator Wall Heat Leakage (qwrl) ****\n');
```

```
% for i = 1:1:37
% freq = 5:5:185;
qwrl = cqwr*(twh - twk)/freq;
% end
```

```
fprintf(' qwrl = %.3f (W)\n\n', qwrl*freq);
```

```
fprintf('*****\n\n');
```

```
fprintf('===== pressure drop Simple analysis =====\n');
```

```
dwork = worksimple(var,dvar);
% save('dwork.mat','dwork');
```

```
% for i = 1:1:37
% freq = 5:5:185;
%
% Dwork = dwork*freq;
% end
```

```
fprintf(' **** Pressure Drop Available Work Loss (dwork) ****\n');
```

```
fprintf(' dwork = %.4f (W)\n\n',dwork*freq);
```

```
fprintf('*****\n\n');
```

```
for i = 1:1:37
for j = 1:1:37
```

```

% freq =5:5:37;
%

% Outputpower = Wpower - dwork*freq;

Outputpower = Wpower - dwork*freq;

Heatpowerin = Qhpower + qrloss*freq + qwrl*freq;

% acteff = actWpower(i)/actQhpower(i);

    end
end

Efficiency = Outputpower/Heatpowerin;

save('Effeciency.mat', 'Effeciency');
save('Heatpowerin.mat', 'Heatpowerin');
save('Outputpower.mat', 'Outputpower');

fprintf('==== Output Work, Heat and Efficency for Simple Analysis =====\n\n');
fprintf(' ***** Total Power Output From Simple Analysis *****\n');
fprintf('      Outputpower = %.3f (W)\n\n', Outputpower);
fprintf('*****\n\n');
fprintf(' ***** Heat power Added to the Heater From Simple Analysis *****\n');
fprintf('      Heatpowerin = %.3f (W)\n\n', Heatpowerin );
fprintf('*****\n\n');
fprintf(' ***** Efficency From Simple Analysis *****\n');
fprintf('      Efficiency = %.3f (%%)\n\n', Efficiency*100);
fprintf('*****\n\n');

% Temperature plotting of the Simple simulation results
figure
x = 0:10:360;
Tcomp = var(TC,:);
Texp = var(TE,:);
plot(x,Tcomp,'b-*',x,Texp,'r-*','LineWidth',1);
xlim([0 360]);
hold on
x = [0,360];
y = [twk,twk];
ylim([200 1100]);
plot(x,y,'b--','LineWidth',1)
y = [tk,tk];
plot(x,y,'b','LineWidth',1)
y = [tr,tr];
plot(x,y,'g','LineWidth',1)
y = [th,th];
plot(x,y,'r','LineWidth',1)
y = [twh,twh];
plot(x,y,'r--','LineWidth',1)
hleg = legend('Tcomp','Texp','twk','tk','tr','th','twh');
hold off
grid on
xlabel('Crank Angle (theta) [degree]');
ylabel('Temperature [K]');
% title('Simple analysis simulation - Wall and Gas Temps vs Crank Angle');

```

```

% various plots of the quasi steady flow analysis

plotsimple(var,dvar);

end

function [vc,ve,dvc,dve,v] = volume(theta)

% determine working space volume variations and derivatives
% Argument: theta - current cycle angle [radians]
% Returned values:
% vc, ve - compression, expansion space volumes [m^3]
% dvc, dve - compression, expansion space volume derivatives

[vc,ve,dvc,dve,v] = freepiston(theta);

%=====

function [vc,ve,dvc,dve,v] = freepiston(theta)

% determine drive volume variations and derivatives of FPSE
% Argument: theta - current cycle angle [radians]
% Returned values:
% vc, ve - compression, expansion space volumes [m^3]
% dvc, dve - compression, expansion space volume derivatives

global vclc % compression clearance volume [m^3]
global vcle % expansion clearance volume [m^3]
global vswc % compression swept volume [m^3]
global vswe % expansion swept volume [m^3]
global alpha % phase angle advance of expansion space [radians]

% theta = 0:5:360;
vc = vclc + 0.5*vswc*(1 + cos(theta));
ve = vcle + 0.5*vswe*(1 + cos(theta + alpha));
dvc = -0.5*vswc*sin(theta);
dve = -0.5*vswe*sin(theta + alpha);
v = vc +ve;

end

end

function dwork = worksimple(var,dvar)

% Evaluate the pressure drop available work loss [J]
% Arguments:
% var(23,37) array of variable values every 10 degrees (0 - 360)
% dvar(16,37) array of derivatives every 10 degrees (0 - 360)
% Returned value:

```

% dwork - pressure drop available work loss [J]

% Row indices of the var, dvar arrays:

TC = 1; % Compression space temperature [K]  
TE = 2; % Expansion space temperature [K]  
QK = 3; % Heat transferred to the cooler [J]  
QR = 4; % Heat transferred to the regenerator [J]  
QH = 5; % Heat transferred to the heater [J]  
WC = 6; % Work done by the compression space [J]  
WE = 7; % Work done by the expansion space [J]  
W = 8; % Total work done (WC + WE) [J]  
P = 9; % Pressure [Pa]  
VC = 10; % Compression space volume [m<sup>3</sup>]  
VE = 11; % Expansion space volume [m<sup>3</sup>]  
MC = 12; % Mass of gas in the compression space [kg]  
MK = 13; % Mass of gas in the cooler [kg]  
MR = 14; % Mass of gas in the regenerator [kg]  
MH = 15; % Mass of gas in the heater [kg]  
ME = 16; % Mass of gas in the expansion space [kg]  
TCK = 17; % Conditional temperature compression space / cooler [K]  
THE = 18; % Conditional temperature heater / expansion space [K]  
GACK = 19; % Conditional mass flow compression space / cooler [kg/rad]  
GAKR = 20; % Conditional mass flow cooler / regenerator [kg/rad]  
GARH = 21; % Conditional mass flow regenerator / heater [kg/rad]  
GAHE = 22; % Conditional mass flow heater / expansion space [kg/rad]  
V = 23; % Total volume ([m<sup>3</sup>])

% Size of var(ROWV,COL), dvar(ROWD,COL)

ROWV = 23; % number of rows in the var matrix  
ROWD = 16; % number of rows in the dvar matrix  
COL = 37; % number of columns in the matrices (every 10 degrees)

% \*\*\*\*\*

global tk % cooler temperatures [K]  
global tr % regenerator temperatures [K]  
global th % heater temperatures [K]  
global omega % cycle frequency [rads/s]  
global vh % heater void volume [m<sup>3</sup>]  
global ah % heater internal free flow area [m<sup>2</sup>]  
global dh % heater hydraulic diameter [m]  
global lh % heater effective length [m]  
global vk % cooler void volume [m<sup>3</sup>]  
global ak % cooler internal free flow area [m<sup>2</sup>]  
global dk % cooler hydraulic diameter [m]  
global lk % cooler effective length [m]  
global vr % regen void volume [m<sup>3</sup>]  
global ar % regen internal free flow area [m<sup>2</sup>]  
global lr % regenerator effective length [m]  
global dr % regen hydraulic diameter [m]  
global qrloss % Regenerator net enthalpy loss  
global kgas

dtheta = 2\*pi/36;

dwork = 0; % initialise pumping work loss

for i = 1:1:37

```

% dwork = 0; % initialise pumping work loss

gk = (var(GACK,i) + var(GAKR,i))*omega/(2*ak);

% tk
% dk
% gk

[mu,kgas,re(i)] = reynum(tk,gk,dk);

[ht,fr] = pipefr(dk,mu,re(i));

dpkol(i) = 2*fr*mu*vk*gk*lk/(var(MK,i)*dk^2);

gr = (var(GAKR,i) + var(GARH,i))*omega/(2*ar);

[mu,kgas,re(i)] = reynum(tr,gr,dr);

[st,fr] = matrixfr(re(i));

dpreg(i) = 2*fr*mu*vr*gr*lr/(var(MR,i)*dr^2);

gh = (var(GARH,i) + var(GAHE,i))*omega/(2*ah);

[mu,kgas,re(i)] = reynum(th,gh,dh);

[ht,fr] = pipefr(dh,mu,re(i));

dphot(i) = 2*fr*mu*vh*gh*lh./(var(MH,i)*dh^2);

% dphot(i) = 18.03*gh*v^3*re(i)^(-0.316)*(Pt/dh)^(-0.927)*(Pt/Pd)^0.515;

dp(i) = dpkol(i) + dpreg(i) + dphot(i);

dwork = dwork + dtheta*dp(i)*dvar(VE,i); % pumping work [J]

pcom(i) = var(P,i);

pexp(i) = pcom(i) + dp(i);

pcombar = pcom*1e-5;
pexpbar = pexp*1e-5;

save('com_space_pressure.mat','pcombar');
save('exp_space_pressure.mat','pexpbar');

% end
end

dpkol(COL) = dpkol(1);
dpreg(COL) = dpreg(1);

```

```

dphot(COL) = dphot(1);
dp(COL) = dp(1);
pcom(COL) = pcom(1);
pexp(COL) = pexp(1);

save('pressure_drop_cooler.mat', 'dpkol');
save('pressure_drop_regen.mat', 'dpreg');
save('pressure_drop_heater.mat', 'dphot');
save('pressure_drop_drop.mat', 'dp');
save('pressure_drop_comp.mat', 'pcom');
save('pressure_drop_exp.mat', 'pexp');

fprintf('quitting pressure plots...\n\n');
fprintf('*****\n\n');

end

```

## Appendices 4: Matlab computer model result:

>> sea

start sim

Create a new data file? (y/n)y

enter new filename: mm

===== FPSE Data configuration =====

enter compression space clearance volume (vclc) [m<sup>3</sup>]: 0.0002

enter compression space swept volume (vswc) [m<sup>3</sup>]: 0.00013

enter expansion space clearance volume (vcle) [m<sup>3</sup>]: 0.0002

enter expansion space swept volume (vswe) [m<sup>3</sup>]: 0.000314

enter expansion phase angle advance (alpha) [degrees]: 90

===== free piston stirling engine data summary =====

compression clearance volume: vclc = 200.0 (cc)

compression swept volume: vswc = 130.0 (cc)

expansion clearance volume: vcle = 200.0 (cc)

expansion swept volume: vswe = 314.0 (cc)

expansion phase angle advance: alpha = 1.6 (rad)

\*\*\*\*\*

===== Available cooler type is smooth annulus =====

enter annular gap outer diameter (dout) [m] : 0.193

enter annular gap inner diameter (din) [m] : 0.192

enter heat exchanger length (len) [m] : 0.2

===== cooler data summary =====

cooler void volume: vk = 60.48 (cc)

cooler free flow area: ak = 3.02 (cm<sup>2</sup>)

cooler wetted area: awgk = 1212.65 (cm<sup>2</sup>)

cooler hydraulic diameter: dk = 1.00 (mm)

cooler length: lk = 20.00 (cm)

\*\*\*\*\*

===== Available heater type is smooth annulus =====

enter annular gap outer diameter (dout) [m] : 0.193

enter annular gap inner diameter (din) [m] : 0.192

enter heat exchanger length (len) [m] : 0.06

===== heater data summary =====

heater void volume: vh = 18.14 (cc)

heater free flow area: ah = 3.02 (cm<sup>2</sup>)

heater wetted area: awgh = 363.80 (cm<sup>2</sup>)

heater hydraulic diameter: dh = 1.00 (mm)

heater length:lh = 6.00 (cm)

\*\*\*\*\*

=== Available regenerator is annular nonmatrix regenerator ===

enter housing external diameter (dout) [m]: 0.198

enter housing internal diameter (din) [m]: 0.193

enter matrix internal diameter (dimat) [m]: 0.188

enter regenerator length (lr) [m]: 0.12

===== regenerator data summary =====

regenerator hydraulic diam: dr = 5.000 (mm)

regenerator total wetted area: awgr = 0.143634 (sq.m)

regenerator void volume: vr = 179.54 (cc)

\*\*\*\*\*

Available gas types are:

hy)drogen)

he)lium

ai)r

enter gas type: ai

gas type is air

enter mean pressure (Pa) : 100000

enter cold sink temperature (tk) in [K] : 298.15

enter hot source temperature (th) in [K] : 623.15

enter operating frequency in (freq) in [Hz] : 10.47

\*\*\*\*\*

===== operating parameters =====

mean pressure: pmaen = 100.000 (kPa)

cold sink temperature: tk = 298.1 (K)

hot source temperature: th = 623.1 (K)

effective regenerator temperature: tr = 440.9 (K)

operating frequency: freq = 10.5 (Hz)

\*\*\*\*\*

pressure phase angle: (beta) = 49.1(degrees)

total mass of gas: (mgas) = 0.723(gm)

\*\*\*\*\*

===== Schmidt analysis =====

Work:  $w = 2.686e+00$  (joules)

Power:  $power = 2.813e+01$  (Watts)

Heat removed from compression space:  $q_c = w_c = -2.464e+00$  (joules)

Heat added to the expansion space:  $q_e = w_e = 5.151e+00$  (joules)

Schmidt efficiency:  $eff = 5.46$

\*\*\*\*\*

===== The Ideal Analysis =====

Cooler temperature:  $T_k = 298.1$  (K)

Heater temperaturer:  $T_h = 623.1$  (K)

\*\*\*\*\*

iteration 0:  $y(TC) = 298.1(K)$  &  $y(TE) = 623.1(K)$

iteration 1:  $y(TC) = 298.0(K)$  &  $y(TE) = 597.1(K)$

iteration 2:  $y(TC) = 298.4(K)$  &  $y(TE) = 586.3(K)$

iteration 3:  $y(\text{TC}) = 298.8(\text{K})$  &  $y(\text{TE}) = 581.5(\text{K})$

iteration 4:  $y(\text{TC}) = 299.2(\text{K})$  &  $y(\text{TE}) = 579.4(\text{K})$

iteration 5:  $y(\text{TC}) = 299.5(\text{K})$  &  $y(\text{TE}) = 578.5(\text{K})$

iteration 6:  $y(\text{TC}) = 299.7(\text{K})$  &  $y(\text{TE}) = 578.0(\text{K})$

iteration 7:  $y(\text{TC}) = 299.8(\text{K})$  &  $y(\text{TE}) = 577.8(\text{K})$

iteration 8:  $y(\text{TC}) = 299.9(\text{K})$  &  $y(\text{TE}) = 577.7(\text{K})$

iteration 9:  $y(\text{TC}) = 299.9(\text{K})$  &  $y(\text{TE}) = 577.7(\text{K})$

===== Regenerator simple analysis =====

Average Reynolds number:  $\text{reavg} = 359.4$

Maximum Reynolds number:  $\text{remax} = 650.4$

Stanton number(Average Re):  $\text{st} = 0.062$

Number of transfer units:  $\text{ntu} = 3.0$

Regenerator effectiveness =  
74.713\*\*\*\*\*

===== Heater Simple analysis =====

Average Reynolds number:  $\text{reavg} = 316.4$

Maximum Reynolds number:  $\text{remax} = 565.9$

Heat transfer coefficient:  $\text{ht} = 129.48 (\text{W}/\text{m}^2 \cdot \text{K})$

Heat transferred to the heater:  $\text{qh} = 6.16 (\text{J})$

heater wall temperatures:  $T_{\text{wh}} = 623.1 (\text{K})$

heater gas temperatures:  $T_{\text{gh}} = 609.5 (\text{K})$

\*\*\*\*\*

===== Cooler Simple analysis =====

Average Reynolds number:  $re_{avg} = 434.7$

Maximum Reynolds number:  $re_{max} = 791.2$

Heat transfer coefficient:  $ht = 97.48 \text{ (W/m}^2\text{*K)}$

Heat transferred from the cooler:  $q_k = -3.23 \text{ (J)}$

cooler wall temperatures:  $T_{wk} = 298.1 \text{ (K)}$

cooler gas temperatures:  $T_k = 301.0 \text{ (K)}$

\*\*\*\*\*

===== The Ideal Analysis =====

Cooler temperature:  $T_k = 301.0 \text{ (K)}$

Heater temperature:  $T_h = 609.5 \text{ (K)}$

\*\*\*\*\*

iteration 0:  $y(TC) = 301.0(K) \ \& \ y(TE) = 609.5(K)$

iteration 1:  $y(TC) = 301.0(K) \ \& \ y(TE) = 584.3(K)$

iteration 2:  $y(TC) = 301.4(K) \ \& \ y(TE) = 573.7(K)$

iteration 3:  $y(TC) = 301.9(K) \ \& \ y(TE) = 569.1(K)$

iteration 4:  $y(TC) = 302.3(K) \ \& \ y(TE) = 567.0(K)$

iteration 5:  $y(TC) = 302.6(K) \ \& \ y(TE) = 566.1(K)$

iteration 6:  $y(TC) = 302.8(K) \ \& \ y(TE) = 565.7(K)$

iteration 7:  $y(\text{TC}) = 302.9(\text{K})$  &  $y(\text{TE}) = 565.5(\text{K})$

iteration 8:  $y(\text{TC}) = 303.0(\text{K})$  &  $y(\text{TE}) = 565.4(\text{K})$

iteration 9:  $y(\text{TC}) = 303.1(\text{K})$  &  $y(\text{TE}) = 565.3(\text{K})$

===== Regenerator simple analysis =====

Average Reynolds number:  $\text{reavg} = 364.4$

Maximum Reynolds number:  $\text{remax} = 659.3$

Stanton number(Average Re):  $\text{st} = 0.061$

Number of transfer units:  $\text{ntu} = 2.9$

Regenerator effectiveness =  
74.609\*\*\*\*\*

===== Heater Simple analysis =====

Average Reynolds number:  $\text{reavg} = 324.8$

Maximum Reynolds number:  $\text{remax} = 580.6$

Heat transfer coefficient:  $\text{ht} = 130.16 (\text{W}/\text{m}^2\cdot\text{K})$

Heat transferred to the heater:  $\text{qh} = 6.06 (\text{J})$

heater wall temperatures:  $\text{Twh} = 623.1 (\text{K})$

heater gas temperatures:  $\text{Tgh} = 609.8 (\text{K})$

\*\*\*\*\*

===== Cooler Simple analysis =====

Average Reynolds number:  $\text{reavg} = 432.0$

Maximum Reynolds number:  $\text{remax} = 786.6$

Heat transfer coefficient:  $\text{ht} = 97.74 (\text{W}/\text{m}^2\cdot\text{K})$

Heat transferred from the cooler:  $\text{qk} = -3.27 (\text{J})$

cooler wall temperatures:  $\text{Twk} = 298.1 (\text{K})$

cooler gas temperatures:  $T_k = 301.0$  (K)

\*\*\*\*\*

===== converged heater and cooler mean temperatures =====

heater wall temperatures:  $T_{wh} = 623.1$  (K)

heater gas temperatures:  $T_h = 609.8$  (K)

cooler wall temperatures:  $T_{wk} = 298.1$  (K)

cooler gas temperatures:  $T_k = 301.0$  (K)

\*\*\*\*\*

===== Ideal Adiabatic analysis results =====

Heat transferred to the cooler:  $Q_{kpower} = -34.289$  (W)

\*\*\*\*\*

Heat transferred to the regen.:  $Q_{rpower} = 0.036$  (W)

\*\*\*\*\*

Heat transferred to the heater:  $Q_{hpower} = 63.433$  (W)

\*\*\*\*\*

Total power output:  $W_{power} = 29.221$  (W)

\*\*\*\*\*

Ideal Adiabatic Thermal efficiency:  $eff = 46.065$ (%)

\*\*\*\*\*

===== REGENERATOR ANALYSIS RESULTS =====

\*\*\*\* Regenerator Net Enthalpy Losses (q<sub>rloss</sub>) \*\*\*\*

$$q_{rloss} = 115.294 \text{ (W)}$$

\*\*\*\*\*

\*\*\*\* Regenerator Wall Heat Leakage (q<sub>wrl</sub>) \*\*\*\*

$$q_{wrl} = 103.963 \text{ (W)}$$

\*\*\*\*\*

===== pressure drop Simple analysis =====

quitting pressure plots...

\*\*\*\*\*

\*\*\*\* Pressure Drop Available Work Loss (d<sub>work</sub>) \*\*\*\*

$$d_{work} = 7.5172 \text{ (W)}$$

\*\*\*\*\*

===== Output Work, Heat and Efficiency for Simple Analysis =====

\*\*\*\*\* Total Power Output From Simple Analysis \*\*\*\*\*

$$\text{Outputpower} = 21.704 \text{ (W)}$$

\*\*\*\*\*

\*\*\*\*\* Heat power Added to the Heater From Simple Analysis \*\*\*\*\*

Heatpowerin = 282.690 (W)

\*\*\*\*\*

\*\*\*\*\* Effecieny From Simple Analysis \*\*\*\*\*

Effeciency = 7.677 (%)

\*\*\*\*\*

quitting Simple plots...

quitting simulation...

>>

## Appendices 4:

### Consideration variable frequency versus power output and efficiency

Frequency(Hz)	Power output (W)			Efficiency (%)		
	Schmidt	Adiabatic	Simple	Schmidt	Adiabatic	Simple
At $T_h = 573$ (K)						
11	14.32	11.40	6.73	5.28	39.47	3.25
13	16.92	13.45	6.08	6.24	39.41	2.60
15	19.53	15.49	4.60	7.20	39.36	1.75
17	22.13	17.52	2.19	8.16	39.31	0.75

Frequency(Hz)	Power output (W)			Efficiency (%)		
At $T_h = 673$ (K)	Schmidt	Adiabatic	Simple	Schmidt	Adiabatic	Simple
11	18.14	15.74	11.32	6.13	49.24	4.53
13	21.44	18.58	11.60	7.24	49.20	4.15
15	24.74	21.41	11.10	8.36	49.15	3.57
17	28.04	24.23	9.72	9.47	49.11	2.84

Frequency(Hz)	Power output (W)			Efficiency (%)		
At $T_h = 773$ (K)	Schmidt	Adiabatic	Simple	Schmidt	Adiabatic	Simple
11	21.52	19.56	15.35	6.76	56.30	5.28
13	25.44	23.09	16.44	7.99	56.26	5.10
15	29.35	26.61	16.79	9.22	56.22	4.73
17	33.27	30.13	16.31	10.44	56.19	4.20